OCTA

6-8 February, 2020

ALECSO, Tunis -Tunisia

Multi-Conference OCTA

OCTA International Multi-Conference on:

Organization of Knowledge and Advanced Technologies

https://multiconference-octa.loria.fr/

Unifying the scientific contributions of the following conferences:

SIIE

8th. International Conference on:

Information Systems and Economic Intelligence

ISKO-Maghreb

Digital Sciences: impacts and challenges on Knowledge Organization

CITED

2nd. International Symposium on:

Advanced Technologies, Renewable Energies and Economic Development

TBMS

1st. international symposium on:

Big-Data-Analytics Technologies for Strategic Management: innovation and competitiveness

ORGANIZERS

Université de Tunis

ISKO-Maghreb

UNIVERSITÉ DE LORRAINE

IEEE Tunisia Section

www.ieee.tn

المنظمة العربية للتربية والثقافة والعلوم

SPONSORS

Tunisia China Friendship Association

ATLAS

SPECIAL ISSUES JOURNALS & BOOKS

Financial Innovation

Cambridge Scholars Publishing

isprs International Journal of Geo-Information

IEEE Xplore® Digital Library

PROCEEDINGS
2nd. International Symposium CITED'2019 on:

"Advanced Technologies, Renewable Energies and Economic Development".

February 6-7-8, 2020 Tunis (Tunisia)

https://cited2019.loria.fr

Organization in the event of the International Multi-Conference OCTA'2019 on: « Organization of Knowledge and Advanced Technologies » (https://multiconference-octa.loria.fr/)

Multi-Conference OCTA
OCTA'2019
IEEE Tunisia Section
www.ieee.tn
UNIVERSITÉ DE LORRAINE
ISKO-Maghreb

CFP_ CITED 2019 & *Special issues in Journals & Books*

Description :

In a global context, more aware than ever, about climate change and challenges, from one hand and, shortages of current energy resources, from the other hand. It remains an undeniable fact today to observe that advanced technologies for industrial purposes and the implementation of efficient use of renewable energies, will be the pillars of modern economies and future challenges.

Shumpeter 1912, highlighted the relationship between the innovation factor and economic conjuncture; pattern of economic transition; i.e, theory of economic evolution. Analyzed in the context of economic cycles, the horizons of 2020-2030, appear according to the cycles of Kondratiev 1926, as the beginning of the transition to a new era of production, industrialization and means, which can now be explained by the rise of the green economy theme.

The international symposium CITED'2019, in its second edition, aims to bring together the work on concerted and reflective research on the establishment of sustainable economic development based on technological advances, the optimal use of means and resources, and on renewable energies.

For researchers, technologists and R&D professionals, both public and private, in CITED'2019 int. event, will be the opportunity to present, share and evaluate scientific research, R&D and innovation, towards the rise of the green economy.

Committees

Steering Committee in OCTA:

Honorary President
Pr. Habib SIDHOM, President of the University of Tunis (Tunisia)

Presidents
Sahbi SIDHOM (LORIA – Université de Lorraine, France)
Amira KADDOUR (ENSTAB – Université de Carthage, Tunisia)
Anass EL HADDADI (ENSA Al-Hoceima, Morocco)
Mohamed ADDAM (ENSAH Al Hoceima, Morocco).
Abdelkrim MEZIANE (Centre de Recherche CERIST, Algeria)
Davy MONTICOLO (ENSGSI – Université de Lorraine, France)
Xi LU (Tsinghu University, China & Harvard University, Cambridge MA, USA)
Saoussen KRICHEN (Vice-President Université de Tunis, Tunisia)
Khaled KCHIR (Vice-President Université de Tunis, Tunisia)

Program committee / Comité scientifique :

Presidents
LU Xi, School of Environment, Tsinghu University & Harvard University, Cambridge, MA (USA).
Kaddour Amira, ENSTAB & Université de Carthage Tunisie.
Sidhom Sahbi, President ISKO-Maghreb & Université de Lorraine France.
.
Members
Abbesi Mohamed Ammar, University of Gafsa, Tunisia
Aboub Nedia, University la Manouba, Tunisia
Addam Mohamed, ENSA Al Hoceima, Morocco
Ahmadi Fatma (IEEE Tunisia, National Engineering School of Gabes (ENIG), Tunisia)

Alain Sylvestre, University of Grenoble, France
Arouri Mohamed, University Nice Côte d'azur, France
Batista Paulo (University of Évora, Portugal)
Befort Nicolas, Chair of Industrial Bioeconomy Neoma Business School, France
Bellow Edgar, Chair of Industrial Bioeconomy Neoma Business School, France
Berrada Ilham, ENSIAS University Mohammed V de Rabat, Morocco
Boubakeur Ahmed, Ecole Nationale Polytechnique d'Alger, Algeria
Boussaid Omar, ERIC Lab & University Lumière Lyon2, France
Bouzaiene Afef, University of Carthage, Tunisia
CHICHTI Jameleddine, Montpellier Business School, France & Tunisie
Djebali Ridha, University of Jendouba, Tunisia
El-Bouhdidi Jaber, ENSA de Tetouan, Morocco
El-Ghoul Mansour, University of Lorraine, France
El-Haddadi Anass, Vice-President ISKO-Maghreb & ENSA Al Hoceima, Morocco
Hagui Abdelhamid, VAD Lab. University of Carthage, Tunisia
Hajlaoui Makki, University of Carthage, Tunisia
Henry Carole, Société Générale Insurance, Luxembourg
Jomni Fethi, University of Tunis El Manar, Tunisia
KADDOUR Amira (Vice-President ISKO-Maghreb & ENSTAB Université de Carthage, Tunisia)
KALLEL Ilhem (IEEE SMC Society chair, ISIMS, University of Sfax, Tunisia)
KAMMOUN Habib (IEEE Tunisia Section Chair, & University of Sfax, Faculty of Science, Tunisia)
Kendo Sandra, University of Lorraine Neoma Business School, France
Khabbouchi Imed, University of Carthage, Tunisia
Khalfa Sana (IEEE Tunisia, Private Polytechnic School – Monastir, Tunisia)
LAABIDI Nadia (Université de Carthage, Tunisia)
Lhuillery Stéphane, Chair of Industrial Bioeconomy Neoma Business School, France
MEZIANE Abdelkrim (Vice-President ISKO-Maghreb for Algeria & CERIST, Algeria)
Mhamdi Faouzi, University of Jendouba, Tunisia
Monticolo Davy, ENSGSI-ERPI & Université de Lorraine, Tunisia
Naoui Kamel, University la Manouba, Tunisia
Pecquet Pascal, University of Montpellier, France
Rouahi Ahlem, Université de Jendouba, Tunisia
Sidhom Sahbi (President ISKO-Maghreb Chapter & University of Lorraine, France)
Tanti Marc, Center for Epidemiology and Public Health of the Armed Forces-SESSTIM, France
Zouaoui Mhamed, University la Manouba, Tunisia

A combined fault location methodology for radial power distribution systems

HAMDOUCHE Tarek
dept. Process Automation and Electrification
University of Boumerdes
Boumerdes, Algeria
t.hamdouche@univ-boumerdes.dz

BENDJEGHABA Omar
dept. Process Automation and Electrification
University of Boumerdes
Boumerdes, Algeria
bendjeghaba@univ-boumerdes.dz

AHRICHE Aimed
Electrical Engineering
University of Boumerdes
Boumerdes, Algeria
a.ahriche@univ-boumerdes.dz

***Abstract*—power distribution systems (PDS) are becoming more complex and dispersed at long distances and different locations. With its radial and several laterals configuration, loads could be connected at similar distances from the substation which leads to a multi estimation of fault location and consuming more time for iterative fault location algorithms. In order to overcome those limitations, a new practical combined fault location methodology is presented in this paper. By knowing the topology of the feeder, it can be segmented into a number of mono lateral systems (MLSs) using a proposed communicant sensor (CS), which is judicially installed in radial PDS. Then, a fault location process is applied only at the affected MLS basing on an equivalent model of the feeder. To examine the proposed approach, a real PDS from the Algerian distribution grid is used and the obtained results show a significant accuracy and feasibility of the approach.**

Keywords—Power distribution systems; fault location; service continuity ;comminicant sensor

I. INTRODUCTION

Service continuity and power quality are great challenges for power distribution companies, and it is also a very important condition needed by customers and investors. Outage time caused by faults is considered as a paid and not supplied power which is a failure for distribution companies. Due to the increasing demand on electric power, electric grid become more extended and more complex, which make it subject to faults caused by different events, such as atmospheric factors, equipments degradation, transport accidents, etc. In order to improve the operation indexes such as SAIDI (System Average Interruption Duration Index) and CAIDI (Customers Average Interruption Duration Index), faults location must be done very fast. This objective is quite mature in transmission power systems (TPS) where lines are homogeneous and have a simple topology. On the other hand, in distribution power systems (DPS), fault location task is very complex because of some inherent characteristics such as; radial architecture, laterals and sub laterals, different kinds and sections of cables, dynamic topology, unbalanced operation, time varying load and fault resistance. All of these make PDS a heterogeneous system. Until now, when a fault occurs in the PDS, a maintenance crew is sent to patrol the feeder, guided by fault indicator (FI) devices installed at different line-sections. Often, these devices are not operational and needing a regular maintenance. Another method is the dividing of the feeder into isolate sub regions using breaker recloser and sensors of SCADA (Supervisory Control And Data Acquisition). This method is practical and efficient, but it is not suitable for feeder equipment. It caused damages when reclose on the short circuit current. Owing to the cost and time consuming, these methods may not be an economical solutions. Hence, automatic fault location is an essential issue to speed up the restoration system and improve the operation indexes for distribution companies. Before, several efficient algorithms have been proposed for fault location in PDS. They can be classified into three main families; travel wave based algorithms [1]-[3], artificial intelligent based algorithms [4]-[11] and impedance based algorithms [12]-[19]. The first category is based on the high frequencies signals generated by faults and traveling along the feeder. These methods are fast and show a high accuracy. However they require high sampling rate for digital relays and high number of sensors due to the huge number of laterals and ramifications in PDS. In addition, in case of high resistive faults the generated wave is weak and can be fully dissipated which affect the efficiency of travel wave methods. In the second category, a machine learning rule is used to interpret the complex relationship between the fault and its distance from the source. Different artificial intelligent techniques are used such as; Fuzzy Logic (FL) [4], [5]. Artificial Neural Networks (ANN) [6], [7], Supporting Vector Regression (SVR) [8], [9], Genetic Algorithms (GA) [10], [11]. Providing an adequate and sufficient dataset is the common condition of those techniques. For example in work [7] a fault location technique for radial distributions networks is proposed. In this method short circuit power peaks are measured at the main substation during faulty conditions at different distances from the source. The method presents a good accuracy, but it is not a generalized one. Because two phase to ground (LLG) and tree phase to ground (LLLG) faults are not considered. In addition, loads variations are supposed fixed in the time, which need to update the gathering dataset at any change of the feeder topology, and leading to time consuming at the ANN learning step. The third category is the impedance based methods, when fault voltages and currents seen at the beginning of the feeder are used to calculate the apparent impedance. Because of their simplicity and low implementation cost, they are the most used one. However, owing to multi branches, loads uncertainty and faults resistances multi estimation location is the main drawback of these methods. Generally, impedance based algorithms used iterative estimations which may converge at false solution. In reference [13], an iterative fault location algorithm is proposed. The algorithm use a load current estimation model base on the assumption that, impedance load is constant and known, which it's not always true and available in PDS. So, the fault distance can be out of the section and the algorithm would be executed for the next section, leading to more time consuming. Paper [14] presents a novel fault location method. By traversing all value of fault distance the algorithm overcomes the problem of false solution for iterative methods. A high accuracy has obtained, but the effect of load uncertainty is not treated. In work [15], an iterative approach is presented considering load variations by aggregating the total load at the end of the feeder. An initial fault distance at each line section is assumed and incremented from zero to the section length. Then the fault location is obtained were the fault reactance is minimum. The method shows a good performance, but it requires a high number of tests. On the other hand, this algorithm neglects the problem of multiple estimation location, which is the main pitfall of all impedance based methods. In order to overcome this problem, an effective and fast fault location technique is proposed in this paper. By knowing the topology of the feeder, it can be segmented into a number of mono lateral systems (MLSs) using a proposed communicant sensor (CS), which is judicially installed in radial PDS. Then, a fault location process is applied only at the affected MLS basing on an equivalent model of the feeder. The proposed method can help impedance based algorithms by reducing the number of iterations and giving a unique fault location. The rest of the paper is organized as follows; section II describes the proposed fault location approach. Next, in section III the application and test of the proposed method on a real PDS is presented. Then, section IV is reserved for the conclusion.

II. PROPSED FAULT LOCATION METHOD

The basic idea of the proposed approach is to partition a multi laterals distribution system to possible MLSs by the proposed CSs. The number and placement of the used CSs is depending on the feeder topology. The here presented approach bases on two steps. Firstly, a transmitted fault signal is generated from the CS to the Operation station. So, the faulty MLS is precisely detected and the service could be speedily restored. Then, in the second step an equivalent model for the feeder during faulty conditions is established and used for fault distance estimation. Details of each step are described in the following sections.

A. Proposed Communicant sensor

The sensor presented in this work is based on a current transformer connected to a communication interface as shown in *Fig. 1*. The calibration of the CS is sited according to the over current relay (OCR) threshold in order to satisfy the coordination.

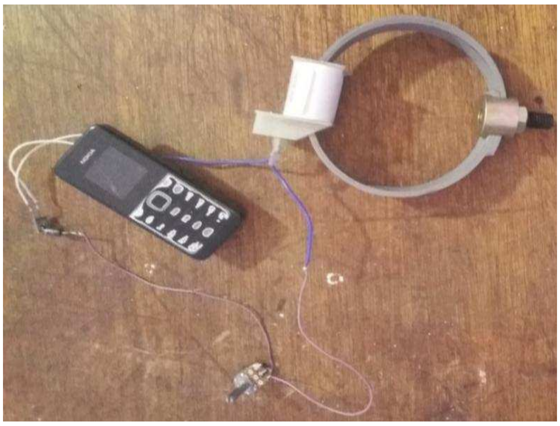

Fig.1. Proposed communicant sensor

B. Fault location estimation

The fact that voltages and currents measurement are often available only at the beginning of the feeder, it is difficult to obtain the online impedance at each node. In order to consider the load variations, several impedance based algorithms proceeding to aggregate the total load at the end of the feeder, as in [15]. This strategy is adopted in this study, basing on the assumption that load impedance is bigger than line impedance ($Z_C >> Z_L$). From *Fig 1.* We are:

$$Z_C = (V_S / I_S) - Z_L \quad (1)$$

Where:

$\mathbf{V_S}$**:** the pre-fault voltage at the substation.

$\mathbf{I_S}$**:** the pre-fault current at the substation.

$\mathbf{Z_L = \Sigma Z_{LMLSj}}$: the total line impedance, *j* is varied from 1 to total MLSs number *n*

$\mathbf{Z_C}$: the total load impedance aggregated at the farthest point of the feeder.

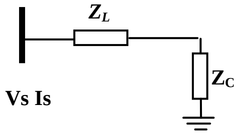

Fig.2. Simplified single line feeder model during prefault conditions

One of the difficulties of the technique proposed in [15] is the multiple fault location estimation caused by feeder laterals. In the here presented method, by detecting the exact faulty MLS the other MLSs can be eliminated from the fault location process which leads to reduce the number of analyzed line sections and giving a unique location. During a fault, the equivalent model of the feeder is presented as shown in *Fig. 3*. Where:

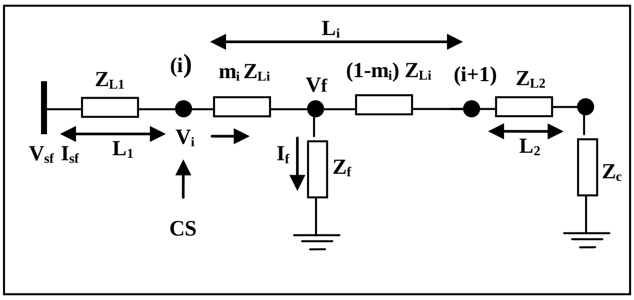

Fig.3. Equivalent model of the feeder during fault conditions

L_1: The distance from the substation to the faulted MLS.
L_2: The distance from the faulted MLS to the end of the feeder.
i: the faulty MLS.
L_i: The faulty MLS length.
Z_{Li}: the faulty MLS impedance.
Z_{L1} $= \Sigma Z_{LMLSj}$, j is varied from 1 to (i-1).
Z_{L2} $= \Sigma Z_{LMLSj}$, j is varied from (i+1) to n.
V_{sf}: voltage at the substation during the fault.
I_{sf}: current at the substation during the fault.
m_i: the per unit fault distance at MLS_i.
From *Fig. 2* the fault location **L_f** is determined using (2).

$$L_f = L_1 + m_i L_i \tag{2}$$

The incoming voltage V_i at node (i), voltage at fault point and fault current I_f are obtained using (3), (4) and (5) respectively.

$$V_i = V_{sf} - Z_{L1} I_{sf} \tag{3}$$

$$V_f = V_i - m_i Z_{li} I_{sf} \tag{4}$$

$$I_f = I_{sf} - (((1 - m_i) Z_{Li} + Z_{L2} + Z_c)^{-1} V_s) \tag{5}$$

Then the fault impedance is;

$$Z_F (m_i) = (V_f (m_i) / I_f (m_i)) \tag{6}$$

$$X_F (m_i) = \text{imag} (Z_F (m_i)) \tag{7}$$

Basing on the resistive character of faults, and by incrementing the assumed distance (m_i) from zero to the total length (L_i) of the MLSi, the fault location is assumed at the distance where the fault reactance is minimal. The flow chart of the proposed method is depicted in *Fig. 4.* The most commonly used digital OCRs are configured for detecting all types of faults, (phases-phases) faults by comparing currents to a phase threshold value $|I_{tp}|$, and (phases-ground) faults by comparing currents to a ground threshold value $|I_{tg}|$. *Table. 1* summarizes faults types conditions.

TABLE I. FAULTS TYPE DETERMINATION

Fault type	Conditions
ag	$\|I_a\|>=\|I_{tp}\|$ & $\|Ig\| > 0$
bg	$\|I_b\|>=\|I_{tp}\|$ & $\|Ig\| > 0$
cg	$\|I_c\|>=\|I_{tp}\|$ & $\|Ig\| > 0$
abg	$\|I_a\|>=\|I_{tp}\|$, $\|I_b\|>=\|I_{tp}\|$ & $\|Ig\| > 0$
bcg	$\|I_b\|>=\|I_{tp}\|$, $\|I_c\|>=\|I_{tp}\|$ & $\|Ig\| > 0$
acg	$\|I_a\|>=\|I_{tp}\|$, $\|I_c\|>=\|I_{tp}\|$ & $\|Ig\| > 0$
abc	$\|I_a\|>=\|I_{tp}\|$, $\|I_b\|>=\|I_{tp}\|$, $\|I_c\|>=\|I_{tp}\|$, & $\|Ig\| = 0$
ab	$\|I_a\|>=\|I_{tp}\|$, $\|I_b\|>=\|I_{tp}\|$ & $\|Ig\|= 0$
bc	$\|I_b\|>=\|I_{tp}\|$, $\|I_c\|>=\|I_{tp}\|$ & $\|Ig\|= 0$
ac	$\|I_a\|>=\|I_{tp}\|$, $\|I_c\|>=\|I_{tp}\|$ & $\|Ig\|= 0$
abcg	$\|I_a\|>=\|I_{tp}\|$, $\|I_b\|>=\|I_{tp}\|$, $\|I_c\|>=\|I_{tp}\|$, & $\|Ig\| > 0$

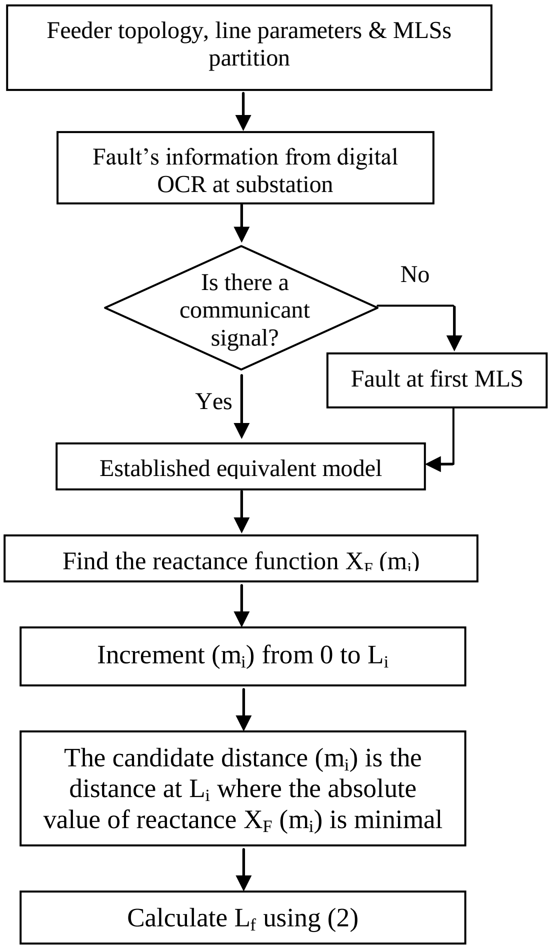

Fig.4. Flow chart of the proposed method

III. TESTS AND ANALYSIS

To examine the method, a real underground PDS from Sonelgaz SDC in Algeria is used; its topology is presented in *Fig. 1.* The selected system is 51 nodes, 30KV underground feeder dispersed at a total length of 18,357Km with a total power of 15,933MVA. The additional information of this feeder is shown in Table II in Appendix. From the topology of the feeder, it can be divided into four MLSs. Thus, three CSs are needed to be installed, as shown in *Fig. 5.*

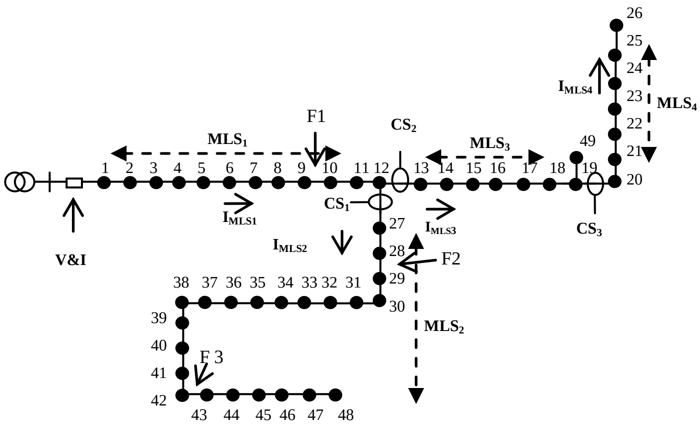

Fig.5. Test feeder topology

To evaluate the performance of the proposed method, three real faults cases are used. Those faults are happened at different locations and different conditions along the feeder length. F1 (node9–node10), F2 (node28-node29), and F3 (node42-node43). Fig. 6, presents informations of a case fault extracted from the digital OCR at the substation.

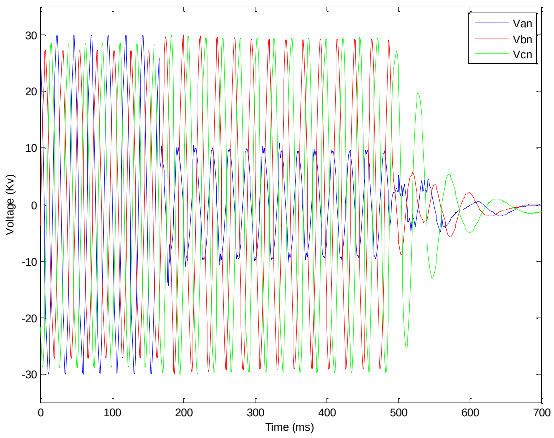

Fig.6. F2 volatges measurement at substation

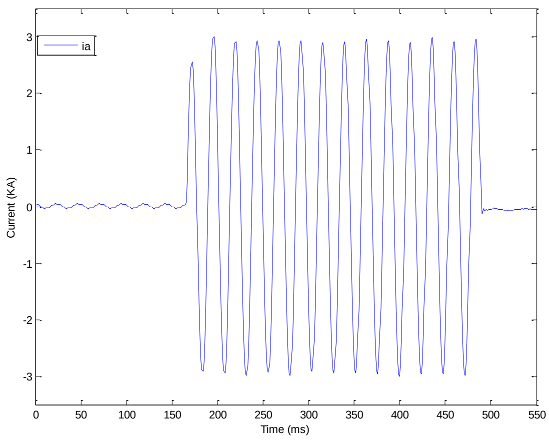

Fig.7. F2 current of faulty phase measured at substation

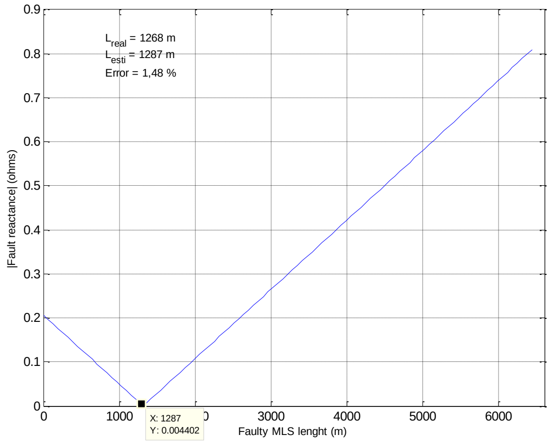

Fig.8. F2 reactance values along faulty MLS

From Fig. 8, it is shown that the minimum absolute value of fault reactane is obtained at a distance of 1287 m giving an error of 1,48 %. Compared to the method presented in [15], the here proposed method investigate only a partion of the PDS and giving a unique fault location. The error is calculated by (8).

$$\text{Error}(\%) = (|\, l_{real} - l_{estimated} \,|/\, l_{teal}\ ) \times 100 \qquad (8)$$

IV. Conclusion

A fast and practical technique to locate faults in radial distribution systems is exposed in this paper. This method overcomes the problem of multi fault location estimation, which is the main drawback of impedance based algorithms. By segmenting the PDS to possible MLSs, the fault location process executed only at a one partition of the system which leading to reduce the number of tests and giving a unique fault location. The method requires only information of feeder topology, series line impedance of each homogeneous section, and fundamental components of voltages and currents measured at substation pre and during faulty conditions.

References

[1] H. Fernando Magnago, A. Aburn, "A New Fault Location Technique for Radial Distribution Systems Based on High Frequency Signals," IEEE Power Engineering Society Summer Meeting. Conference Proceedings (Cat. No.99CH36364), vol.1, pp. 421-431, 1999.

[2] M. Goudarzi, B.Vahidi, R.A. Naghizadeh, S.H. Hosseinian, "Improved fault location algorithm for radial distribution systems with discrete and continuous wavelet analysis," Electrical Power and Energy Systems 67 (2015) 423-430.

[3] A. Ghaderi, H. Ali Mohammadpour, H. Giin "Active Fault Location in Distribution Network using Time-Frequency Reflectometry," IEEE Power and Energy Conference at Illinois (PECI), pp. 1-7, 2015.

[4] J. Moshtagh, A. Rafinia, "A New Approach to High Impedance Fault Location in Three-Phase Underground Distribution System Using Combination of Fuzzy Logic & Wavelet Analysis," 11th International Conference on Environment and Electrical Engineering, pp. 90-97, 2012

[5] S. Bunjongjit, A. Ngaopitakkul, C. Pothisarn "A Discrete Wavelet Transform and Fuzzy Logic Algorithm for Identifying the Location of

Fault in Underground Distribution System," International Conference on Fuzzy Theory and Its Applications (iFUZZY), pp. 415-419, 2013.

[6] H. Zayandehroodi, A. Mohamed, M. Farhoodnea and A. Heidari "New Training Strategies for RBF Neural Networks to Determine Fault Location in a Distribution Network with DG Units," IEEE 7th nternational Power Engineering and Optimization Conference (PEOCO), pp. 450-454, 2013.

[7] P. Farzan, M. Izadi, C. Gomes, and M. Zainal"Short Circuit Power Based Fault Location Algorithm in Distribution Networks," IEEE 8th International Power Engineering and Optimization Conference (PEOCO2014), pp. 105-109, 2014.

[8] L. Ye, D. You, X. Yein, K. Wang, and J. Wu "An improved fault location method for distribution system using wavelets and support vector regression," Electrical Power and Energy Systems 55 (2014) 467-472.

[9] S. Shilpa, H. Mokhlis, H. Azil, A. Abu bakar, and L. Awalin "Fault Location in an Unbalanced Distribution System using Support Vector Classification and Regression Analysis," IEEJ Transactions on Electrical and Electronic Engeneering. 2018; 13: 237–245.

[10] S. Jamali, A. Bahmanyar, and H. Borhani-Bahabadi "A Fast and Accurate Fault Location Method for Distribution Networks with DG Using Genetic Algorithms," Smart Grid Conference (SGC), pp. 110-114, 2015.

[11] J. Qiyan, J. Rong "Fault Location for Distribution Network Based on Genetic Algorithm and Stage Treatment," Spring Congress on Engineering and Technology, pp. 1-4, 2012

[12] IEEE Guide for Determining Fault Location on AC Transmission and Distribution Lines, pp. 1-76, 2015.

[13] S. Lee, M. Choi, S. Kang, B. Jin, D. lee, B. Ahn, N. Yoon, H. Kim, and S. Wee. "An Intelligent and Efficient Fault Location and Diagnosis Scheme for Radial Distribution Systems," IEEE Transactions on power delivery, vol. 19, NO. 2, April 2004.

[14] Y. Lei, Y. Dahai, Y. Xianggen, T. Jinrui, L. Baolei, and Y. Yuan, "A Novel Fault-Location Method for Radial Distribution Systems," Asia pacific power and energy engineering conference, pp. 1-5, 2012.

[15] G. Espana, M. Florez, and V. Tores, "Fault location method based on the determination of the minimum fault reactance for uncertainty loaded and unbalanced power distribution systems," IEEE/PES Transmission and Distribution conference and exposition; Latina America, pp. 803-809, 2010

APPENDIX1

TABLE II TEST FEEDR CHARACTERISTIC

N°_Tr	From	To	Cond	Sec (mm2)	Long (m)	Longt(m)	R(Ω/km)	X(Ω/km)	St(Kva)	Longd(m)
1	1	2	AL	120,000	1021,000	1021,000	0,250	0,100	0,00	1021
2	1	2	AL	120,000	318,000	1339,000	0,250	0,100	0,00	1339
3	1	2	CU	70,000	418,000	1757,000	0,257	0,100	250,00	1757
4	2	3	CU	70,000	138,000	138,000	0,257	0,100	0,00	1895
5	2	3	AL	120,000	19,000	157,000	0,250	0,100	250,00	1914
6	3	4	AL	120,000	19,000	19,000	0,250	0,100	0,00	1933
7	3	4	CU	70,000	33,000	52,000	0,257	0,100	400,00	1966
8	4	5	CU	70,000	67,000	67,000	0,257	0,100	250,00	2033
9	5	6	CU	70,000	52,000	52,000	0,257	0,100	0,00	2085
10	5	6	AL	120,000	170,000	222,000	0,250	0,100	400,00	2255
11	6	7	AL	120,000	170,000	170,000	0,250	0,100	0,00	2425
12	6	7	CU	70,000	196,000	366,000	0,257	0,100	630,00	2621
13	7	8	AL	120,000	127,000	127,000	0,250	0,100	400,00	2748
14	8	9	AL	120,000	72,000	72,000	0,250	0,100	160,00	2820
15	9	10	CU	120,000	40,000	40,000	0,150	0,100	0,00	2860
16	9	10	AL	120,000	150,000	190,000	0,250	0,100	0,00	3010
17	9	10	AL	120,000	459,000	649,000	0,250	0,100	400,00	3469
18	10	11	AL	120,000	481,000	481,000	0,250	0,100	250,00	3950
19	11	12	AL	120,000	119,000	119,000	0,250	0,100	400,00	4069
20	12	13	AL	120,000	310,000	310,000	0,250	0,100	250,00	4379
21	13	14	AL	120,000	805,000	805,000	0,250	0,100	400,00	5184
22	14	15	AL	120,000	597,000	597,000	0,250	0,100	250,00	5781
23	15	16	AL	120,000	518,000	518,000	0,250	0,100	250,00	6299
24	16	17	AL	120,000	315,000	315,000	0,250	0,100	250,00	6614
25	17	18	AL	120,000	203,000	203,000	0,250	0,100	250,00	6817
26	18	19	AL	120,000	515,000	515,000	0,250	0,100	250,00	7332
27	19	20	AL	120,000	1247,000	1247,000	0,250	0,100	400,00	8579
28	20	21	AL	120,000	29,000	29,000	0,250	0,100	0,00	8608
29	20	21	CU	120,000	340,000	369,000	0,150	0,100	400,00	8948
30	20	21	AL	120,000	695,000	695,000	0,250	0,100	160,00	9643
31	22	23	AL	120,000	586,000	586,000	0,250	0,100	250,00	10229
32	23	24	AL	120,000	338,000	338,000	0,250	0,100	400,00	10567
33	24	25	AL	120,000	426,000	426,000	0,250	0,100	250,00	10993
34	25	26	AL	120,000	586,000	586,000	0,250	0,100	250,00	11579
35	26	27	AL	120,000	343,000	343,000	0,250	0,100	250,00	11922
36	27	28	AL	120,000	490,000	490,000	0,250	0,100	410,00	12412
37	28	29	AL	120,000	103,000	103,000	0,250	0,100	160,00	12515
38	29	30	AL	120,000	492,000	492,000	0,250	0,100	0,00	13007
39	29	30	CU	70,000	190,000	682,000	0,257	0,100	0,00	13197

40	29	30	CU	120,000	143,000	825,000	0,150	0,100	100,00	13340
41	30	31	CU	120,000	194,000	194,000	0,150	0,100	0,00	13534
42	30	31	AL	120,000	33,000	227,000	0,250	0,100	630,00	13567
43	31	32	AL	120,000	33,000	33,000	0,250	0,100	0,00	13600
44	31	32	CU	120,000	138,000	171,000	0,150	0,100	250,00	13738
45	32	33	AL	120,000	159,000	159,000	0,250	0,100	630,00	13897
46	33	34	AL	120,000	114,000	114,000	0,250	0,100	0,00	14011
47	33	34	CU	120,000	58,000	172,000	0,150	0,100	0,00	14069
48	33	34	CU	120,000	23,000	195,000	0,150	0,100	630,00	14092
49	34	35	CU	120,000	20,000	20,000	0,150	0,100	0,00	14112
50	34	35	CU	120,000	239,000	259,000	0,150	0,100	160,00	14351
51	35	36	CU	70,000	248,000	248,000	0,257	0,100	630,00	14599
52	36	37	CU	70,000	210,000	210,000	0,257	0,100	463,00	14809
53	37	38	AL	120,000	346,000	346,000	0,250	0,100	0,00	15155
54	37	38	AL	120,000	119,000	465,000	0,250	0,100	0,00	15274
55	37	38	AL	120,000	190,000	655,000	0,250	0,100	250,00	15464
56	39	40	AL	120,000	229,000	229,000	0,250	0,100	0,00	15693
57	39	40	AL	120,000	37,000	266,000	0,250	0,100	400,00	15730
58	40	41	AL	120,000	42,000	42,000	0,250	0,100	400,00	15772
59	41	42	CU	70,000	231,000	231,000	0,257	0,100	0,00	16003
60	41	42	CU	70,000	46,000	277,000	0,257	0,100	0,00	16049
61	41	42	AL	120,000	148,000	425,000	0,250	0,100	400,00	16197
62	42	43	AL	120,000	142,000	142,000	0,250	0,100	0,00	16339
63	42	43	CU	120,000	86,000	228,000	0,150	0,100	0,00	16425
64	42	43	CU	70,000	58,000	286,000	0,257	0,100	250,00	16483
65	43	44	AL	120,000	245,000	245,000	0,250	0,100	400,00	16728
66	44	45	AL	120,000	240,000	240,000	0,250	0,100	0,00	16968
67	44	45	AL	120,000	35,000	275,000	0,250	0,100	250,00	17003
68	45	46	AL	120,000	34,000	34,000	0,250	0,100	0,00	17037
69	45	46	CU	70,000	185,000	219,000	0,257	0,100	160,00	17222
70	46	47	CU	70,000	32,000	32,000	0,257	0,100	0,00	17254
71	46	47	CU	120,000	70,000	102,000	0,150	0,100	0,00	17324
72	46	47	AL	120,000	142,000	244,000	0,250	0,100	160,00	17466
73	47	48	AL	120,000	148,000	148,000	0,250	0,100	160,00	17614
74	48	49	CU	120,000	70,000	70,000	0,150	0,100	0,00	17684
75	48	49	CU	70,000	170,000	240,000	0,257	0,100	0,00	17854
76	48	49	CU	70,000	163,000	403,000	0,257	0,100	0,00	18017
77	48	49	CU	120,000	30,000	433,000	0,150	0,100	400,00	18047
78	49	50	CU	120,000	30,000	30,000	0,150	0,100	0,00	18077
79	49	50	CU	70,000	60,000	90,000	0,257	0,100	0,00	18137
80	49	50	CU	120,000	110,000	200,000	0,150	0,100	250,00	18247
81	50	51	CU	120,000	110,000	110,000	0,150	0,100	400,00	18357

For farmers who want to automatically take care of their plants (diagnosis & cure), FarmerAid will take care of plants' health and report immediately if there are any detected diseases and take the right decision to cure plants. FarmerAid's product uses is very low electricity consumption, easy to install, makes decisions in real-time and suggests solutions for farmers to make better decisions.

Our product is a combination of many cutting-edge technologies, like AI, IoT and cloud computing.

The aim of this project is to solve an energy management problem that led to an exorbitant energy bill for the production area of an automotive company. In order to solve it wisely, it was essential to monitor the energy consumption, analyse its behaviour and make a diagnosis on the lighting system, compressed air production system and air conditioning system being the highest consumers of energy.

Solutions that address the problems encountered have been suggested, studied and analysed energetically, environmentally and financially.

This work can serve as a standard model toward energy transition in the case of automotive industry.

Key words: Energy management, energy efficiency, lighting, compressed air, air conditioning

ZBOUNA EMNA
Docteur en droit public,
Assistante à l'institut supérieur des langues appliquées et de l'informatique de Béja

Amira KADDOUR
ENSTAB - UCAR

L'administration tunisienne à l'épreuve des nouvelles technologies

Mots clés : Administration, service public, e-gouvernement, e-dinar, crypto monnaie.

Résumé

L'évolution et l'apparition des nouvelles technologies, ont bouleversé non seulement notre vie quotidienne, mais aussi toutes les institutions de l'Etat.

L'administration tunisienne, en tant qu'outil exécutif de l'Etat, s'est trouvée confronter à une nouvelle réalité créée par la globalisation et la genèse des nouvelles technologies qui ont envahi le quotidien des citoyens-administrés et qui ont crée d'autres formes d'entreprises, de sociétés, de commerce, de contrat, de signature… (Électroniques et virtuel).

Comment l'administration tunisienne peut s'adapter avec ce « tsunami » technologique ?

Est-il facile de se métamorphoser rapidement, pour une administration profondément fidèle et attachée à ces traditions, une administration longtemps gouvernée par la logique sécuritaire qui appréhende les nouvelles technologies comme une source de méfiance à cause des lacunes juridiques dans ce domaine ?

L'administration tunisienne à l'épreuve des nouvelles technologies sera une occasion afin de répondre à cette myriade d'interrogations et de disséquer les différentes périodes passées par l'administration tunisienne, jusqu'à l'adoption du e- gouvernement et du e- dinar.

Une évolution certes prépondérante, mais encore insuffisante pour une administration cherchant à être à la fois efficace et efficiente à l'échelle interne, et compétitive à l'échelle internationale.

Plan :

I) Une adaptation imposée
   A) Crise de l'administration traditionnelle
   B) Les mutations vers une administration moderne
II) Une adaptation malaisée
   A) L'imbroglio du cadre juridique
   B) Les méfiances des crypto monnaies

Techniques de traitement et de reconnaissance d'IRM cérébrale

AMMAR Karam

JEBARI Nessrine

Résumé :

Les bases de données médicales spécialisées jouent actuellement un rôle majeur dans l'archivage et la recherche de données comparables acquises par différentes modalités d'imagerie médicale. Dans le contexte du stockage et de la recherche de données dans des bases de données médicales, il est primordial de trouver une méthode d'extraction et de représentation des contenus trouvés dans l'image qui assurerait un accès rapide et des résultats satisfaisants aux recherches d'enregistrements d'images. Ce qui est important, cette représentation doit également être indépendante de la forme de l'image. La large diffusion des bases de données médicales multimédias qui peuvent stocker non seulement des images uniques mais aussi des séquences vidéo a montré que le problème de la recherche efficace d'images contenant des cas de maladies spécifiques significatifs pour le diagnostic médical est toujours très difficile. Notre projet, présente des méthodes de de reconnaissance d'image. Les méthodes proposées, bien que prédestinées principalement aux applications médicales, peuvent également servir de base à d'autres solutions, notamment pour l'acquisition et l'analyse sémantique sophistiquée de motifs d'images complexes pour des raisons

FinTech : a post crisis answer to increased financial institutions compliance obligations

Dr. Amira KADDOUR

ENSTAB – CARTHAGE UNIVERSITY TUNISIA

Pr. Jameleddine CHICHTI

ESC – UNIVERSITE DE LA MANOUBA

Abstract:

It's an indeniable fact today that the global financial crisis of 2008 was a major financial episode that has deeply impacted general evaluation of past financial methods and models. The important role of bank's behavior, strategy and choices that have fueled deep reasons of this turbulence, have enhanced the shift from less regulated models to more and severe regulations such as Basel III in order to limit risk taking behavior, to straighten financial situation of banks and to increase their compliance obligation. Regarding these conditions, the general perception of banks role has been negatively impacted leading to a shift toward new kind of financial services under a general era of digitalization. This paper investigates FinTech as a post-crisis result.

Keywords: Financial crisis, FinTech, digitalization, Financial risks.

ESG approach, the new perspective of financial analysis: challenges and limits for MENA region

Dr. Amira KADDOUR

ENSTAB – CARTHAGE UNIVERSITY TUNISIA

Yasmine DAKOUMI

AVICENNE BUSINESS SCHOOL TUNISIA

Abstract:

When we talk about financial markets, we say challenges, and we can enumerate many examples, new technologies, various emerging markets , financial and political crisis and the list goes on, but we cannot forget about climate change. Climate change is certainly affecting all firms on various levels, it affects their financial stability, and changes the nature of the environment they belong to. Here came along the concept of green finance, Green finance can be explained as any financial tool or service that has a positive impact on both the society and the environment on a long term note or what we call sustainability. With a basic criteria for being labeled as a 'green' activity or business, is the act of reducing greenhouse emissions. Along this awareness, companies started to shift their attention to the real impact of climate change, that they are contributing to, and therefore, they are starting to inject this environmental responsibility in their business module DNA, weather directly by changing their business strategies, or indirectly by investing in projects that have an environmentally friendly vision and plan of action.

Traditional financial models focuses on firm's profit as main measure of financial profitability, these models have fuled overuse of resources and negative impacts linked to the absence of ecofriendly compliance obligations. ESG approach stipulates a general revision of companies vision toward more responsible behavior from owners to employees and all the different stakeholders.

Keywords: Green Finance, ESG, Financial assessment, Green economy

La transition green et digitale : une question de culture et de valeur

Dr. Amira KADDOUR

ENSTAB – CARTHAGE UNIVERSITY TUNISIA

Mariem MAAZI et Nour DRIDI

ENSTAB – CARTHAGE UNIVERSITY TUNISIA

Abstract:

Discuter la transition digitale et green autour des techniques, méthodes et systèmes à implementer semble rester sans efficacité escomptée en dehors de l'existence d'un consenus ethique general cadrant l'implication des acteurs dans ces efforts. En effet allant du fait que l'économie est à la base une interaction entre travail et capital, dans l'objectif de satisfaire des besoins illimités sous contraintes des resources limités, les repercussions néfastes jusqu'à présent des pratiques économiques de l'Homme laissent présager la nécessité de revoir sa relation avec l'environnement. Dans ce sens les experiences de transition réussites sont renforcées à la base par un cadre culturel et éducatif fondant les préceptes d'un comportement humain facilitant et consolidant la notion d'économie verte et de développement durable.

Keywords: Green culture, green education.

Iterated Granular Neighborhood Algorithm for Multi-Station Taxi-Sharing Problem IEEE Computer Society Conferences

Houssem E-B Smida
Université de Tunis and
Universidad de Malaga
Institut Superieur de Gestion
Tunisia, Bouchoucha 2000
Email: he.bensmida@gmail.com

Saoussen Krichen
Université de Tunis
Institut Superieur de Gestion,Tunis
Email: saoussen.krichen@gmail.com

Francisco Chicano
Universidad de Malaga
E.T.S. Ingeniería Informática, 3.2.47
Email: chicano@lcc.uma.es
Web: http://www.franciscochicano.es/

***Abstract*—A rush hour is the time during which the most people commute, its impact on traffic congestion and pollution in cities is very important. Usually we find a crowd of travelers waiting in the same origin, willing to travel to different destinations. On the other hand, taxis are a quick and reliable mean of transportation, but rarely travel with full capacity. For this reason, it is interesting to share taxis instead of traveling alone. A new problem formulation is presented to the Taxi Sharing Problem, in this paper we will manage all the origins in the same system. We propose a Mixed Integer Linear Programing formulation (MILP) for the Multi-Station Taxi Sharing Problem (MSTSP) for small instances and iterated granular neighborhood algorithm (IGNA) for medium , large and very large instances. The model will be tested on a real life case study (Tunisia).**

1. Introduction

The known taxi sharing problem requires the travelers to walk towards the common origin whatever the distance from their starting points, and then they can share their trips. Imagine that we have more than 300 travelers decided to share taxis and they meet in a common station at the same time. We need at least 75 taxis to assign travelers in taxis. This situation can cause traffic congestion and increase clutter. To solve these limitaions, we have to generalize the taxi sharing problem to the multi-stations taxi sharing problem. We can assign the travelers to a close and suitable station to minimize the first mile for passengers and the traveling cost.
In this problem, the taxis depart from one of the available stations and finish their trip at their last passenger's destination.
Figure 1 shows an example of a solution of the MSTSP composed of 10 passengers and 2 Stations. In this solution, we used 4 taxis, 2 taxis starts from station 1 and visit a total of 5 destinations along their routes, and 2 cubs starts from the second station with the same number of visit.

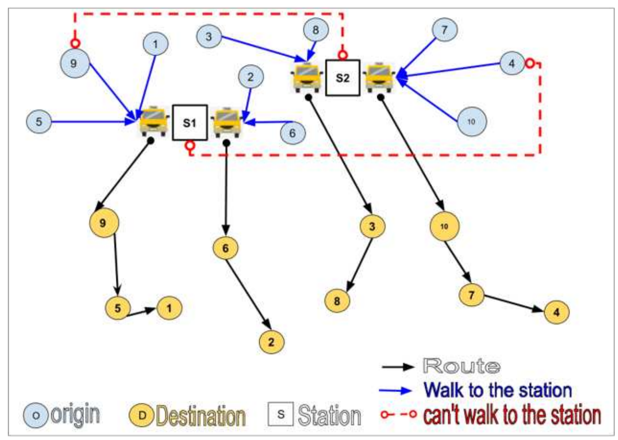

Figure 1. Example of a solution for the MSTSP. This example is composed of 10 passengers and 2 depots

In real-world contexts, we can find a multitude of environments in which the Taxis may depart from different stations when starting their routes. This practical issue is addressed by the multi-station taxi-sharing problem (MSTSP). The Multi-Staion Taxi Sharing Problem differs from the well-known Taxi Sharing Problem. That is, the routes of Taxis start from different stations and finishes at their last destination. The goal of this paper is to provide a new mathematical formulation for the MSTSP. The remainder of this paper is organized as follows. The proposed mathematical formulation for the MSTSP is introduced in Sect. 2. The real case study carried out in this work is presented in Sect. 3. Finally, some conclusions are drawn in Sect. 4.

2. Mathematical formulation

The Multi-Station Taxi Sharing Problem presented in the previous section can be transformed into a Capacitated Multi-Depot Vehicle Routing Problem instance where the number of vehicles is unknown. This served as a motivation to adapt existing Multi-Depot Vehicle Routing MILP formulations to solve Multi-Station Taxi Sharing. In particular, we base our formulation in that of Golden, Magnanti, and Nguyen [?].

In the MDVRP, The objective is to serve all customers while minimizing the number of vehicles and travel distance. A MDVRP requires the assignment of customers to depots. A fleet of vehicles is based at each depot. Each vehicle originate from one depot, service the customers assigned to that depot, and return to the same depot. Each vehicle has a maximum capacity that cannot be exceeded. Each customer must be visited only once by one vehicle. There is a similarity between MDVRP and MSTSP if we relate the customers with the passengers and the depots with the Stations of all the passengers. The vehicles are the taxis and the maximum capacity is the number of people each taxi can take. The main differences are:

- The taxis do not have to go back to the depot (as in MDVRP)
- There is a minimum fare that is not related to the distance traveled
- There can be several passengers that want to go to the same location
- The distance between the starting point of the traveler and the available stations.
- Every passenger can't walk to a station far from his origin.

We can transform a MSTSP instance into a MDVRP instance if we find a way to deal with these differences. In order to model the fact that taxis do not need to go back to the depot, we can do the cost of return equals zero.
This way, although the solutions will be composed of closed paths, there is no cost related to the final segment (that goes back to the origin).
The minimum fare can be added to the cost of the first segment of any path. In particular, it can be added to all the edges that leave the origin.
All the passenger destinations can be considered as different. If some of them are the same in a particular instance of the problem, we add a zero cost edge between them.
We will add another constraint in our future work, which does not allow the traveler to travel from a station far from its origin. With these considerations, we can adapt the MILP formulation of MDVRP to MSTSP.
We assume c_{0i} is the cost from the origin to the location plus the minimum fare that the customers have to pay to the taxi. The values c_{0i} will be 0 as explained above.
We assume that each passenger can be affected to any station without calculating the distance from his starting point to the assigned station.

The MSTSP can be defined as follows. The taxi sharing problem is extended to the case wherein we have multiple origin.

Let $G = (V, A)$ be a complete graph, where $V = V_p \cup V_s$ is the node set and A is the arc set. V_p is the subset of passengers nodes where $V_p = \{1, ..., n\}$, and V_s is the subset of station nodes where $V_s = \{n+1, ..., m\}$ for $m = n+w$. we provide enough taxis to transport people. K is the set of taxis where $K = \{1, ..., r\}$.
The parameters included in this new formulation are the following:

- c_{ij} cost between nodes i and j. The travelling cost is represented according to the travelling distance.
- Q_k capacity of taxi k.
- w number of stations.
- n number of passengers.

A travelling cost, $c_{ij} \geq 0$ is defined for each arc between each pair of vertices (i, j), where $i, j \in V$, $i \neq j$. The travelling cost c_{ij} from each passenger destination i to each station j is set to zero, where $c_{ij} = 0$, $\forall i \in V_p, j \in V_s$. Each station $s \in V_s$ can provide enough taxis to transport all the passengers. For this purpose, each station has an unlimited space to pause taxis for the pick up of passengers. Each taxi has the same positive capacity, denoted as Q_K. The decision variable x_{ijk} is a binary variable that indicates whether taxi k travels directly from customer i to customer j. The complete formulation is given below:

$$\min \sum_{i=0}^{m} \sum_{j=0}^{m} \sum_{k=0}^{m} c_{ij} x_{ijk}, \tag{1}$$

subject to:

$$\sum_{i=0}^{m} \sum_{k=0}^{m} x_{ijk} = 1 \qquad \forall k \in K, \forall j \in V_p \tag{2}$$

$$\sum_{j=0}^{m} \sum_{k=0}^{m} x_{ijk} = 1 \qquad \forall k \in K, \forall i \in V_p \tag{3}$$

$$\sum_{i=0}^{m} x_{ihk} - \sum_{j=0}^{m} x_{hjk} = 0 \qquad \forall k \in K, \forall h \in V \tag{4}$$

$$\sum_{i=0}^{n} \sum_{j=0}^{m} x_{ijk} \leq Q_k \qquad \forall k \in K \tag{5}$$

$$\sum_{j=0}^{n} x_{ijk} \leq 1 \qquad \forall k \in K_i, \forall i \in V_s \tag{6}$$

$$u_i - u_j + n \times x_{ijk} \leq n - 1 \text{for } 1 \leq i \neq j \leq n, k \in K \tag{7}$$

$$u_i \in R \quad \text{ for } 1 \leq i \leq n \tag{8}$$

The objective function (1) minimizes the total travelling distance, where x_{ijk} are binary variables and $x_{ijk} = 1$ if and only if a taxi k visits node j after node i. Constraints (2) and (3) ensures that each node except the origin are visited exactly once. Constraint (4) guarantee the route continuity, every taxi must exit the destination visited and Eq. (5) ensures that the capacity of any taxi is not exceeded. Constraint (6) ensure that each vehicle will leave the station at most once. Eq. (7) avoids subtour and Constraint (8) define the domains of u_i.

3. Iterated Granular Neighborhood Algorithm

The idea of this paper is to show the efficiency and the importance of the extension of the taxi sharing problem towards the taxi sharing with several station. We will show the effectiveness of this contribution by solving a real cases study which has several stations and several travelers. We compare our new contribution by the previous work. In the previous work we group the travelers in stations according to the distance criterion, so each passenger has to go to his nearest station. That's mean we create small instances from large instance and we apply our MILP formulation for each station to solve the previous taxi sharing problem. In this paper, we solve the problem as the MSTSP, we treat all the stations together in order to minimize the sum of the traveling costs related to the performed routes. Since the MSTSP is NP-Hard problem, and the exact techniques can't solve large instances. We adapt our IGNA to solve this new problem.

The proposed algorithm is based on the Iterated Local Search metaheuristic (ILS) [?] with a Granular neighborhood (GN) [?], [?] in the local search phase. The iterated Granular neighborhood Algorithm (IGNA) uses restricted swap neighborhoods, called granular neighborhoods, obtained from a sparse graph which includes all the edges with a cost not greater than a granularity threshold value ϑ, defined by

$$\vartheta = \beta \cdot \frac{z'}{n+m}$$

[?].
The objective of this approach is to obtain high quality solutions within short computing times. The main body of algorithm IGNA considers three parts: In the first part, we construct an initial solution by applying new heuristic, in the second part we calculate the threshold value to eliminate long edges and the third part we apply the iterated swap neighborhood algorithm.

3.1. Initial solution

We construct an initial solution which is able to find good initial solutions within short computing times. We execute the following steps :

- Assign passengers to the stations by using the well known K-means algorithm
- We arrange travelers randomly by generating a random path for each station, starting and returning to the same origin while visiting each vertex exactly once.
- Divide each path into groups so as to avoid exceeding the capacity of each taxi. The partitioning method is sequential follow the logic that each traveler will be affected to a taxi, regardless of the distance traveled.

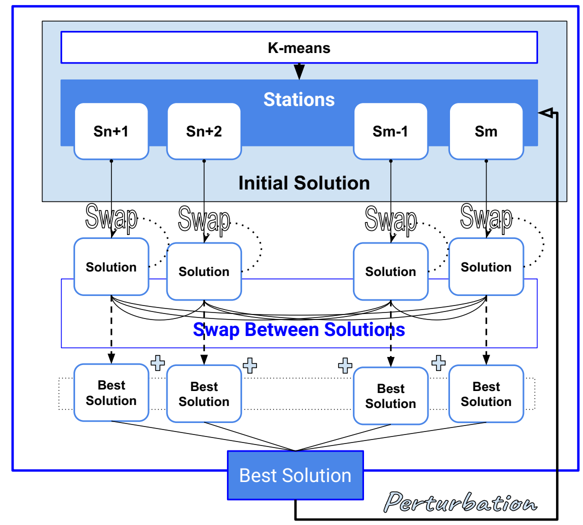

Figure 2. Iterated Granular Neighborhood Algorithm IGNA

3.2. Algorithm Structure

The basic idea of the IGNA is extended from the ILS [?] to perform randomized walks in solution space. This algorithm escape from being trapped in a local minimum by perturbing the local optima. The search in the IGNA starts from an initial solution, commonly generated by a fast heuristic. In the first step, we apply our swap neighborhood to the current solution until the search is stuck in a local optimum. In the second step, an acceptance criteria can determine whether the new solution must replace the current solution or not, whenever a new overall best solution is found in the local search step and has not been accepted before, it replaces the current solution. The third mechanism is to escape from the current local optimum by perturbing the solution. Then, it repeatedly utilizes these three steps to improve this solution. The proposed IGNA is shown in figure 2. The perturbation should be strong enough to get away from the current local optimum, but low enough to exploit knowledge from previous iterations [?].

4. Real Case Study

we did a little investigation to find out the maximum distance that a traveler is ready to walk from his starting point to the station. Most of people agree to walk 5 minutes on feet to get the station, which is equivalent to 500 meters following google maps. In this problem we assume that we have the necessary number of taxis to satisfy all the requests. in a future work, we will take into consideration the real distance of the taxis from the original stations and we add some constraint like a traveler cannot assign to an origin station if the distance between his point of departure and the station is greater than 500 meters. The distance between the departure point of a traveler and his taxi station will not be calculated in the travelling costs, even it has influence on the choice of origin station. Like all countries in the world, each municipality has its property; residential or industrial... Rush hour in Tunisia represents a migration from residential municipality to industrial municipality or vice versa. El Mourouj is a town and commune in the southern suburbs of Tunis in the Ben Arous Governorate, Tunisia. It has 130 K inhabitants as of 2018, making it the most populous commune in the Ben Arous Governorate. The city gradually expanded to cover around 15 km. According to a survey that I did for 1000 inhabitants who are between 25 and 50 years old, 90% of travelers arrived late because of transport. The stations that we have chosen are the most popular stations in this city. In our future work, the choice of stations will depend on the positioning of travelers and taxis, we will apply some techniques of the p-median problem. the criteria for selecting travelers are as follows:

- they travel at the same instant (an interval of 20 minutes)
- people who are used to take an individual taxi and accept to share with other people.
- people who are used to use their car and prefer a shared taxi to minimize the cost and eliminate the cost of parking
- people who match public transport and are looking for a reliable way to travel by one means of transport.

The number of stations is fixed to 4 and the number of travelers is 67. Table 1 shows the solution quality (cost) and the run-time required by our approach for the MSTSP and the MILP to solve the 4 real-like instances of the Taxi Sharing Problem. Our approach save the cost and required less run-time.

Instances	MSTSP		TSP	
	IGNA	Runtime(s)	MILP	Runtime(s)
18	154.6	7.4	43.2	3.1
14			39.5	3.8
19			62.0	5.4
16			34.8	4.6
Total			179.5	16.9

5. Conclusion

In this paper we propose Iterated Granular Swap Neighborhood Algorithm to solve the Multi-Station Taxi Sharing Problem. We compared this approach with the previous Taxi sharing problem, and we can observe in this real-case that the cost obtained by the MSTSP is lower than the cost obtained by TSP. In our future work we will try to reduce the time complexity by dynamic and parallel techniques. We will try to extend the optimization problem by creating new formulation, adding the delay as a second objective and impose the distance as new constraint.

Financial risk assessment using neural network: case of Tunisian banking sector

Fadwa Srasra

ENSTAB UCAR

Adnen Arbi

ENSTAB UCAR

Amira Kaddour

ENSTAB UCAR

Since the global financial crisis, concerns have risen over whether policy makers are able to maintain financial stability. Nowadays, assessing the financial risk of banks had gained more prominence. There has been focus around how risk is being detected, measured and managed. At the same time, machine learning has been established as one of the most important tools of risk management. Many efforts have been made for providing an efficient model for more accurate evaluation and classification. Neural networks have been considered because of its high flexibility. Building a neural network enables a more accurate risk model by identifying complex nonlinear patterns within large datasets. The predictive power of these models is enhancing over time. The aim of this project is to assess the financial situation of a bank using neural networks.

Criteria weight elicitation of fuzzy ARAS-H method for healthcare waste treatment technologies assessment

M. Ghram , H. M. Frikha

Abstract—Healthcare waste management (HCW) is considered nowadays to be major problem especially in developing countries such as Tunisia. However, choosing the appropriate HCW technique is not an easy task. Therefore, the Multi-Criteria Decision Making (MCDM) methods find naturally their place to solve such a problem. In this paper, we address the choice of the best waste treatment technology for care activities through the fuzzy ARAS-H method (F-ARAS-H). Howbeit, developing the F-ARAS-H method requires criteria weight elicitation. Getting them directly from the decision maker (DM) makes the results unreliable. So, to reduce the subjectivity of the data, we thought of preference disaggregation technique. It involves the DM in the weight elicitation process by taking some preference information. Thus, the process of weight elicitation is considered to be a set of mathematical programs which are solved by LINGO software. Thereupon, to choose the best HCW treatment technology in Tunisia, several alternatives which present different technologies to treat HCW (Sterilization by autoclave, microwave disinfection, landfill, chemical disinfection in situ, encapsulation, physio- chemical disinfection off situ, NEWSTER, incineration) are evaluated according to nine elementary criteria (net cost per ton, waste residuals, noise, release with health effects, reliability, treatment effectiveness, occupational hazards public acceptance and employment generation).

Keywords —Multi-Criteria Decision Making, Healthcare waste management, criteria weights, F-ARAS-H, mathematical programming.

1 INTRODUCTION

Due to the rapid industrialization and population growth, HCW have been increasing worldwide [1]. As a matter of fact, the World Health Organisation [2] classified healthcare wastes into nine categories (infectious waste, pharmaceutical waste, chemical waste, wastes with high content of heavy metals, pressurized containers, pathological waste, sharps, genotoxic waste and radioactive waste). In tunisia, 24 HCW management societies are authorized by the ministry of environment and local affairs. Their mission resides in the collection, transport and treatment of wastes generated from care activities. In this paper, we are interested in the treatment of HCW. Actually, the Tunisian legislation authorizes the following HCW treatment technologies (Sterilization by autoclave, microwave disinfection, landfill, chemical disinfection in situ, encapsulation, physio- chemical disinfection off situ, treatment by NEWSTER process and incineration). Thus, these HCW treatment technologies are evaluated according to a set of intermediate criteria (economic, environmental, technical and social and their related sub-ones (net cost per ton, watste residuals, noise, release with health effects, reliability, treatment effectiveness, occupational hazards and public acceptance).

The paper is divided into five sessions. In section 2, a state of the art survey on criteria wight elicitation within fuzzy MCDM methods in HCW management problem is given. In Section 3, the criteria weight elicitation of the fuzzy ARAS-H method model is described. In section 4, an empirical study conducted in Sfax, Tunisia will be presented to discuss the feasibility of the proposed model. In section 5, a conclusion with our main perspectives will be given.

2 LITERATURE REVIEW

HCW presents a major and a crucial environmental problem namely in developing countries. Inappropriate HCW treatment causes pollution, rodents, contamination of diseases like hepatitis. For that reason, it is very important to separate healthcare wastes from domestic and industrial ones to protect the municipal workers mostly.
So to improve HCW management, some studies focused on the selection of the best HCW treatment technology using fuzzy multi-level hierarchical structure of criteria methods. However, most of these methods require fixing criteria weights in order to be implemented. In theliterature, very few authors worked on criteria weight elicita-

- *Maroua Ghram is with laboratory "Optimisation, Logistique et Informatique Décisionnelle" (OLID), University of Sfax, Higher Institute of Industrial Management of Sfax Road of Tunis km 10.5, 3021, Sfax, Tunisia, maroua.ghram@gmail.com, +21653352046, ORCID: 0000-0002-6798-5209.*
- *Hela Moalla Frikha is with laboratory "Optimisation, Logistique et Informatique Décisionnelle" (OLID), University of Sfax, Higher Institute of Industrial Management of Sfax Road of Tunis km 10.5, 3021, Sfax, Tunisia, hela_frikha_moalla@yahoo.fr.*

tion within fuzzy hierarchical methods. To start with, [3], [4] used the Ordered Weighted Averaging (OWA) operator to aggregate DM's opinions [5]. To determine the weights of the OWA operator, the authors used fuzzy linguistic quantifiers. On the other hand, [6] determined criteria weights using the AHP method [7]. Additionally, [8] used 2-tuple DEMATEL [9] to highlight the relationship between HCW treatment technologies criteria and therefore building the influential relation map among them. The aim is to determine influential criteria weights while considering the hierarchy of criteria. Correspondingly, our aim is to elicit criteria weights of F-ARAS-H method. Thus, we propose a new procedure of weight elicitation via mathematical programming which takes into account the DM's preferences.

3 The Proposed Model for Fuzzy ARAS-H Criteria Weight Elicitation

The F-ARAS-H method is an extension of the ARAS-H one in the context of a fuzzy environment. In fact, the ARAS-H method is on its turn an extension too of the classical ARAS method [10] in the case of hierarchically structured criteria [11]. Therefore, in order to develop the F-ARAS-H method, we need criteria weights of the hierarchy tree. Thus, we suggested a new procedure of criteria weight determination within ARAS method through mathematical programming [12]. Also, we developed a set of mathematical programs to elicit ARAS-H criteria weights [13]. Likemanner, we proceed in this paper to criteria weight inference of F-ARAS-H method through mathematical programming. The DM has to introduce some preference information which report his value system. The process of weight elicitation is considered to be a set of mathematical programs. Their number depends on the number of the levels in the hierarchy. Henceforth, we adopt a bottom-up approach in criteria weight inference. First we start by the last level *l*. The aim is to obtain all elementary criteria weights from preference relations given by the DM on some pairs of alternatives according to intermediate criteria of the upward level, some weight partial pre order and some comparisons between differences of criteria weights. This process is generated until we reach the root criterion. So, our aim is to elicit F-ARAS-H criteria weights at each node of the hierarchy tree. As a matter of fact, we adopted the preference disaggregation technique in the weight inference procedure. The principle is as follow. After the normalization of the performance matrix given by the DM, we proceed in the modeling of the first linear program. The objective function consists in maximizing the sum of the slack variables between the pairs of alternatives. As we said before, the constraints concern the comparisons of the differences of adjacent weights, some weight partial pre order, thresholds on slack variables and criteria weights. Also, we must consider criteria weight normalization constraint.

The main contribution of this model is that the DM interfers partially in the weight elicitation process through his preference information which reveals his value system.

4 An Empirical Example

In this case study, we intend to elicit HCW treatment technologies' criteria weights using F-ARAS-H. Thus, the criteria are organized into a hierarchy tree as presented in Fig. 1. Indeed, the set of elementary criteria are at the last level of the hierarchy tree. Hence, the DM can directly evaluate the alternatives through these criteria listed as follow:

The set of elementary criteria (*EL*) is defined as follow:
g1,1,1: Cost (to be minimized)
g1,2,1: Waste residuals (to be minimized)
g1,2,2: Noise (to be minimized)
g1,2,3: Release with health effects (to be minimized)
g1,3,1: Reliability (to be maximized)
g1,3,2: Effectiveness (to be maximized)
g1,3,3: Occupational hazards (to be minimized)
g1,4,1: Public Acceptance (to be maximized)
The set of intermediate criteria (I_G) is:
g1,1: Economic
g1,2: Environmental
g1,3: Technical
g1,4: Social
g1: root criterion
The set of alternatives (A) is listed as follow:
A1: Sterilization by autoclave
A2: Microwave disinfection
A3: Treatment by NEWSTER process
A4: Incineration
A5: Chemical disinfection in situ
A6: Physio- chemical disinfection off situ
A7: Encapsulation
A8: Landfill

Remark: The landfill can be operated only after the trivialization of hazardous waste by eliminating the infectious risk and the physical one of the HCW with infectious risk.

The chemical disinfection in situ, encapsulation and physio- chemical disinfection off situ concern only HCW with chemical risk.

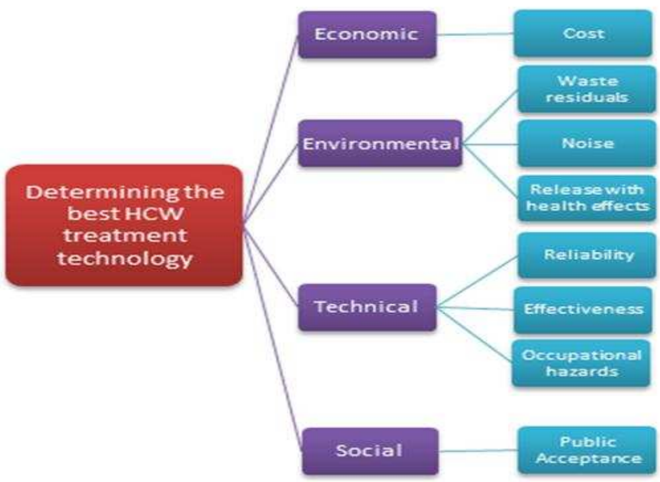

Fig. 1. The hierarchy structure of criteria

TABLE 1

FUZZY PERFORMANCE MATRIX

A \ EL	$g_{1,1,1}$	$g_{1,2,1}$	$g_{1,2,2}$	$g_{1,2,3}$	$g_{1,3,1}$	$g_{1,3,2}$	$g_{1,3,3}$	$g_{1,4,1}$
A1	H	H	L	L	H	H	ML	H
A2	VH	H	ML	L	H	H	M	MH
A3	H	H	M	L	H	H	ML	VH
A4	VH	VL	M	H	VH	VH	MH	L
A5	MH	H	L	H	M	M	MH	ML
A6	H	MH	L	L	H	MH	H	M
A7	MH	VH	M	ML	M	M	ML	M
A8	L	H	ML	MH	M	L	MH	VL
W_j	0,151	0,125	0,061	0,159	0,125	0,144	0,137	0,098

TABLE 2

LINGUISTIC VARIABLES

Linguistic variable	Fuzzy numbers
Very Low (VL)	(0,0,1)
Low (L)	(0,1,3)
Moderate Low (ML)	(1,3,5)
Moderate (M)	(3,5,7)
Moderate High (MH)	(5,7,9)
High (H)	(7,9,10)
Very High (VH)	(9,10,10)

Besides the performance matrix, the DM is asked to give some preference relations between some pairs of alternatives according to intermediate criteria.

On economic family criteria, the DM prefers NEWSTER process on microwave (i.e A3 ≻ A2).

On environmental family criteria, the DM prefers microwave on incineration (i.e A2 ≻ A4).

On technical family criteria, the DM prefers Physio-chemical disinfection off situ on chemical disinfection in situ (i.e A6 ≻ A5).

Finaly, on social family criteria, the DM prefers NEWSTER process on landfill (i.e A3 ≻ A7).

Also, the DM provides us other information type, that is to say:

$w_{121} \geq w_{122}$

$w_{132} \geq w_{131}$

$w_{141} \geq w_{111}$

$w_{141} - w_{111} \geq w_{133} - w_{131}$

$w_{132} - w_{122} \geq w_{121} - w_{123}$

In addition, we ask the DM to fix thresholds of elementary criteria weights as well as of the slack variables.

Then, we integrate those preference relations as constraints into the first linear program. Its resolution by the LINGO software give us all elementary criteria weights as shown in table 1 (W_j). At this stage, we construct the weighted normalized decision matrix in which we calculate the fuzzy optimality values and the utilty degrees.

Subsequently, we rank the alternatives from the best one to the worst with respect to intermediate criteria (economic, environmental, technical and social) as shown in figures Fig. 2., Fig. 3., Fig. 4. and Fig. 5. Respectively.

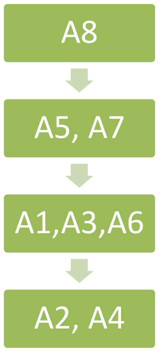

Fig. 2. The partial pre-orders obtained from Economic family criteria

Fig. 3. The partial pre-orders obtained from Environmental family criteria

Fig. 4. The partial pre-orders obtained from Technical family criteria

Fig. 5. The partial pre-orders obtained from Social family criteria

In order to determine sub-criteria weights, we take a preference relation between a pair of aternatives according to the root criterion. The DM precises that sterilization by autoclave is preferred to landfill (i.e A1 ≻ A8). Also, the DM provides us other information type:

$w_{12} \geq w_{14}$

$w_{11} \geq w_{13}$

$w_{12} - w_{14} \geq w_{11} - w_{13}$

$w_{12} - w_{11} \geq w_{13} - w_{14}$

In addition, we ask the DM to fix thresholds of elementary criteria weights as well as of the slack variables.

Then, we integrate those preference relations as constraints into the second linear program. Its resolution by the LINGO software give us the intermediate criteria weights. Thus, the weights of economic, technical, environmental and social criteria are: w_{11}=0.246, w_{12}=0.315, w_{13}=0.234 and w_{14}=0.205 respectively.

The final step consists in constructing the complete preorder of the alternatives (Fig. 6.).

Fig. 6. The complete pre-order of alternatives

The final ranking of alternatives according to the root criterion is: A1 ≻ A2 ≻ A7 ≻ A3 ≻ A8 ≻ A4 ≻ A6 ≻ A5.

So, we can conduct that the sterilization by autoclave (A1) present the best HCW treatment technology whereas chemical disinfection in situ is considered to be the worst. In fact, sterilization by autoclave present major advantages. First, it can sterilize a large number of HCW types (sharps included). Second, it is considered to be risk free for the environment. Third, it is an economic technique.

5 Conclusion

In this paper, we presented a procedure for criteria weight elicitation of F-ARAS-H method. The aim of this procedure is to overcome the imprecise weighting through preference programming which takes into account the DM's preferences. Therefore, the DM can express his preference information not only in a comprehensive way but also in a partial way that is considering preference information with respect to each criterion in the hierarchy tree. Thus, he can analyze the obtained rankings according to each criterion apart to detect the anomalies of the given problem.

References

[1] R. Mato and G. R. Kassenga, 'A study on problems of management of medical solid wastes in Dar es Salaam and their remedial measures', Resour. Conserv. Recycl., vol. 21, no. 1, pp. 1–16, 1997.

[2] A. Prüss-Üstün, E. Giroult, P. Rushbrook, and W. H. Organization, Safe management of wastes from health-care activities. World Health Organization, 1999.

[3] M. Dursun, E. E. Karsak, and M. A. Karadayi, 'Assessment of health-care waste treatment alternatives using fuzzy multi-criteria decision making approaches', Resour. Conserv. Recycl., vol. 57, pp. 98–107, 2011.

[4] *H. C. Liu, J. Wu, and P. Li, 'Assessment of health-care waste disposal methods using a VIKOR-based fuzzy multi-criteria decision making method', Waste Manag., vol. 33, no. 12, pp. 2744–2751, 2013.*

[5] *R. R. Yager, 'On ordered weighted averaging aggregation operators in multicriteria decisionmaking', IEEE Trans. Syst. Man Cybern., vol. 18, no. 1, pp. 183–190, 1988.*

[6] *M. A. A. Samah, L. A. Manaf, A. Z. Aris, and W. Nor, 'Solid waste management: analytical hierarchy process (AHP) ppplication of selecting treatment technology in Sepang Municipal council, Malaysia', Curr. World Environ., vol. 6, no. 1, p. 1, 2011.*

[7] *T. L. Saaty, 'The analytic hierarchy process McGraw-Hill', N. Y., vol. 324, 1980.*

[8] *H. C. Liu, J.-X. You, C. Lu, and Y.-Z. Chen, 'Evaluating health-care waste treatment technologies using a hybrid multi-criteria decision making model', Renew. Sustain. Energy Rev., vol. 41, pp. 932–942, 2015.*

[9] *Z. P. Fan, W.-L. Suo, and B. Feng, 'Identifying risk factors of IT outsourcing using interdependent information: An extended DEMATEL method', Expert Syst. Appl., vol. 39, no. 3, pp. 3832–3840, 2012.*

[10] *E. K. Zavadskas and Z. Turskis, 'A new additive ratio assessment (ARAS) method in multicriteria decision-making', Technol. Econ. Dev. Econ., vol. 16, no. 2, pp. 159–172, 2010.*

[11] *M. Ghram and H. M. Frikha, 'Multiple Criteria Hierarchy Process within ARAS method', in 2019 6th International Conference on Control, Decision and Information Technologies (CoDIT), 2019, pp. 995–1000.*

[12] *M. Ghram and H. M. Frikha, 'A New Procedure of Criteria Weight Determination Within the ARAS Method', Mult. Criteria Decis. Mak., vol. 13, pp. 56–73, 2018.*

[13] *M. Ghram and H. M. Frikha, A new procedure of criteria weight determination for ARAS-H method. Djerba-Tunisia, 2019.*

Interval-valued intuitionistic fuzzy CODAS-SORT method: A case study on natural resources in Tunisia

A. Ouhibi, H. Frikha

Abstract— In this study, a fuzzy extension of CODAS-SORT method is developed to deal with multi-criteria decision-making problems in an uncertain environment In fact, in CODAS SORT, the assignment rules are based on the use of two measures. The first measure is related to the Euclidean distance and the second one is the Taxicab distance. The assignment rules are based on the difference between these two distances. However, the Euclidean and Taxicab distances are defined in a crisp environment and we cannot use them in fuzzy problems. The aim of this study is to develop an intuitionistic fuzzy CODAS-SORT method, namely Interval-Valued Intuitionistic Fuzzy CODAS-SORT (IVIF-CODAS-SORT) taking into consideration the hesitancy of decision makers based on both Euclidean and Taxicab distances according to the negative-ideal point. We have validated our developed method by an application classifying 24 towns of Tunisia into five classes, representing areas with different Natural resources. This research provides appropriate results with respect to the development of sorting models in the form of outranking relations.

Index Terms— Multi-criteria decision aid, Sorting method, CODAS SORT, Interval-Valued Intuitionistic Fuzzy,

1 Introduction

In recent years, multi-criteria decision aid (MCDA) approaches have grown significantly. They provide some answers to the problem of evaluation of alternatives according to multiple contradictory points of view. MCDA deals with three types of decision-making problems: choice, ranking, and sorting [1]. The choice problems consist in choosing a subset of better alternatives from those envisaged; the ranking problems consist in classifying all the alternatives from the best to the worst while the sorting problems consist in assigning each alternative to one of the categories ordered and predefined by the decision maker (DM). The first two problems have been widely studied and applied in several fields, whereas relatively little works have been devoted to the sorting problems.

In MCDA, the allocation of alternatives in predefined classes is a classic problem encountered in several fields such as medicine, financial and economic management, technical diagnosis and production systems.

To tackle sorting problems, several approaches have been proposed including outranking methods such as ELECTRE-TRI [1] [2], FlowSort [3], multi-attribute utility theories such as UTADIS [4], the rough sets [5], etc. These methods differ in the way the categories are defined a priori (i.e. by limiting profiles, thresholds, decision rules, etc.). For this reason, the CODAS-SORT [6] method based on CODAS [7] (Combinative Distance-based Assessment) ranking multi-criteria method has been developed.

Uncertainty is one of the important factors that can affect the process of decision-making. Fuzzy MCDM approaches have been designed to deal with the uncertainty of decision-making problems. Fuzzy Set Theory is an extension of classical set theory. However there is a relaxation of the concept of membership that occurs in the classical theory [6]. According to [7], a fuzzy set is a class of objects with a continuum of grades of membership. Such a set is characterized by a membership function, which assigns a grade of membership ranging between zero and one to each object. That is, in fuzzy set there is no well-defined boundary between those elements that belong to a group and those that do not [4].

Fuzzy set theory is an excellent tool to capture the uncertainty in humans' thoughts and linguistic assessments. Ordinary fuzzy sets have been extended to new types offuzzy sets in order to define membership and hesitancy degrees of decision makers. The new extensions of ordinary fuzzy sets are type-2 fuzzy sets, intuitionistic Fuzzy Sets (IFSs), Hesitant Fuzzy Sets (HFSs) [8], Pythagorean fuzzy sets (PFSs) [9], and Neutrosophic sets (NSs) [10]. Among all these types, IFSs are the most popular fuzzy sets and PFSs and NSs are the extensions of IFSs. Atanassov [11] proposed the concept of IFS. An IFS is represented by a membership degree and a non-membership degree together. Later, Atanassov and Gargov [12] generalized IFSs to interval-valued intuitionistic fuzzy sets. In this paper, we develop an interval-valued intuitionistic fuzzy extension of the CODAS-SORT method combining the interval-valued intuitionistic fuzzy set theory and CODAS-SORT method.

- *A. Ouhibi is with University of Sfax, Higher Institute of Industrial management of Sfax, Road of Tunis km 10.5, 3021, Sfax, Tunisia (corresponding author to provide phone: +21621464321; e-mail: abirouhibi22@gmail.com).*
- *H. Frikha is with University of Sfax, Higher Institute of Industrial management of Sfax, Road of Tunis km 10.5, 3021, Sfax, Tunisia. (E-mail: hela_frikha_moallla@yahoo.com).*

In the rest of the paper is organized as follows: In section 2, preliminaries of the interval-valued intuitionistic fuzzy sets are given. In Section 3, the proposed interval-valued intuitionistic fuzzy CODAS (IVIF-CODAS-SORT) method are given. In Section 4, an application is given for natural ressources in Tunisia. In Section 5, conclusion and suggestions for further research are presented.

2 Intervale-Valued Intuitionistic Fuzzy Sets

In this sub-section, we will give the preliminaries on interval-valued intuitionistic fuzzy (IVIF) numbers and steps of the methodology.

Definition 1. Let X be a non-empty set. An IVIF set in X is an object A given as in Equation (1) [12]:

$$A = \{\langle x, [\mu_A^-, \mu_A^+], [\upsilon_A^-, \upsilon_A^+]\rangle, x \in X\} \quad (1)$$

where $0 \leq \mu_A^-, \mu_A^+ \leq 1$ for every $x \in X$.

Definition 2. Let $A = ([\mu_A^-, \mu_A^+], [\upsilon_A^-, \upsilon_A^+])$ and $B = ([\mu_B^-, \mu_B^+], [\upsilon_B^-, \upsilon_B^+])$ be two IVIFS numbers [13]:

$$A \oplus B = ([\mu_A^- + \mu_B^- - \mu_A^- \mu_B^-, \mu_A^+ + \mu_B^+ - \mu_A^+ \mu_B^+], [\upsilon_A^- \upsilon_B^-, \upsilon_A^+ \upsilon_B^+]) \quad (2)$$

$$A \oplus B = ([\mu_A^- \mu_B^-, \mu_A^+ \mu_B^+], [\upsilon_A^- + \upsilon_B^-, -\upsilon_A^- \upsilon_B^-, \upsilon_A^+ + \upsilon_B^+ - \upsilon_A^+ \upsilon_B^+]) \quad (3)$$

Definition 3. Let $A = ([\mu_A^-, \mu_A^+], [\upsilon_A^-, \upsilon_A^+])$ and $B = ([\mu_B^-, \mu_B^+], [\upsilon_B^-, \upsilon_B^+])$ be two IVIFS numbers.

The distance between these two IVIF numbers is obtained by Hamming distance as in Equation (4) [14]:

$$HD = \frac{1}{4} \sum(|\mu_A^- - \mu_B^-| + |\mu_A^+ - \mu_B^+| + |\upsilon_A^- - \upsilon_B^-| + |\upsilon_A^+ - \upsilon_B^+)| \quad (4)$$

Definition 4. Let $A = ([\mu_A^-, \mu_A^+], [\upsilon_A^-, \upsilon_A^+])$ is an IVIF number. Defuzzification formula ($\mathfrak{D}(x)$) for A is given in Equation (5) [15].

$$\mathfrak{D}(x) = \frac{\mu_A^- + \mu_A^+ + (1-\upsilon_A^-) + (1-\upsilon_A^+) + \mu_A^- \mu_A^+ \sqrt{(1-\upsilon_A^-)1-\upsilon_A^+}}{4} \quad (5)$$

3 The Proposed IV-IF-CODAS-SORT Method

Ghorabaee et al. [7] presented CODAS method for complex MCDM problems. To determine the desirability of an alternative, this method uses the Euclidean distance as the primary and the Taxicab distance as the secondary measure, and these distances are calculated according to the negative-ideal point. The alternative which has greater distances, is more desirable in the CODAS method. Some nmerical examples are given to illustrate the steps of the proposed method.

Ouhibi and Frikha [6] extend a new sorting method based on CODAS. The CODAS-SORT method is simple to process easy to use especially for decision-makers.The assignment rules are based on the use of two measures. The first measure is related to the Euclidean distance and the second one is the Taxicab distance. The assignment rules are based on the difference between these two distances. However, the Euclidean and Taxicab distances are defined in a crisp environment and we cannot use them in intuitionistic fuzzy problems. The aim of this study is to develop an interval-valued intuitionistic fuzzy extension of the CODAS method. In order to reach this aim, we use the fuzzy weighted Euclidean distance and the fuzzy weighted Hamming distance, which were presented by Li [16], instead of the crisp distances. Suppose that we have n alternatives, m criteria and q decision-makers (DMs).

In a sorting problem, the decision maker wants to assign a set of actions $A = \{a_1,..., a_n\}$ to K predefined categories $C_1,C_2,...,C_K$. There is a complete order on the categories such that category C_1 is the best and C_K is the worst category. Each action is evaluated on q criteria g_j (j = 1,..., q).

In the CODAS-Sort method, the K categories are predefined either by limiting profiles or central profiles. In the former case, each category is defined by an upper and a lower boundary.

In the IVIF-CODAS-SORT, firstly we construct IVIF decision matrix and the IVIF profiles matrix. After that, we determine the fuzzy negative ideal solution of the decision and profiles matrix. Then, we calculate the IVIF weighted Euclidean and hamming distances of alternatives from the fuzzy negative-ideal solution. Following, we calculate the IVIF weighted Euclidean and hamming distances of profiles from the fuzzy negative-ideal solution.

Next, we determine relative assessment matrix, which is the difference between the Euclidean and hamming distances.Finally, we assign alternatives to categories: To assign an alternative to one of the predefined categories, there are two ways that depend on the type of available profile provided by the decision maker: Central and limiting profiles.

4 Application

Tunisia is an African nation found on the northern part of the continent. The Tunisian economy is considered one of the top economies in the region with a GDP of $41.662 billion in 2018. The success of the Tunisian economy can be attributed to the proper utilization of the country's natural resources as well as the economic policies put in place by the Tunisian government. Some of Tunisia's most important natural resources include the country's beautiful scenery, petroleum, and arable land among others.

Natural resources are components that exist in the world without the input of humans. These natural resources are diverse ranging from renewable resources to non-renewable resources, living to non-living resources, tangible to intangible resources. Natural resources are essential to the survival of humans and all other living organisms. All the products in the world use natural resources as their basic component, which may be water, air, natural chemicals or energy. The high demand for natural resources around the world has led to their rapid depletion. As a result, most

nations are pushing for proper management and sustainable use of natural resources.
Natural resources could be classified into different categories such as renewable and non-renewable resources, biotic and abiotic resources, and stock resources.
Five criteria are used to classify Tunisian's towns on the Natural resources: natural vegetation (c_1), wind energy (c_2), weather conditions (c_3), water (c_4), and solar energy (c_5). Therefore, Class 1 is considered as the best and then Classes 2 to 4 are ranked respectively.
The scores of 24 tows of Tunisia according to the criteria were collected and entered into the decision matrix (Tab. 2).

Table 1: linguistic terms

Linguistic terms	Corresponding IVIFNs
Very high (VH)	([0.75, 0.95], [0.00, 0.05])
High (H)	([0.50, 0.70], [0.05, 0.25])
Medium (M)	([0.30, 0.50], [0.20, 0.40])
Low (L)	([0.05, 0.25], [0.50, 0.70])
Very low (VL)	([0.00, 0.05], [0.75, 0.95])

Step 1. We construct the IVIF decision matrix of decision-maker as in Table 2 by using linguistic terms in Table 1.

Table 2: Decision matrix

	C_1	C_2	C_3	C_4	C_5
A_1	L	L	H	H	M
A_2	L	VL	VH	VH	L
A_3	VL	L	H	H	M
A_4	L	VL	VH	VH	H
A_5	L	VH	L	VL	H
A_6	VL	H	L	L	L
A_7	L	VL	VH	VH	M
A_8	VH	M	M	M	VL
A_9	VH	M	M	M	L
A_{10}	VL	VH	VL	VL	VH
A_{11}	VH	L	H	M	VL
A_{12}	H	M	M	M	H
A_{13}	L	L	H	M	M
A_{14}	VH	VH	L	VL	H
A_{15}	VL	M	M	M	H
A_{16}	H	L	H	VH	VH
A_{17}	H	M	L	L	H
A_{18}	M	H	L	L	VL
A_{19}	H	L	H	VH	L
A_{20}	H	L	M	M	H
A_{21}	M	VH	VL	VL	H
A_{22}	VL	VH	VL	VL	VH
A_{23}	VL	L	H	M	M
A_{24}	L	L	H	M	M

Step 2. We construct the IVIF profiles matrix of decision-maker as in Table 3 by using linguistic terms in Table 1.

Table 3: Profiles matrix

	C1	C_2	C_3	C_4	C_5
P_1	VH	VH	H	VH	L
P_2	H	H	M	H	M
P_3	L	M	L	M	H
P_4	VL	H	VL	L	VL

Step 3. Calculate the weighted Euclidean (EDi) and weighted Hamming (HDi) distances of alternatives from the fuzzy negative-ideal solution.

Table 4: Table of Euclidien and Hamming distances (actions)

	Distances	
	E_{a_i}	H_{a_i}
A_1	0.125	0.7
A_2	0.125	0.5
A_3	0.125	0.7
A_4	0.29	1
A_5	0.3	0.3
A_6	0.05	0.3
A_7	0.36	1.2
A_8	0.323	0.9
A_9	0.29	1
A_{10}	0.05	0.79
A_{11}	0.125	0.5
A_{12}	0.125	0.7
A_{13}	0.125	0.7
A_{14}	0.3	0.5
A_{15}	0.29	1
A_{16}	0.79	0.7
A_{17}	0.79	0.7
A_{18}	0.28	1
A_{19}	0.29	1
A_{20}	0.7	0.7
A_{21}	0.323	0.9
A_{22}	0.05	0.3
A_{23}	0.05	0.3
A_{24}	0.11	1

Step 4. Calculate the weighted Euclidean (E_{b_i}) and weighted Hamming (H_{b_i}) distances of profiles from the fuzzy negative-ideal solution.

Table 5: Table of Euclidien and Hamming distances (profiles)

	Distances	
	E_{b_i}	H_{b_i}
P_1	0.19	0.29
P_2	0.05	0.17
P_3	0.17	0.3
P_4	0.125	0

Step 7. Determine relative assessment matrix and calculate the assessment score of each alternative and profiles.

Table 6: Relative evaluation matrix

	P_1	P_2	P_3	P_4
A_1	-0.065	0.075	-0.045	0
A_2	-0.065	0.075	-0.045	0
A_3	-0.065	0.075	-0.045	0
A_4	0.1	0.24	0.12	0.165
A_5	0.11	0.05	0.13	0.175
A_6	-0.14	0	-0.12	-0.075
A_7	0.17	0.31	0.19	0.235
A_8	0.18	0.12	0.153	0.198
A_9	0.1	0.24	0.12	0.165
A_{10}	-0.14	0	-0.12	-0.075
A_{11}	-0.065	0.075	-0.045	0
A_{12}	-0.065	0.075	-0.045	0
A_{13}	-0.065	0.075	-0.045	0
A_{14}	0.11	0.25	0.13	0.175
A_{15}	0.1	0.24	0.12	0.165
A_{16}	0.6	0.74	0.62	0.665
A_{17}	0.133	0.273	0.153	0.198
A_{18}	0.15	0.25	0.11	0.155
A_{19}	0.1	0.24	0.12	0.165
A_{20}	0.51	0.65	0.53	0.575
A_{21}	-0.065	0.075	-0.045	0
A_{22}	-0.14	0	-0.12	-0.075
A_{23}	-0.14	0	-0.12	-0.075
A_{24}	-0.08	0.06	-0.06	-0.015

Step 9. According to the decreasing values of assessment scores, we can rank the alternatives. The alternative with the highest assessment score is the most desirable alternative.

Table 7: the final classification of the actions

Actions	Categories
Class 1	A_4, A_7, A_9 ,A_{14} ,A_{15} ,A_{16} ,A_{17} ,A_{19} ,A_{20}
Class 2	A_1 , A_2 , A_3, A_5 ,A_8, A_{11}, A_{12}, A_{13}, A_{21}
Class 3	A_6 A_{10} A_{18} , A_{22} , A_{23} A_{24}
Class 4	-

5 Discussion

The IVIF CODAS-Sort method, proposed in this paper, pertains to the extension of the classic CODAS-SORT method in order to sort the alternatives. In the proposed method, the profile and reference points determine a range from the best to the worst values independently from the data. Application of the proposed approach was demonstrated by classifying 24 towns of Tunisia into four classes (but none of the towns fits into Classe 4).

The results obtained by the IVIF-CODAS-Sort give credence to its success, because the results of sorting confirm our and specialists' evaluation of the towns. This research provides appropriate results with respect to the development of sorting models in the form of outranking relations. The model, proposed by this study, is applicable to the other sorting methods such as ELECTRE-Tri, Flowsort, etc

6 CONCLUSION

It is a quite hard process since it includes several types of conflicting and intangible criteria. Decision makers generally prefer linguistic assessments rather than exact numerical assessments because of vagueness and impreciseness in the decision problem. Fuzzy set theory presents an excellent tool to capture the vagueness and uncertainty existing in decision making problems. One of the most popular extensions of ordinary fuzzy sets is IFSs. We proposed IVIF-CODAS-SORT method in order to consider hesitancy parameter in decision making processes. For further research, we suggest other extensions of ordinary fuzzy sets such as Pythagorean fuzzy sets, hesitant fuzzy sets, neutrosophic sets . The outcomes of those new extensions can be compared with the ones of this paper

REFERENCES

[1] Dias J, Jose Figuiera (2010) Electre Tri-C A multiple criteria sorting method based on characteristic reference actions. Eur J Oper Res 204(3):565–580

[2] Wei Y (1992) ELECTRE TRI. Document du Lamsade, Université Paris-Dauphine, Aspects méthodologiques et manuel d'utilisation 74

[3] Nemery Ph, Lamboray C (2008) FlowSort: a flow-based sorting method with limiting and central profiles. TOP 16:90–113

[4] Zopounidis Doumpos M (1999) Business failure prediction using UTADIS multicriteria analysis. J Oper Res Soc 50–11:1138–1148

[5] Pawlak Z (1982) Rough sets. Int J Comput Inf Sci 11:341–356

[6]

[7] M.Keshavarz Ghorabaee, E.K. Zavadskas, Z .Turskis and J. Antucheviciene, A new combinative distance-based assessment (CODAS) method for multi-criteria decision-making, Economic Computation & Economic Cybernetics Studies & Research 50(3) (2016), 25–44.

[8] O.Senvar, I.Otayand E.Bolturk, Hospital site selection via hesitant fuzzy TOPSIS, IFAC-Papers on Line 49 (12) (2016), 1140–1145.

[9] S.C¸. Onar, B. Oztaysi and C. Kahraman, Multicriteria evaluation of cloud service providers using pythagorean fuzzy TOPSIS, Journal of Multiple-Valued Logic and Soft Com-puting 30(2-3) (2018), 263–283.

[10] E. Bolturk and C. Kahraman, A novel interval-valued537 neutrosophic AHP with cosine similarity measure, Soft538 Computing (2018), 1–18.

[11] K.T. Atanassov, Intuitionistic fuzzy sets, Fuzzy sets and577 Systems 20(1) (1986), 87–96

[12] K.T. Atanassov and G. Gargov, Interval-valued intuitionistic fuzzy sets, Fuzzy sets and Systems 31(3) (1989), 343–349

[13] Z. Xu, Methods for aggregating interval-valued intuitionistic fuzzy information and their application to decision making, Kongzhi Yu Juece/Control and Decision 22(2) (2007), 215–219.

[14] L. Abdullah and W.K. Ismail, Hamming distance in intuitionistic fuzzy sets and interval-valued intuitionistic fuzzy sets: A comparative analysis, Advances in Computational Mathematics and its Applications 1(1) (2012), 7–11.

[15] A. Karasan and C. Kahraman, A noval intuitionistic fuzzy dematel – anp – topsis integrated methodology for freight village location selection, Journal of Intelligent & Fuzzy Systems (2017), 1–18.

[16] Li, D.-F. 2007. Compromise ratio method for fuzzy multi-attribute group decision making, Applied. Soft Computing 7 (3): 807–817.

The Triangular Intuitionistic Fuzzy Extension of the CODAS Method for Solving Multi-Criteria Group Decision Making

Fedia Daami Remadi, Hela Moalla Frikha

***Abstract*— Crisp values are insufficient to model real-life situations and vague concepts are frequently represented in multicriteria decision aid. Intuitionistic fuzzy sets are more suitable to deal with uncertainty than other generalized forms of fuzzy sets. Furthermore, to avoid project failures, involving the significant group of experts should be essentially accounted for selecting the optimal solution. As results, this paper develops an extended CODAS method for addressing multiple criteria group decision-making problems in the framework of Triangular intuitionistic fuzzy sets. The rating of each alternative is described by linguistic terms and converted to triangular intuitionistic fuzzy numbers. To validate our extension, an illustrative example of green material selection of companies in agri-food sector is presented.**

Keywords—CODAS method, Multicriteria group decision making, Triangular Intuitionistic Fuzzy Numbers

I. Introduction

Multi-criteria decision making (MCDM) is the process of structuring and solving decision problems when multiple conflicting criteria are deployed. It is one of the most important parts of management science and operations research. It provides a wide arsenal of methodologies and techniques since the 1970's. Several methods have been introduced by many researchers, including the Analytic Hierarchy Process [18] (AHP), Technique for Order Preference by Similarity to Ideal Solution [5] (TOPSIS), PROMETHEE [4], and ELECTRE [16] etc. Moreover, MCDM is used by many researchers in various fields of society, economy, medicine, management and military affairs, etc.

Recently, a new COmbinative Distance-based ASsessment (CODAS) [10] method have been proposed by Keshavarz Ghorabaee et al. (2016). It has some features that have not been considered in the other MCDM methods [10]. It defines the desirability of an alternative by using the Euclidean distance as the primary. If the Euclidean distances of two alternatives are very close to each other, the Taxicab distance is used to compare them. These distances are calculated according to the negative-ideal point. In addition, as an advantage, in the CODAS method, the Euclidean and the Taxicab distances are measured for l2-norm and l1-norm indifference spaces, respectively (Yoon, 1987). In fact, the comparison of each pair of alternatives should first assess in a L2-norm indifference space. If there is a non-comparability, the alternative will be evaluated on a L1-norm indifference space.

The process of decision making is often prone to uncertainty and imprecision as it implies human judgement and cognitive thinking. It is hard for DMs to give the accurate evaluation on complex things in practical decision problems. Thus, Keshavarz Ghorabaee et al. (2017) introduced the Fuzzy extension of the CODAS method [11] for multicriteria market segment evaluation. Furthermore, Yalçın and Pehlivan (2019) proposed an application of the fuzzy CODAS method based on fuzzy envelopes for hesitant fuzzy linguistic term sets [20]. To solve uncertainty, the concept of intuitionistic fuzzy sets (IFS) theory [1] is more suitable to deal with uncertainty than other generalized forms of fuzzy sets [7]. It is a generalization of the Fuzzy Set theory [22]. It is characterized by a membership function and a non-membership function. It gives a powerful tool to handle ambiguity in real-world case studies principally when to express a pair-wise comparison.

The IFS achieved great success in various MCDA researches: Park et al. [14] prolonged the group decision making VIKOR method for an interval-valued intuitionistic fuzzy environment. In this method, the attribute weights information was partially known. Chen [5] developed an extended TOPSIS method with an inclusion comparison approach to address multiple criteria group decision-making medical problems in the interval-valued intuitionistic fuzzy set framework. Some significant extensions of CODAS under intuitionistic fuzzy numbers (IFNs) are narrated below. Ren [15] developed a novel intuitionistic fuzzy MCDM combinative distance-based assessment (CODAS) method for prioritizing the alternative energy storage technologies. Bolturk and Kahraman [3] introduced an interval-valued intuitionistic fuzzy CODAS method and applied it to wave energy facility location selection problem. Roy et al. [17] presented an extension of the CODAS approach using IVIFS Set for sustainable material selection in construction projects with incomplete weight information.

To present the ill-known input data of the IFS on the real number set, the triangular intuitionistic fuzzy number

*Research supported by ABC Foundation.

D.R. Fedia is with the faculty of economics and management of sfax, university of Sfax Tunisia (corresponding author to provide phone: +216 20 161 416; e-mail: Fedia.daami008@gmail.com).

F.M. Hela is in the Department of Mathematics of the University of Sfax, Business School ESC (hela_frikha_moalla@yahoo.fr).

TIFN [12] are very useful for decision makers (DMs) to depict their fuzzy preference information. TIFNs can precise different dimension decision information and reflect DM's information more perfectly than IFNs. In addition, applying TIFNs to decision making field have an important theoretical value and practical significance [20]. As an extension of TIFNs, Wang [19]presented the concepts of trapezoidal intuitionistic fuzzy numbers (TrIFN) and interval valued trapezoidal intuitionistic fuzzy numbers (IVTrIFN).

Motivated by the following fact:

- Single decision-makers are unable to express their opinions or preferences on multiple criteria to solve the complexity of the social-economic environment. In fact, when multiple actors are involved in the decision process, it becomes even more efficient, since each one seeks to present his own influence on the process, according to his individual and group interests.
- Human beings usually tend to make preferences based on the comparative analysis. These preferences are generally invoked vagueness because the choices are linguistically rated and compared.
- The existing researches about TIFNs mainly discussed the ranking methods and the aggregation operators; there was no investigation on introducing classic CODAS method to solve the MAGDM problems with TIFNs.

This paper focuses on a group decision making problem where a group of individuals or a committee collectively shares the responsibility for making a sort among a set of alternatives for action. Indeed, the aim of our research is to develop an extension of the CODAS method to deal with imprecision by the IFS theory and to solve MCGDM problems. Indeed, our proposed describe decisional matrix by linguistic terms and convert them to triangular intuitionistic fuzzy numbers.

This paper is organized as follows: in the second section, we will introduce the TIFNs definitions and operations. In the third section, we will present the CODAS method using crisp evaluations. The fourth section will be devoted to develop an extension of the CODAS method based on IFS theory to solve MCGDM problem. In section five, we will include a numerical example and comparison of results with other MCDA methods. The final section will conclude the paper and outline further research.

II. Triangular Intuitionistic fuzzy set theory

A. *Definition*

Let a set X be fixed. An intuitionistic fuzzy set (IFS) [1] A in X can be defined as follows:

A= {<x, μ_A (x), ν_A(x)>| x ∈ X},

where μ_A (x), ν_A(x) ∈ [0, 1] define the degree of membership and the degree of non-membership of the element x ∈ X respectively, $0 \leq \mu_A(x) + \nu_A(x) \leq 1$.

The TIFN [13] will be represented by the two sets of triplets $A_{(TIFN)}= \{(a_1, a_2, a_3);(a'_1, a_2, a'_3)\}$ where a_2 is the mean value of the intuitionistic fuzzy numbers μ_A (x) and ν_A (x), a_1 and a_3 are respectively the left and the right boundary of μ_A (x), a'_1 and a'_3 are respectively the left and the right boundary of ν_A (x), and $a'_1 \leq a_1 \leq a_2 \leq a_3 \leq a'_3$.

The membership and the non-membership of TIFN are given as follows:

$$\mu_{A_{(TIFN)}}(x) = \begin{cases} \frac{x-a_1}{a_2-a_1}, for\ a_1 \leq x \leq a_2 \\ \frac{a_3-x}{a_3-a_2}, for\ a_2 \leq x \leq a_3 \\ 0\ otherwise \end{cases} \quad (1)$$

$$\nu_{A_{(TIFN)}}(x) = \begin{cases} \frac{a_2-x}{a_2-a'_1}, for\ a'_1 \leq x \leq a_2 \\ \frac{x-a_2}{a'_3-a_2}, for\ a_2 \leq x \leq a'_3 \\ 1\ otherwise \end{cases} \quad (2)$$

Operations of Triangular Intuitionistic Fuzzy numbers

Let have $A_{(TIFN)}= \{(a_1, a_2, a_3);(a'_1, a_2, a'_3)\}$ and $B_{(TIFN)}= \{(b_1, b_2, b_3);(b'_1, b_2, b'_3)\}$. The operations on triangular intuitionistic fuzzy number are the following:

$A_{(TIFN)}+ B_{(TIFN)}$ =

$$\{(a_1+ b_1, a_2+ b_2, a_3+ b_3);(a'_1+ b'_1, a_2+ b_2, a'_3+ b'_3)\}; \quad (3)$$

$A_{(TIFN)}- B_{(TIFN)}$ =

$$\{(a_1- b_3, a_2- b_2, a_3- b_1); (a'_1- b'_3, a_2- b_2, a'_3+ b'_1)\}; \quad (4)$$

$A_{(TIFN)}* B_{(TIFN)}$ =

$$\{(a_1* b_1, a_2* b_2, a_3* b_3); (a'_1* b'_1, a_2* b_2, a'_3* b'_3)\}; \quad (5)$$

Let k be a scalar number:

If k >0 then k* $A_{(TIFN)}$=

$$\{(k * a_1, k * a_2, k * a_3);(k * a'_1, k * a_2, k * a'_3)\}$$

If k <0 then k* $A_{(TIFN)}$=

$$\{(k * a_3, k * a_2, k * a_1);(k * a'_3, k * a_2, k * a'_1)\} \quad (6)$$

Hepzibah and Vidhya [8] proposed the following division operator:

$$\frac{A_{(TIFN)}}{B_{(TIFN)}} = \{(\min(\frac{a_1}{b_1}, \frac{a_1}{b_3}, \frac{b_1}{a_1}, \frac{b_3}{a_3}) ; \frac{a_2}{b_2} ; \max(\frac{a_1}{b_1}, \frac{a_1}{b_3}, \frac{b_1}{a_1}, \frac{b_3}{a_3})) ;(\min(\frac{a'_1}{b'_1}, \frac{a'_1}{b'_3}, \frac{b'_1}{a'_1}, \frac{b'_3}{a'_3}) ; \frac{a'_2}{b'_2} ; \max(\frac{a'_1}{b'_1}, \frac{a'_1}{b'_3}, \frac{b'_1}{a'_1}, \frac{b'_3}{a'_3})) \quad (7)$$

The deffuzzification of the TIFNs [4] to ordinal number is the following:

$$A_d = \frac{(a_1+2a_2+a_3)+(a'_1+2a_2+a'_3)}{8} \quad (8)$$

The aggregation of multiple TIFNs into single TIFN (Zhang et al. 2010) presented as the following.

$$f_w(I_1, I_2, \ldots, I_n) = \{(a^1, a^2, a^3);(a'^1, a^2, a'^3)\}, \text{ i=1,2,..,n} \quad (9)$$

Where:

$a^1 = 1 - \prod_{i=1}^{n}(1 - a_i^1)^{w_i}$, $a^2 = 1 - \prod_{i=1}^{n}(1 - a_i^2)^{w_i}$,

$a^3 = 1 - \prod_{i=1}^{n}(1 - a_i^3)^{w_i}$, $a'^1 = \prod_{i=1}^{n}(a_i'^1)^{w_i}$,

$a^2 = \prod_{i=1}^{n}(a_i^2)^{w_i}$, $a'^3 = \prod_{i=1}^{n}(a_i'^3)^{w_i}$.

W_i is the weight vector of I_i, i=1,2,…,n.

Zhang et al. (2013) defined the normalized TIFNs decision matrix as follow:

$$\hat{a}_{ij} = \{(\frac{a_{ij}^1}{a_j^+}, \frac{a_{ij}^2}{a_j^+}, \frac{a_{ij}^3}{a_j^+});(\frac{a_{ij}'^1}{a_j^+}, \frac{a_{ij}^2}{a_j^+}, \frac{a_{ij}'^3}{a_j^+})\}, \text{ i=1,2,..,n; j=1,2,..,m.} \quad (10)$$

Where $a_j^+ = max\, a_{ij}$, i=1,2,..,n; j=1,2,..,m

III. COMBINATIVE DISTANCE-BASED ASSESSMENT (CODAS) METHOD

CODAS method is proposed for ranking A = $\{a_1, a_2, .., a_n\}$ actions according to q criteria G= $\{g_1, g_2, .., g_m\}$ evaluated by a weight w_j, j=1..m. As a second step, the decision matrix and the weighted decision matrix should be normalized.

Second, it is necessary to determine the negative-ideal solution of each criterion $ns_j = \min_i r_{ij}$, j=1...m, where r_{ij} is the normalized decision matrix

Then, as clearly stated above, the ranking of alternatives is determined by using two measures; the principal measure is the Euclidean distance of alternatives from the negative-idea in an l2-norm indifference space for criteria:

$$E_i = \sqrt{\sum_{j=1}^{m} r_{ij} - ns_j}. \quad (11)$$

If there are two incomparable alternatives, the secondary measure is the Taxicab distance, which is related to the l1-norm indifference space, should be calculated:

$$T_i = \sum_{j=1}^{m} \left| r_{ij} - ns_j \right|. \quad (12)$$

The alternative which has higher distances from the negative-ideal solution is more desirable.

IV. THE CODAS FOR MULTICRITERIA GROUP DECISION MAKING IN INTUITIONISTIC FUZZY SET THEORY

Our research aimed to develop an IFS CODAS method where the input data is expressed with triangular intuitionistic fuzzy number to solve multicriteria group decision making problem. Our method constructed by linguistic values as input data to simplify its collection. It consists in aggregating the individual sorting results in a collective one and calculating the personal and the group satisfaction degrees. If satisfaction is low, it will be necessary to recollect the input data.

The procedure of our proposed extension divided in 3 principal parts:

The first part is to collect data. A group of DMs are called to give their preference rating and their criteria weight as linguistic term. This input data should be then transformed to triangular intuitionistic fuzzy numbers (TIFNs). Table 1 and Table 2 show the linguistic scales and corresponding IFNs according to the following tables: :

Very Poor (VP)	{(0.5,0.5,0.5); (0.5,0.5,0.5)}
Poor (P)	{(0,1,3); (0.5,1,4)}
Medium Poor (MP)	{(1,3,5); (0.5,3,5.5)}
Fair (F)	{(3,5,7); (2,5,8)}
Medium Good (MG)	{(5,7,9);(4.5,7,9.5)}
Good (G)	{(7,9,10); (6,9,10)}
Very Good (VG)	{(10,10,10); (10,10,10)}

Table 1: Linguistic variable for the rating [4]

Very Low(VL)	{(0,0,0.1); (0,0,0.2)}
Low(L)	{(0,0.1,0.3); (0,0.1,0.4)}
Medium Low(ML)	{(0.1,0.3,0.5; 0.05,0.3,0.5.0.5)}
Medium(M)	{(0.3,0.5,0.7); (0.2,0.5,0.8)}
Medium High(MH)	{(0.5,0.7,0.9);(0.45,0.7,0.95)}
High(H)	{(0.7,0.9,1); (0.6,0.9,1)}
Very High(VH)	{(0.9,1,1); (0.8,1,1)}

Table 2:Linguistic variables for the weight importance of each criterion [4]

The second part consists to Construction and exploitation of the individual TIFNS-CODAS procedure. This extension developed to deal with uncertainty by integrated the TIFS theory in the CODAS method. In fact, by using the arithmetic operations given in section 2, the TIFNs adopt the following steps:

- The compute of the TIFNs normalized matrix of each decision maker.
- The compute of the TIFNs weighted normalized matrix.
- The Determination of the TIFNS negative- ideal solution.

- DMs should defuzzify the results given in the last steps to crisp number by using the Gani and Abbas (2014) operator.
- The implementation the steps of the original CODAS method by calculating the Euclidian and taxicab distances and by computing the relative assessment matrix and the assessment score.

The third phase is the implementation of the Group decision making TIFS- CODAS procedure. It consists in aggregating the individual sorting results in a collective one. As in the CODAS method the alternative which has greater Euclidian and Taxicab distances is more desirable.

V. Using TIFNs-CODAS method for MCGDM problem to solve Green Supplier Selection problem

For any organization, purchasing is a principal function, so supplier selection is a beneficial strategy for business relationship. Since, the performance of an organization in a supply chain (SC) depends on the performance of its suppliers. Consequently, this field is one of the most important multi-criteria decision-making (MCDM) problems. In fact, multicriteria ranking methods usually make a comparison among suppliers and rank them from the best to the worst.

At this step of our research, we tested the applicability of the proposed TIFS-CODAS method for the MCGDM through its application to the Green supplier selection problem. We have considered the example given by Banaeian et al. [2]. In their decision problem, food processing companies in agri-food sector are under various pressures to measure, control and reduce the environmental burdens of their supply chains.

After a preliminary screening, four suppliers of Olive oil $\{A_1, A_2, A_3, A_4\}$ evaluated according to four criteria g_1 Service level, g_2 quality and g_3 price were identified as the primary conventional criteria and g_4 the Environmental Management Systems (EMS) as the green criterion. To collect input data for our analysis, a panel of three industry experts $\{DM_1, DM_2, DM_3\}$ was formed to provide opinions. The weights of the DMs are assumed to be a crisp number $\lambda_l = \{0,5; 0,3; 0.2\}$. The weights of the four criteria and the preference rating are described using the linguistic term set in table 3 and 4.

By using the table given by Gautam et al. [4], we transformed the linguistic input values to Triangular Intuitionistic Fuzzy Numbers (TIFNs) (table 5-6). After normalizing and calculating the weighted normalized matrix, we determinate the TIFNs negative-ideal solution of each DM separately as given in table 7.

Criteria	Alternatives	Decision Makers		
		DM_1	DM_2	DM_3
g_1	A_1	F	P	MP
	A_2	G	F	VG
	A_3	MP	VG	P
	A_4	P	MP	F
g_2	A_1	MP	G	F
	A_2	F	G	P
	A_3	VG	MP	G
	A_4	VP	VP	P
g_3	A_1	MP	MP	G
	A_2	F	MG	G
	A_3	MG	VG	G
	A_4	P	F	G
g_4	A_1	VG	F	MG
	A_2	MG	F	G
	A_3	G	VG	G
	A_4	MP	MG	G

Table 3: Linguistic Suppliers Decision Matrix

Decision Maker	g_1	g_2	g_3	g_4
DM_1	H	H	MH	ML
DM_2	VH	MH	H	M
DM_3	H	VH	MH	MH

Table 4: linguistic criteria weights

Criteria	Alternatives	Decision Makers		
		DM_1	DM_2	DM_3
g_1	A_1	{(3,5,7);(2,5,8)}	{(0.5,1,3);(0.5,1,4)}	{(1,3,5);(0.5,3,5)}
	A_2	{(7,9,10);(6,9,10)}	{(3,5,7);(2,5,8)}	{(9,10,10);(8,10,10)}
	A_3	{(1,3,5);(0.5,3,5)}	{(9,10,10);(8,10,10)}	{(0.5,1,3);(0.5,1,4)}
	A_4	{(0.5,1,3);(0.5,1,4)}	{(1,3,5);(0.5,3,5)}	{(3,5,7);(2,5,8)}
g_2	A_1	{(1,3,5);(0.5,3,5)}	{(7,9,10);(6,9,10)}	{(3,5,7);(2,5,8)}
	A_2	{(3,5,7);(2,5,8)}	{(7,9,10);(6,9,10)}	{(0.5,1,3);(0.5,1,4)}
	A_3	{(9,10,10);(8,10,10)}	{(1,3,5);(0.5,3,5)}	{(7,9,10);(6,9,10)}
	A_4	{(0.5,0.5,0.5);(0.5,0.5,0.5)}	{(0.5,0.5,0.5);(0.5,0.5,0.5)}	{(0.5,1,3);(0.5,1,4)}
g_3	A_1	{(1,3,5);(0.5,3,5)}	{(1,3,5);(0.5,3,5)}	{(7,9,10);(6,9,10)}
	A_2	{(3,5,7);(2,5,8)}	{(5,7,9);(4.5,7,9.5)}	{(7,9,10);(6,9,10)}
	A_3	{(5,7,9);(4.5,7,9.5)}	{(9,10,10);(8,10,10)}	{(7,9,10);(6,9,10)}
	A_4	{(0.5,1,3);(0.5,1,4)}	{(3,5,7);(2,5,8)}	{(7,9,10);(6,9,10)}
g_4	A_1	{(9,10,10);(8,10,10)}	{(3,5,7);(2,5,8)}	{(5,7,9);(4.5,7,9.5)}
	A_2	{(5,7,9);(4.5,7,9.5)}	{(3,5,7);(2,5,8)}	{(7,9,10);(6,9,10)}
	A_3	{(7,9,10);(6,9,10)}	{(9,10,10);(8,10,10)}	{(7,9,10);(6,9,10)}
	A_4	{(1,3,5);(0.5,3,5)}	{(5,7,9);(4.5,7,9.5)}	{(7,9,10);(6,9,10)}

Table 5: TIFNs Suppliers Decision Matrix

Decision Maker	C_1	C_2	C_3	C_4
DM_1	{(0.7,0.9,1); (0.6,0.9,1)}	{(0.7,0.9,1); (0.6,0.9,1)}	{(0.5,0.7,0.9); (0.45,0.7,0.95)}	{(0.1,0.3,0.5); (0.05,0.3,0.5.0.5)}
DM_2	{(0.9,1,1); (0.8,1,1)}	{(0.5,0.7,0.9); (0.45,0.7,0.95)}	{(0.7,0.9,1); (0.6,0.9,1)}	{(0.3,0.5,0.7); (0.2,0.5,0.8)}
DM_3	{(0.7,0.9,1); (0.6,0.9,1)}	{(0.9,1,1); (0.8,1,1)}	{(0.5,0.7,0.9) ;(0.45,0.7,0.95)}	{(0.5,0.7,0.9); (0.45,0.7,0.95)}

Table 6: TIFNs criteria wieghts

TNS_j	C_1	C_2	C_3	C_4
DM_1	{(0.08, 0.25, 0.43) ; 0.04, 0.25, 0.43)}	{(0.08, 0.25, 0.43) ; 0.04, 0.25, 0.43)}	{(0.04,0.05,0.07); (0.03,0.05,0.08)}	{(0.03,0.09,0.15); (0.02,0.09,0.24)}
DM_2	{(0.05,0.1,0.3); (0.05,0.1,0.4)}	{(0.07,0.2,0.35); (0.04,0.2,0.0.35)}	{(0.04, 0.04, 0.04); (0.04, 0.04, 0.04)}	{(0.15,0.25,0.35); (0.1,0.25,0.4)}
DM_3	{(0.09,0.25,0.4); (0.4,0.25,0.5)}	{(0.05,0.1,0.3); (0.05,0.1,0.7)}	{(0.03,0.07,0.3) ;(0.03,0.07,0.0.4)}	{(0.35,0.5,0.63); (0.3, 0.5, 0.66)}

Table 7: The triangular intuitionistic fuzzy negative-ideal solution of each decision maker

We calculated the Euclidian and the taxicab distances by using the defuzzified $\mathrm{TNS_j}$ shown in table 8. Then we computed the relative assessment and the assessment score H_i of each decision making separately (table 9). To implement the group decision making part, we aggregate the individual relative assessment and the assessment score HG□ in collective one. The ranking is given by the group results are evaluated according to the aggregated assessment score (table 10).

Decision Maker		A_1	A_2	A_3	A_4
DM_1	E_i	0,79	0,97	0,89	0,36
	T_i	0,63	0,95	0,78	0,52
DM_2	E_i	0,76	0,82	1,03	0,75
	T_i	0,58	0,68	1,0	0,56
DM_3	E_i	0,46	0,85	0,72	0,50
	T_i	0,21	0,72	0,78	0,32

Table 8: Euclidian and Taxicab distances

R_a		A_1	A_2	A_3	A_4
DM_1	A_1	0	0,11	-0,28	-0,43
	A_2	-0,12	-0,39	0	-0,62
	A_3	-0,08	0	0,10	-0,53
	A_4	0,48	0,38	0,88	0
	H_i	0,28	0,10	0,71	-1,58
DM_2	A_1	0	0,27	-0,48	-0,01
	A_2	-0,05	0,21	0	-0,06
	A_3	-0,14	0	-0,13	-0,14
	A_4	0,01	0,28	0,08	0
	H_i	-0,18	0,76	-0,51	-0,22
DM_3	A_1	0	0,26	0,45	0,046
	A_2	-0,19	-0,13	0	-0,21
	A_3	-0,11	0	0,12	-0,12
	A_4	-0,04	0,22	0,48	0
	H_i	-0,34	0,36	1,06	-0,28

Table 9: The relative assessment matrix and the assessment score of each decision maker

Hg_{ik}	A_1	A_2	A_3	A_4
A_1	0	0,23	0,03	-0,07
A_2	-0,14	-0,08	0	-0,25
A_3	-0,11	0	0,04	-0,21
A_4	0,08	0,27	0,44	0
HG_i	-0,17	0,43	0,51	-0,52
Rank	3	2	1	4

Table 10: The group relative assessment matrix and assessment score

Rank	TOPSIS	VIKOR	GRA	TIFNs-CODAS
A_1	3	3	3	3
A_2	2	2	2	2
A_3	1	1	1	1
A_4	4	4	4	4

Table 11: comparison with other MCDM method

The results given in table 11 proved the applicability of the triangular intuitionistic fuzzy Number in the CODAS method for treating imprecise elements and for solving the green supplier selection problem. The same input data were used and applied into the TOPSIS, the VIKOR, the GRA and the IVF-CODAS methods. It can be seen, that the ranking of the olive oil suppliers is the same $A_3 > A_2 > A_1 > A_4$

VI. Conclusion

CODAS method is considered as potential MCDM method. It is the process of finding the best compromise among the feasible alternatives by using Euclidian and taxicab distances. This method uses crisp numbers as input data. But, it is hard for decision makers to precisely express their preferences. For this reason, we propose to develop an IFS-CODAS method based on the Triangular Intuitionistic Fuzzy Numbers for describing imprecise evaluations. To simplify the process of collecting data, we choose to work with linguistic terms. These linguistic terms should be then converted to TIFNs. Because single decision maker cannot present the preference rating of the group perfectly, our extension overcome this drawback and integrates the MCGDM problem into CODAS method. The notion of green supply chain management developed as a response to integrate consciousness of environmental protection to costumers. It can be a remarkable real MCGDM problem. To validate this extension, a practical example of green supplier selection problem is treated and validated by a comparison with other MCDM method. As Future search, we can develop a model of green supplier selection problem based on the TIFNs. We can we can modify our extension to solve MCGDM based on the input aggregation procedure.

References

[1] K.T. Atanassov, Intuitionistic fuzzy sets, Fuzzy Sets and Systems 20, 87–96, 1986.

[2] N. Banaeian, H. Mobli, B.Fahimnia, I. E. Nielsen, Mahmoud Omid, “Green Supplier Selection Using Fuzzy Group Decision Making Methods: A Case Study from the Agri-Food Industry”, *Computers and Operation Research*, 2016.

[3] E. Bolturk, C. Kahraman, “Interval-valued intuitionistic fuzzy CODAS method and its application to wave energy facility location selection problem, *Journal of Intelligent & Fuzzy Systems*, 2018.

[4] J.P. Brans, "L'ingénierie de la décision: élaboration d'instruments d'aide à la décision. La méthode PROMETHEE". *Presses de l’Université Laval*, 1982.

[5] T.Y. Chen, The inclusion-based TOPSIS method with interval-valued intuitionistic fuzzy sets for multiple criteria group decision making, *Applied Soft Computing* 26, 57-73, 2015.

[6] A. Gani, S. Abbas, A New average method for solving intuitionistic fuzzy transportation problem, International Journal of Pure and Applied Mathematics 93, 491-499, 2014.

[7] S.S. Gautam, Abhishekh, S. R. Singh, TOPSIS for Multi Criteria Decision Making in Intuitionistic Fuzzy Environment, International Journal of Computer Applications 156, 0975 – 8887, 2016.

[8] R. I. Hepzibah, R.Vidhya, Modified new operations for triangular intuitionistic fuzzy numbers(TIFNS), *Malaya J. Mat.* 2(3), 301–307, 2014.

[9] C.L Hwang, K. Yoon, , “Multiple Attribute Decision Making: Methods and Applications : A State-of-the-ArtSurvey”, *Springer-Verlag*; 1981

[10] M. Keshavarz Ghorabaee, E. K. Zavadskas, Z. Turskis, J. Antucheviciene,“A new combinative distance-based assessment (CODAS) method for multi-criteria decision-making,” *Economic Computation & Economic Cybernetics Studies & Research*, vol.50 (3), 2016, pp. 25–44.

[11] M. Keshavarz ghorabaee, m. Amiri2,e. K. Zavadskas3, r. Hooshmand, j. Antuchevičienė, “fuzzy extension of the codas method for multi-criteria market segment evaluation”, *Journal of Business Economics and Management,* Vol 18(1) 1–19, 2017.

[12] D.F. Li, J.X. Nan, M.J. Zhang, A ranking method of triangular intuitionistic fuzzy numbers and application to decision making, *International Journal of Computational Intelligence Systems* 3 522–530, 2010.

[13] D.F. Li, J. X. Nan, M. J. Zhang, A Ranking Method of Triangular Intuitionistic Fuzzy Numbers and Application to Decision Making,

International Journal of Computational Intelligence Systems 3, 522-530, 2012.

[14] J.H. Park, H.J. Cho, Y.C. Kwun, "Extension of the VIKOR method for group decision making with interval-valued intuitionistic fuzzy information", *Fuzzy Optimization and Decision Making* 10, 233-253, 2011.

[15] J. Ren, Sustainability prioritization of energy storage technologies for promoting the development of renewable energy: A novel intuitionistic fuzzy combinative distance-based assessment approach, *Renewable Energy*, vol 121 , 666-676, 2018.

[16] B. Roy, "Classement et choix en présence de points de vue multiples (la méthode ELECTRE*)". La Revue d'Informatique et de Recherche Opérationelle (RIRO)* (8): 57–75, 1968.

[17] J. Roy, S. Das, S. Kar, D. Pamucar, "An Extension of the CODAS Approach Using Interval-Valued Intuitionistic Fuzzy Set for Sustainable Material Selection in Construction Projects with Incomplete Weight Information", *Symmetry*, 2019.

[18] L. Thomas Saaty "Response to Holder's Comments on the Analytic Hierarchy Process" The Journal of the Operational Research Society, Vol. 42, 909-914, 1991.

[19] J.Q. Wang, Overview on fuzzy multi-criteria decision-making approach, Control and Decision 23 601–607, 2008.

[20] S. Wan Q. Y. Wang, J. Dong, "The extended VIKOR method for multi-attribute group decision making with triangular intuitionistic fuzzy numbers", *Knowledge-Based Systems*, vol52, 65-77, 2013.

[21] N. Yalçın, N. Yapıcı Pehlivan, Application of the Fuzzy CODAS Method Based on Fuzzy Envelopes for Hesitant Fuzzy Linguistic Term Sets: A Case Study on a Personnel Selection Problem, *Symmetry* , vol *11*(4), 493, 2019.

[22] L.A. Zadeh, Fuzzy sets, Information and Control 8, 338-353, 1965.

General Variable Neighborhood Search Approach for Solving the Electric Two-Echelon Vehicle Routing Problem

Mannoubia Affi
Laboratory of Modeling and Optimization for Decisional, Industrial and Logistic Systems (MODILS)
Faculty of Economics and Management Sciences of Sfax, University of Sfax
Sfax, Tunisia
mannoubia.affi@gmail.com

***Abstract*— In this paper, we present an Electric Two-Echelon Vehicle Routing Problem (E2EVRP), which is considered as a VRP problem with Two-Echelon Distribution Systems (TEDS). In the first Echelon Distribution System (EDS), a set of conventional vehicles aims to deliver the goods from the depot to the satellites, while the second EDS aims to deliver the goods from the satellites to the customers using Electric Vehicles (EVs). The EV can stop at Charging Station (CS) to charge their battery. To solve the problem, we propose a General version of the Variable Neighborhood Search algorithm (GVNS) on the basis of the use of three different groups of neighborhood structures. This approach is based on Variable Neighborhood Descent (VND) algorithm as the local search, in which a descent method is used as a subroutine to explore the first echelon, second echelon and two-echelon neighborhoods structures sequentially. In fact, the results indicate that the VNS can easily be applied to ameliorate the quality of the solutions.**

***Keywords*— routing, first echelon, second echelon, satellite, variable neighborhood search, charging station, electric vehicle.**

I. Introduction and Problem Description

The green logistics research is created to reduce the GHG emissions and energy saving. In particular, the transport sector is an important logistic part of CO2 emissions and air pollution. In fact, the introduction of Electric Vehicles (EVs) is one of the main factors to reduce the costs and the pollution caused by the transport operations. In this context, many studies have focused on the VRP problems with fleet of EVs, for example, [1] are the first to proposed a variant of VRP for an EV with time windows and Charging Stations (CSs), [2] suggested a location model for CSs based on the characteristics of travel demands of urban residents and [3] proposed a new model presented as an extension to the work of [1] by considering waiting times at the CSs.

In this work, we consider the Electric Two-Echelon Vehicle Routing Problem (E2EVRP) which was introduced by [4] as a combination of the classical Two-Echelon Vehicle Routing Problem (2E-VRP) [5] with electric vehicle routing problem [6] for the second echelon. The E2EVRP has a single depot, a given number of satellites, a set of customers and a set of CSs (see Fig.1). This problem aims to deliver goods from a depot to the customers through a set of satellites by two types of vehicles: In the first echelon, goods are delivered from the depot to the satellites by large conventional vehicles. In the second echelon, goods are delivered from the satellites to the customers by small EVs. Each EV can stop at CSs to charge their battery.

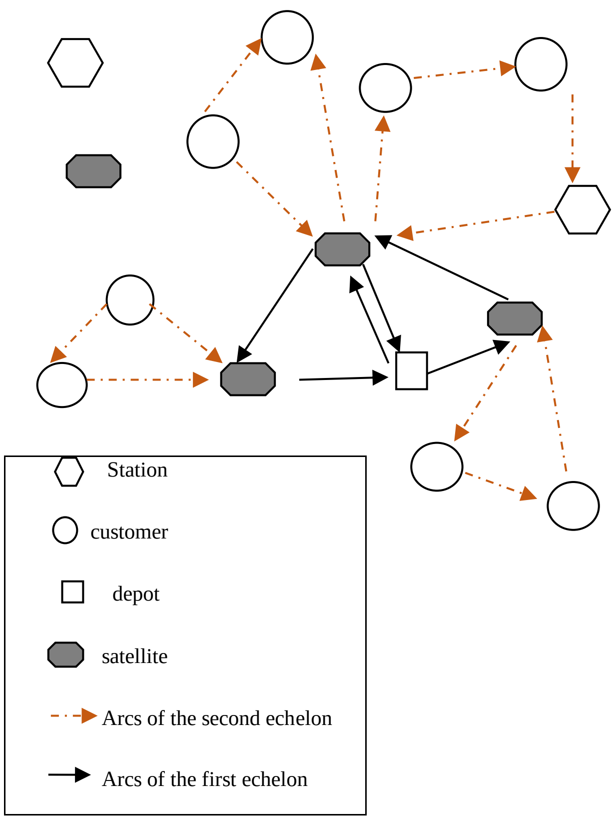

Fig. 1. Solution representation of E2EVRP problem.

The E2EVRP is to find a set of routes at two echelons with the objective of minimizing the sum of the vehicle travel costs (1st- echelon or 2nd- echelon) plus the fixed cost by taking into account the following constraints: Each customer must be visited exactly once by a small EV. By against, not all satellites and CSs have to be used. Each satellite can be served several times without exceeding its maximum capacity of goods and each CS can be visited several times by a small EV in order to charge the battery. Additionally, the capacities of two types of vehicles shall not be violated. The number of large vehicles available at the depot and the number of small EVs available at each satellite are limited and each used vehicle makes a single route. For each used EV, the remaining battery power level at any node does not exceed the battery power limit.

II. Solution Methodology

In this paper, we apply a General Variable Neighborhood Search Algorithm (GVNS) to solve the E2EVRP. GVNS algorithm [7] has been designed as a combination of moves within a set of neighborhood structures used in the local search and perturbation steps to obtain a good quality of the solution. It also has been applied very successfully to many recent problems, for example, we can cite the work of [8] to solve the swap-body vehicle routing problem, the work presented by [9] for solving the Multi-Depot Vehicle Routing Problem and [10] suggested GVNS to effectively solve the Garbage Collection Problem with Time Windows.

Our GVNS algorithm begins with an initial randomly generated solution and employs a set of 10 neighborhood structures that involve different moves for satellites, customers and BSSs between the first and second echelon. *For customer neighborhood*, we propose (i) the shift move of a customer neighborhood: this move is characterized by shifting each customer at the best position in the second echelon of the current solution to get a best neighbor, and (ii) swap move of two customers neighborhood: this move swaps all possible two customers at the second echelon. *For satellite neighborhood*, we propose (iii) close move of a satellite neighborhood: This type of move consists in closing a satellite from the two-echelon routes if his second echelon route does not contain any node, (iv) open move of a satellite neighborhood: This type of move consists in opening a new satellite, (v) the shift move of a satellite neighborhood: this move is characterized by shifting each satellite of the first echelon at the best position, (vi) swap move of two satellites neighborhood: this move is characterized by swapping all possible two satellites of the first echelon, and (vii) replace move of a satellite neighborhood: this move is characterized by replacing a satellite by another satellite in the two-echelon. *For charging station neighborhood*, we propose (viii) replace move of a CS neighborhood: this type of move replaces a CS by another one in a best position, (ix) drop move of a CS neighborhood: this move deletes a CS from a second echelon route and (x) add move of a CS neighborhood: this move inserts a CS at a second echelon route.

These neighborhoods can be grouped into three categories: First echelon subset of neighborhoods (the shift move of a satellite neighborhood, swap move of two satellites neighborhood), second echelon subset of neighborhoods (the shift move of a customer neighborhood, swap move of two customers neighborhood, replace move of a CS neighborhood, drop move of a CS neighborhood, add move of a CS neighborhood) and two-echelon subset of neighborhoods (close move of a satellite neighborhood, open move of a satellite neighborhood, replace move of a satellite neighborhood). Each subset of neighborhoods is explored consecutively around the current solution until there is no further improvement within a Descent Method (DM). Then, our local search is presented by using the VND algorithm [11] where the DM method used as a subroutine to explore the first echelon, second echelon and two-echelon neighborhoods structures sequentially. In the shaking phase, a customer node is selected according to a probability and then removed from its position and insert it at a random position in order to improve the local optimum obtained by VND phase.

III. Experimental Results

To validate the performance of the proposed method, we perform experiments using 12 large instances with 100 customers and 5 or 10 satellites. We compare our results with those obtained with Large Neighborhood Search (LNS) generated by [4]. This method is considered as a combination of various destruction and repair operators, a local search phase, and a fast-labeling procedure to located the charging stations at the best position.

All experiments are conducted on an Intel (R) Core (TM) i5-4460 CPU, 3.20 GHz processor and 4 Go of RAM. The GVNS metaheuristic is coded in C++. The time limit is set for LNS and GVNS to 900 seconds and each instance is running 10 times.

The results are reported in TABLE I. The first column, Instance, reports the name of the instance. The next column BKS shows the value of the Best Known Solution given in [4] . For LNS and GVNS algorithm: Avg is the average solution over ten runs, Best is the best solution quality over ten runs and T*(s) is the computational time in seconds required to obtain the best solution by the LNS and GVNS algorithms. The values in bold in this table correspond to the best obtained costs.

Among the 12 instances of E2EVRP, the GVNS meta-heuristic achieves better solutions for 11 instances. Furthermore, the computational time is significantly better than LNS algorithm for most instances. Overall, we can claim that the proposed method outperforms the LNS algorithm both in solution quality and computational time by comparing the total average best solution and the total average computational time obtained by the GVNS algorithm (10424.5 and 281.1 seconds) with the LNS (10619.2 and 294.4 seconds).

IV. Conclusion

This work has its focus on the Electric Two-Echelon Vehicle Routing Problem (E2EVRP) which is considered as a variant of 2E-VRP. The second echelon of the E2EVRP is handled as an electric VRP. We propose a new application of General VNS algorithm to solve E2EVRP. The idea of this algorithm is to group the set of defined neighborhoods in three subsets of neighborhoods. Each subset of neighborhoods is explored within a descend method. Then, the three obtained descend methods are used sequentially as the subroutines in the VND algorithm. In the shaking phase, a customer node is selected according to a probability and then removed from its position and insert it at a random position in order to improve the local optimum obtained by VND. All the results show that the proposed approach achieves better results (considering the best solution value and the computational time).

References

[1] S. Michael, S. Andreas, and G. Dominik, "The Electric Vehicle Routing Problem with Time Windows and Recharging Stations," *Transportation Science*, vol. 48, no. 4, pp. 500–520, 2012.

[2] Z. Sun, W. Gao, B. Li, and L. Wang, "Locating charging stations for electric vehicles," *Transport Policy*, 2018.

[3] M. Keskin, G. Laporte, and B. Çatay, "Electric Vehicle Routing Problem with Time-Dependent Waiting Times at Recharging Stations," *Computers and Operations Research*, vol. 107, pp. 77–94, 2019.

[4] U. Breunig, R. Baldacci, R. F. Hartl, and T. Vidal, "The electric two-

echelon vehicle routing problem," *Computers and Operations Research*, vol. 103, pp. 198–210, 2019.

[5] T. G. Crainic, G. Storchi, and N. Ricciardi, "Models for evaluating and planning city logistics transportation systems," *Management*, no. December, 2007.

[6] C. S. Liao, S. H. Lu, and Z. J. M. Shen, "The electric vehicle touring problem," *Transportation Research Part B: Methodological*, vol. 86, pp. 163–180, 2016.

[7] N. Mladenović, D. Urošević, S. Hanafi, and A. Ilić, "A general variable neighborhood search for the one-commodity pickup-and-delivery travelling salesman problem," *European Journal of Operational Research*, vol. 220, no. 1, pp. 270–285, 2012.

[8] R. Todosijević, S. Hanafi, D. Urošević, B. Jarboui, and B. Gendron, "A general variable neighborhood search for the swap-body vehicle routing problem," *Computers and Operations Research*, vol. 78, pp. 468–479, 2017.

[9] S. N. Bezerra, S. R. de Souza, and M. J. F. Souza, "A GVNS Algorithm for Solving the Multi-Depot Vehicle Routing Problem," *Electronic Notes in Discrete Mathematics*, vol. 66, pp. 167–174, 2018.

[10] C. Papalitsas and T. Andronikos, "Unconventional GVNS for Solving the Garbage Collection Problem with Time Windows," *Technologies*, vol. 7, no. 3, p. 61, 2019.

[11] W. Maden, R. Eglese, and D. Black, "Vehicle routing and scheduling with time-varying data: A case study," *Journal of the Operational Research Society*, vol. 61, no. 3, pp. 515–522, 2010.

TABLE I. RESULTS ON LARGE SIZE INSTANCES

		LNS			GVNS		
Instance	BKS	Avg	Best	T*(s)	Avg	Best	T*(s)
100-5-1 100	16167	16224.6	16167	403.7	17355.8	**16078**	747.8
100-5-1b 100	11937	12070.2	11937	278.4	12854.5	**11636**	**267.3**
100-5-2 100	**10578**	10578.0	**10578**	**32.9**	11993.9	10790	291.8
100-5-2b 100	8307	8426.1	8307	429.4	9172.2	**8022**	**323.9**
100-5-3 100	10651	10651.4	10651	267.7	10883.7	**10512**	**130.1**
100-5-3b 100	9063	9068.0	9063	244.8	9109.2	**8917**	**144.2**
100-10-1 100	11409	11451.8	11409	435.4	12033.6	**11351**	**342.9**
100-10-1b 100	10168	10194.3	10168	239.5	10056.1	**10043**	**101.3**
100-10-2 100	10525	10561.5	10525	395.9	10774.3	**10250**	**364.6**
100-10-2b 100	8752	8800.7	8752	284.0	8621.4	**8569**	**210.2**
100-10-3 100	10730	10743.6	10730	276.3	11453.2	**10695**	330.2
100-10-3b 100	9144	9209.6	9144	245.2	8241.3	**8231**	**119.4**
Average	10619.2	10664.9	10619.2	294.4	11045.7	**10424.5**	**281.1**

A Comparative Study of Local Search Techniques Addressing an Electric Vehicle Routing Problem with Time Windows

Dhekra Rezgui
ECSTRA Laboratory
ISG, University of Tunis, Tunisia
dhekra.rezgui@live.fr

Hend Bouziri
LARODEC Laboratory,
ESSECT, University of Tunis, Tunisia
hend.bouziri@gmail.com

Wassila Aggoune-Mtalaa
ITIS department
Luxembourg Institute of Science and Technology
wassila.mtalaa@list.lu

Jouhaina Chaouachi Siala
ECSTRA Laboratory
IHEC, University of Carthage, Tunisia
siala.jouhaina@gmail.com

***Abstract*—In this paper, we address a new type of green vehicle routing problems using innovative electric vehicles. Indeed, we study a special variant of the electric Vehicle Routing Problem (e-VRP) in which the vehicles are modular. Local search techniques and their combination with evolutionary schema are proposed. An experimental study on benchmark instances was performed to show the relevance of the evolutionary variable neighborhood descent method.**

***Index Terms*—Evolutionary Algorithm, Variable Neighborhood Descent, Modular Electric Vehicles, Charging Policy, VNS**

I. Introduction

During the last decade, a great interest of research has been devoted to design green supply chains [2], [15] and optimize their related distribution networks in order to limit greenhouse gas emissions [3], [8]. In this paper, we address a new type of green vehicle routing problems using innovative electric vehicles. Indeed, we study a special variant of the electric Vehicle Routing Problem (e-VRP) in which the vehicles are modular.

Hence, in this problem, we have a set of electric vehicles V where each vehicle consists of a set of modules (including the cabin of the driver). Each module has a battery that could be charged separately. We assume that we are in the case of problem of distribution of goods to customers who have charging stations. Thus, if the vehicule charge falls below a certain threshold, the vehicle can detach and leave a module in a client to be recharged and it ends its path. Optionally, the vehicle can recover another module already charged in another customer to benefit from its additional energy. In this work, we consider only releasing modules for recharging. But this idea of modularity can also be used for example to treat the problem of congestion. Several types of modular electric vehicles already exist as prototypes. We can cite basically those developped in the German Research Center for Artificial Intelligence (DFKI) [19].

To show the relevance and effectiveness of our approach, we carried out extensive experiments comparing the proposed method called EVND (Evolutionary Variable Neighborhood Descent) against the VNS technique. In addition, the relevance of the EVND method was emphasized compared to an evolutionary local search. Subsequently a detailed comparison with existing methods was detailed.

The paper provides in section 2, the description of our problem, and we present in section 3 some related works dealing with hybrids and VNS techniques for routing problems. In section 4, we describe in detail the evolutionary based variable neighborhood descent algorithm. The computational study is presented and discussed in section 5 and we conclude the paper in section 6 by giving some perspectives for future works.

II. Problem description

In this paper, we consider the routing problem of modular electric vehicles with time windows. This problem has been formulated as a Mixed Integer Linear Programming (MILP) in [10]. Several constraints have been added compared to the standard Vehicle Routing Problem with Time Windows (VRPTW) with a heterogeneous fleet, notably the constraints related to the modules and their battery charging. These constraints constitute the recharging policy adopted in the studied problem.

A. Recharging policy

As detailed above, each vehicle is composed of a set of modules that can be detached for energy reloading purposes, see [11]. The following assumptions are retained during the routing of this type of electric vehicles.

- All the vehicles, with their modules are fully charged when they leave the depot.

- The charge of the battery of a vehicle is equal to the sum of the charges of batteries of the modules attached including the charge of the cabin.
- A charging threshold is set for each vehicle bellow it the module with the lowest charge is detached to recharge its battery.
- Each customer is provided with an electric charging station by which modules and vehicles can be recharged. The recharging time depends on the level of charge when arriving at the recharging station and should not exceed the time window constraint.
- The cabin module can not be detached. If the charge of its battery falls below a certain threshold, the vehicle is forced to stop to recharge in electricity, this by respecting the predefined time window.

III. Related works

A wide variety of methods has been proposed for the VRPTW problem and its variants which are classified NP-hard. Since our problem is a variant of the VRPTW, our interest has focused on the methods dedicated to this problem and its electric variants. Three major findings can be identified from the study of these methods. First, we can note the great tendency to use metaheuristics with its different types to overcome the difficult nature of the problem. We can cite as example, the work of Schneider et al. [13]. Secondly, the study of the related work has shown the need to adopt methods with diversification mechanisms to visit areas scattered in the research space, which avoids being trapped in local optima. This could explain the use of evolutionary schemas in several methods dedicated to the VRPTW with its different variants as noticed by Braÿsy and Gendreau [4]. We can cite for example the work of Ursani et al. [18]. Finally, we noticed in our study of related literature, the effectiveness of the VNS (Variable Neighborhood Search) method which also contains a component of diversification of the search but its strength lies in its component called VND (Variable Neighborhood Descent) which alters its moves locally between several neighborhood operators to intensify research in promising areas. Several variants have been used in the VRPTW, such as the work of Chen et al. [5] which proposes an adapatation of the VNS, called VNS-C.

The literature review reported previously highlights the relevance of hybridising approaches to deal with the proposed variant of the e-VRPTW problem. More precisely, we are intersted with a method that marries a diversification component and an elaborated intensification component. Hence, the main contribution of this paper is to propose a variable neighborhood descent procedure within an evolutionary to solve the presented problem of VRPTW using a fleet of electric modular vehicles. This idea of hybridizing evolutionary algorithm with a variant of the VNS was also followed by Baniamerian et al. [1] in their method called MVNS (Modified Variable Neighborhood Search).

IV. An Evolutionary Variable Neighborhood Desent Method

In order to guide a search algorithm efficiently in a solution space, it would be necessary to properly define move operators to be used, but also an appropriate objective function that should reflect the properties of the problem being addressed. Indeed, since it concerns the routing of electric vehicles, it is important to minimize as much as possible the number of vehicles used as well as the time allocated for recharging the batteries of the cabin modules (since the vehicle is forced to stop in this case).

A. Objective function

To ensure efficient routing in the context of our specific VRPTW problem using modular and electric vehicles, we opt for an objective function comprising three terms. The first provides the purchase cost of the vehicles used in the routing. The second term corresponds to the distance traveled to serve all customers and the third term penalizes vehicle stops for reloading cabins modules. More formaly, consider a set of vehicles V and C a set of customers. A binary decision variable x_{ij}^v is assigned to each route between two customers i and j, x_{ij}^v is equal to 1 if the vehicle crosses the road from i to j. Further, a transportation cost c_{ij}, which is obtained by multiplying the distance d_{ij} by the variable cost p_k, is also assigned to the road from i to j. Hence, the objective function is defined as follows:

$$\sum_{v\in V}\sum_{j\in C} a^v x_{0j}^v + \sum_{v\in V}\sum_{i,j\in C, i\neq j} c_{ij}x_{ij}^v + \sum_{v\in V}\sum_{i\in C} c_r r_i^v, \quad (1)$$

where a^v is the acquisition cost of a vehicle v, x_{0j}^v indicates if a vehicle v leaves the depot 0 to reach the customer j. The binary variable r_i^v denotes if the vehicle v is recharged at customer i at recharge cost c_r of a cabin module. For the detailed mathematical formulation reflecting all the constraints, please refer to [10].

B. The algorithm

The algorithm of the EVND method is presented in Algorithm 1. An initial population Pop of size S_p is generated, then the individual are ranked according to their cost value calculated by the function f in equation (1). At each generation, a tournament selection procedure is performed to choose two parents $Parent_1$ and $Parent_2$. These routings will be combined within a crossover procedure to generate a $Child$. The VND procedure is then applied on the child to be improved and we have a new routing called $Local$ that will replace the worst routing in the population Pop. The algorithm is stopped when a prefixed number of generations is reached.

a) ***Routing representation*** *:* A vehicle routing is represented by an integer array of length N (number of nodes) where vehicle tours are separated by zeros. Furthermore, for each customer, we report its time service as in classical VRPTW problems. Besides, for our eletric variant, we report for each vehicle, its cost, its recharging stations and the number of attached modules when it visits a customer.

Algorithm 1 Eolutionary Variable Neighborhood Descent Method.

```
Input: C: Customers, d_ij: distance from customer i to j; S_p population size.
Output: Feasible routing
Pop ← Initial population (S_p) ;
best ← Ranking(Pop);
Do while Stopping criterion is not satisfied
    Parent_1,Parent_2 ← Select(Pop);
    Child ← Crossover (Parent_1, Parent_2);
    Local ← VND(Child);
    Pop ← Replacement (Pop, Local);
    If f (Local < best) Then best ← Local
Return Best individual in Pop;
```

b) ***Initial population generation:*** A greedy algorithm is used to provide a feasible routing, where at each time, the nearest customer is served by respecting all constraints related to the recharging constraints reported above. The rest of individuals in the population Pop are generated by using a 2-opt move and adding vehicles when recharging and time windows constraints are violated.

c) ***Crossover operator:*** In this work, we choose the Best Cost Route Crossover (BCRC) firstly proposed by Ombuki et al. [9]. Basically, BCRC provides as offspring, the best combination of tours from each parent that satisfies all the constraints. Routings are valuated according to objective function reported in equation (1).

d) ***The Variable Neighborhood Descent procedure:*** It replaces the classical mutation and tries to improve the child quality by applying local moves. The VND heuristic applies alternatively the neighborhood operators until no improvement is possible. Four neighborhood operators are applied successively on each routing provided by the crossover operator. The sequence of movements retained in this adaptation of VND is: 2-opt, swap, insert and exchange. Approximately, the same order is used for other VRP problems [6] [12]. If the VND can't improve the routing provided as input, i.e. $Child$, VND will return this routing as $Local$.

V. Experimental setup

To test the EVND algorithm, we have used a laptop PC equipped with an Intel Core i3-3217U Processor clocked at 1.8 GHz with 4 GB RAM, running Windows 8.2 Professional. Further, the tests are performed on Solomon instances [16] classified as C1, C2, R1, R2, RCl and RC2 classes, each with 8 to 12 problems. We excecuted for each instance, 10 independent runs of the EVND method. In the experiments we try to show these main issues:

- the comparision between the EVND and the VNS method, since these two algorithms share the same intensification technique and differ in the diversification tool,
- the relevance of the EVND procedure compared to ELS method,
- the performance of our method to treat the electric vehicles routing problem regarding best state of the art methods basically hybrid metaheuristics.

A. Comparison of the EVND with the VNS heuristic

The Variable Neighborhood Search (VNS) is an elaborated search method that showed its performance in solving several optimisation problems including the VRPTW and its variants [7]. Its basic principle is to vary the neighborhood structure over the search process. This is performed by its component called the Variable Neighborhood Descent (VND). To diversify the search, VNS used the so-called shaking procedure. However, EVND replaces this routine of shaking by being population-based. In this part of experiments, we try to compare the performance of the proposed EVND regarding a classical VNS that uses a shaking technique. More specifically, we conducted experiments on all the instances stemmed from Solomon benchmark. In these experiments, we have noted that the EVND is more competitive than the VNS. Table I summarizes the results of the comparison between VNS and EVND. The columns represent the results obtained for each algorithm whereas the lines show the average of the total traveled distance and the average number of vehicles for each class.

TABLE I
Average number of vehicles used and total traveled distance of EVND against VNS.

Benchmark	VNS	EVND
C1	828.78	**825.89**
	9.44	10
C2	585.37	**585.27**
	3	**3**
R1	1189.48	**1183.92**
	11.08	**11**
R2	935.17	**934.52**
	2.72	**2.63**
RC1	1354.84	1357.13
	11.12	11.25
RC2	1050.54	1107.30
	3.12	**3.12**

As shown in Table I, the obtained results indicate that the proposed EVND gives promising results as compared VNS, regarding the decreased numbers of vehicles as in R1 and R2. It is worth noting, that for the group RC1 and RC2, the distances obtained by the VNS are better than the ones obtained with EVND. In the set of instances C1 and C2, EVND provides, in average, a better feasible solution than the one detected by the VNS in terms of distances.

B. Relevance of the EVND procedure compared to the ELS method

Here, we try to assess our theoretical assumptions that the VND could give efficient results by exploring the local neighborhood using the four operators defined before. For this reason, we experiment an Evolutionary Local Search (ELS) procedure that works similarly to the EVND, but replaces the VND procedure by a local descent procedure that iteratively applies the 2-opt move on the child until an improvement is recorded.

Table II summarizes the results of the comparison between ELS and EVND. The columns represent the results obtained for each algorithm whereas the lines show the average of the total traveled distance and the average number of vehicles for each class.

TABLE II
AVERAGE NUMBER OF VEHICLES USED AND TOTAL TRAVELED DISTANCE OF EVND AGAINST ELS.

Benchmark	ELS	EVND
C1	869.62	**825.89**
	8.22	10
C2	592.73	**585.27**
	3	**3**
R1	1186.23	**1183.92**
	11	**11**
R2	940.58	**934.52**
	2.63	**2.63**
RC1	1393.24	**1357.13**
	11.37	**11.25**
RC2	1136.73	**1107.30**
	3.25	**3.12**

As shown in Table II, the obtained results indicate in almost all cases that the proposed EVND gives promising results as compared with the ELS.

C. Comparison with some state-of-the-art local search methods

To prove the effectiveness of our method, we choose to compare our results with three related methods; the Tabu Search (TS) [14] as an efficient competitive metaheuristic, the Localized Genetic Algorithm (LGA) [18] because of its evolutionary framework and the VNS-C [5], an effective VNS procedure. All these methods are tested on the Solomon benchmarks framework.

Since the other authors did not provide the CPU time and since our problem is more constrained than the classical VRPTW, we compare only the total distance and the number of used vehicles to report the effectiveness of our EVND. The idea behind this is to assess the ability of our EVND to overcome electric battery recharging constraints by minimizing the total distance (to serve customers rapidly) and the number of EVs (since their acquisition costs are reported to be high).

A thorough analysis of the results presented in Table III, showed that the proposed EVND competes significantly well against the solutions of the 56 instances, when compared to the other state of the art methods, according to the total distance (underlined distances show an improvement with a competitive number of vehicles). Concerning the NV criterion, the obtained results require in almost all cases, the same number of vehicles as the best one of the other methods (italic numbers show an improvement of the number of vehicles with competitive total distance).

Results highlight clearly that for the group of instances C1 and C2, our approach is able to minimize the TD for all the instances with the same number of vehicles. However, for the R1 and R2 classes, EVND is less performant but it is still very competitive on the two criteria NV and TD. Indeed, it provides excellent performance essentially for the R101 and the R102 instances, where the number of vehicles used dropped to 13 and 14 respectively, against 18 and 17 for the best of the other methods. Also, we note the performance of the EVND for the R109 instance for which the TD is equal to 1109.68 with 11 vehicles, against the TS which needs a total distance of 1205.27 with the same number of vehicles. Also, we can report the R112 instance for which the EVND gains 10,33% of the TD when compared to the TS method, by using the same number of vehicles. Concerning the classes RC1 and RC2, the EVND results are very competitive especially on the number of vehicles and outperforms the other methods in some cases, namely; RC101, RC203 and RC208, where the TD and the NV are the best. All the most interesting performances of the EVND are in bold in Table III.

The results also show that our method has managed to provide routings using the least number of vehicles compared to other existing methods without significantly degrading the total distance traveled. This is more clear for the results underlined in Table III. Indeed, for example, the R205 instance is solved by a routing distance equal to 969,13 using 3 vehicles against VNS-C heuristic whose distance traveled is equal to 964,02 using 4 vehicles. This kind of improvement is suited for our variant of e-VRP since the vehicles are assumed to be expensive. Further, for 13 instances (with results in italic), EVND has succeeded in reducing the number of vehicles compared to state-of-the-art methods.

This performance can be explained by the hybridation mecanism followed by EVND that explores the search space using a population of routings and an effective intensification VND method. In addition, we can note the ability of our method to lead for good tradoffs (NV,TD) suitable for the electric specifity of the problem treated. Indeed, the objective function chosen penalizes the use of added vehicles and the recharging of batteries while looking for routing with minimal distance.

TABLE III
COMPARISON BETWEEN OUR BEST RESULTS AND RELATED METHODS ON THE SOLOMON INSTANCES.

Problem	TS		LGA		VNS-C		EVND	
	NV	TD	NV	TD	NV	TD	NV	TD
C101	10	828.94	10	827.3	10	828.94	**10**	**820.66**
C102	10	828.94	10	827.3	10	828.94	**10**	**823.05**
C103	10	828.07	10	827.3	10	828.94	**10**	**827.54**
C104	10	824.78	10	827.3	10	825.65	**10**	**824.12**
C105	10	828.94	10	827.3	10	898.94	**10**	**828.48**
C106	10	828.94	10	827.3	10	898.94	**10**	**826.35**
C107	10	828.94	10	827.3	10	898.94	**10**	**827.47**
C108	10	828.94	10	827.3	10	898.94	**10**	**827.31**
C109	10	828.94	10	827.3	10	898.94	**10**	**827.99**
C201	3	591.56	3	589.1	3	591.56	**3**	**583.50**
C202	3	591.56	3	589.1	3	591.56	**3**	**591.56**
C203	3	588.49	3	588.7	3	591.17	**3**	**586.45**
C204	3	587.71	3	588.1	3	590.6	**3**	**581.83**
C205	3	588.49	3	586.4	3	588.88	**3**	**581.44**
C206	3	588.49	3	586.0	3	588.49	**3**	**585.43**
C207	3	588.29	3	585.8	3	588.29	**3**	**583.89**
C208	3	588.32	3	585.8	3	588.32	**3**	**588.05**
R101	18	1606.07	20	1640.1	19	1652.47	**13**	**1653.80**
R102	17	1447.36	18	1467.5	18	1476.06	**14**	**1479.22**
R103	13	1257.49	14	1214.0	14	1219.89	**13**	**1248.64**
R104	9	1007.39	11	992.6	11	994.85	**10**	**986.42**
R105	13	1462.39	16	1362.3	14	1381.88	**12**	**1354.98**
R106	12	1263.29	13	1243.3	13	1243.72	***11***	***1250.08***
R107	10	1080.89	11	1069.5	11	1077.24	10	1102.42
R108	9	957.04	10	943.5	10	956.22	**9**	**945.75**
R109	11	1205.27	13	1152.4	13	1157.61	**11**	**1102.68**
R110	10	1128.61	12	1070.6	12	1081.88	**10**	**1118**
R111	10	1102.07	12	1057.3	11	1087.5	10	1064.95
R112	9	1003.76	10	960.8	10	958.7	**9**	**900.05**
R201	4	1248.49	10	1152.7	5	1190.52	**3**	1249.77
R202	3	1177.11	7	1045.4	4	1098.06	**3**	**1164.58**
R203	3	939.54	6	871.2	4	905	3	940.95
R204	2	822.66	5	731.3	3	766.91	2	827.27
R205	3	1005.05	7	965.1	4	964.02	**3**	**969.13**
R206	2	1076.74	5	887.6	3	931.01	**3**	**889.17**
R207	2	883.502	5	807.0	3	855.37	2	894.35
R208	2	730.62	4	703.4	3	708.9	**2**	**725.054**
R209	3	915.07	6	867.0	3	983.75	**3**	**908.48**
R210	3	949.52	6	944.7	4	935.01	**3**	**848.81**
R211	2	864.83	5	754.6	3	794.04	**2**	**862.17**
RC101	14	1685.39	18	1662.5	15	1624.97	**14**	**1607.48**
RC102	12	1503.25	15	1480.6	13	1497.43	**12**	**1502.27**
RC103	10	1305.20	12	1286.7	11	1265.86	**11**	**1255.57**
RC104	10	1118.42	10	1136.1	10	1136.49	10	1135.52
RC105	13	1626.49	16	1549.8	14	1642.81	**13**	**1555.63**
RC106	11	1366.86	13	1382.7	12	1396.59	***10***	***1427.95***
RC107	10	1312.23	12	1215.8	11	1254.68	**10**	**1238.22**
RC108	10	1132.60	11	1115.5	11	1131.23	10	1134.41
RC201	4	1394.81	10	828.93	5	1310.44	***3***	***1417.36***
RC202	3	1326.40	8	828.93	4	1219.49	3	1367.42
RC203	3	1066.66	6	828.93	4	957.1	**3**	**1051.20**
RC204	2	945.44	4	828.93	3	829.13	**3**	**792.11**
RC205	3	1566.16	8	828.93	5	1233.46	4	1243.81
RC206	3	1140.98	7	828.93	4	1107.4	3	1144.37
RC207	3	1055.42	6	828.93	4	1032.78	**3**	**1020.11**
RC208	3	827.58	5	827.52	3	830.06	**3**	**822**

Table IV summarizes the results of the comparison between the algorithms considered in Table III namely the TS, the LGA, the VNS-C and EVND. The columns represent the results obtained for each algorithm whereas the lines show the average of the total traveled distance and the average number of vehicles for each class.

The obtained results in Table IV indicate that, in average, the proposed EVND gives promising results as compared with Schneider's TS [14], Ursani's LGA [18] and Chen's VNS-C [5], regarding the decreased numbers of vehicles, without a significant increase in the total distance. Indeed, in all the classes of problems, we observe that the results obtained by the EVND algorithm are very competitive, in terms of distance despite the lower number of vehicles used to serve the customers. This is particularly convenient for the electric vehicles context.

TABLE IV
AVERAGE NUMBER OF VEHICLES USED AND TOTAL TRAVELED DISTANCE FOR OUR METHOD AGAINST SOME STATE OF THE ART METHODS.

Benchmark	TS	LGA	VNS-C	EVND
C1	828.38	827.3	828.65	**825.89**
	10	10	10	**10**
C2	589.11	587.37	589.86	**585.27**
	3	3	3	**3**
R1	1134.52	1181.15	1079.92	1183.92
	11.75	13.33	13	**11**
R2	909.73	848,54	921.15	934.52
	2.63	6	3.54	**2.63**
RC1	1381.31	1353.71	1368.75	1357.13
	11.25	13.75	12.12	**11.25**
RC2	1165.43	828.93	1064.98	1107.30
	3	6.75	4	3.12

VI. CONCLUSION

In this paper, we have proposed an evolutionary variable neighborhood descent algorithm applied to a vehicle routing problem with time window constraints using heterogeneous fleets of electric modular vehicles. Experimental results show the benefits of combining the evolutionary schema with the variable neighborhood descent procedure. This performance is also confirmed regarding an evolutionary local search technique. This work can be extended to other VRP variants especially those handling electric constraints in emerging freight delivery distribution problems. Moreover, we intend to enhance the variable neighborhood descent procedure by exploring other move operators.

REFERENCES

[1] A. Baniamerian, M. Bashiri and F. Zabihi, "A modified variable neighborhood search hybridized with genetic algorithm for vehicle routing problems with cross-docking," Electronic Notes in Discrete Mathematics, 4th International Conference on Variable Neighborhood Search, vol. 66, pp. 143–150, 2018.

[2] M. Bennekrouf, W. Aggoune-Mtalaa, and Z. Sari, "A generic model for network design including remanufacturing activities. Supply Chain Forum, vol. 14, no 2, pp. 4–17, 2013.

[3] F. Boudahri, W. Aggoune-Mtalaa, M. Bennekrouf, Z. Sari, "Application of a clustering based location-routing model to a real agri-food supply chain redesign," Studies in Computational Intelligence, vol. 457, pp. 323–331, 2013.

[4] O. Braÿsy and M. Gendreau, "Vehicle Routing Problem with Time Windows. Part I: Route construction and local search algorithms," Transportation Science, vol. 39, no. 1, pp. 101-118, 2005.

[5] B. Chen, R. Qu, R. Bai and H. Ishibuchi, "A variable neighbourhood search algorithm with compound neighbourhoods for VRPTW," Springer, pp. 25–35, 2016.

[6] P. Chen, H. Huang, and X. Dong, "Iterated variable neighborhood descent algorithm for the capacitated vehicle routing problem," Expert Systems with Applications, vol. 37, no 2, pp. 1620–1627, 2010.

[7] J. De Armas, B. Melin-Batista, J. A. Moreno-Pérez, and J. Brito, "GVNS for a real-world Rich Vehicle Routing Problem with Time Windows," Engineering Applications of Artificial Intelligence, vol. 42, pp. 45–56, 2015.

[8] W. Mtalaa, R. Aggoune, and J. Schaefers, "CO2 emissions calculation models for green supply chain management," Proceedings of POMS 20th Annual Meeting. http://www.pomsmeetings.org/ConfProceedings/011/FullPapers/011-0590.pdf, 2009.
[9] B. Ombuki, B. J. Ross, and F. Hanshar, "Multi-Objective Genetic Algorithms for Vehicle Routing Problem with Time Windows," Springer Science + Business Media, Inc. Manufactured in The Netherlands, 2006.
[10] D. Rezgui, J. Chaouachi Siala, W. Aggoune-Mtalaa, and H. Bouziri, "Application of a variable neighborhood search algorithm to a fleet size and mix vehicle routing problem with electric modular vehicles," Computers & Industrial Engineering, vol. 130, pp. 537–550, 2019.
[11] D. Rezgui, J. Chaouachi Siala, W. Aggoune-Mtalaa, and H. Bouziri, "Towards smart urban freight distribution using fleets of modular electric vehicles ," Proceedings of the Mediterranean Symposium on Smart City Applications, pp. 602–612, 2017.
[12] D. Rezgui, H. Bouziri, W. Aggoune-Mtalaa, and J. Chaouachi Siala, "A Hybrid Evolutionary Algorithm for Smart Freight Delivery with Electric Modular Vehicles ," International Conference on Computer Systems and Applications (AICCSA), pp. 1–8, 2018.
[13] M. Schneider, A. Stenger, and D. Goeke, "The electric vehicle-routing problem with time windows and recharging stations," Transportation Science, vol. 48, no. 4, pp. 500-520, 2014.
[14] M. Schneider, "The Vehicle-Routing Problem with Time Windows and Driver-Specific Times," European Journal of Operational Research, vol. 250, no. 1, pp. 101–119, 2016.
[15] C. Serrano, W. Aggoune-Mtalaa, and N. Sauer, "Dynamic models for green logistic networks design," IFAC Proceedings Volumes (IFAC-PapersOnline), vol. 46, no. 9, pp. 736–741, 2013.
[16] M.M. Solomon, "Algorithms for the vehicle routing and scheduling problems with time window constraints," Operations Research, vol. 35, pp. 254-265, 1987.
[17] F.H. Liu, and S.Y. Shen, "A Route-Neighborhood-based Metaheuristic for Vehicle Routing Problem with Time Windows," European Journal of Operational Research, vol. 118, pp. 485–504, 1999.
[18] Z. Ursani, D. Essam, D. Cornforth, and R. Stocker, "Localized genetic algorithm for vehicle routing problem with time windows," Applied Soft Computing, vol. 11, pp. 5375–5390, 2011.
[19] DFKI. http://robotik.dfki-bremen.de/de/mediathek/videoarchiv/eo-smart-connecting-6.html. (Accessed on 03/02/2019).

Title: **Web-mapping for ecotourism development: Application in the Ichkeul national park (northern Tunisia)**

Authors: Jaziri Brahim* and Samaali Hamouda*
*Researcher at the Faculty of Human and Social Sciences of Tunis
e-mail**:** jaziribrahim@gmail.com samaalihamouda@yahoo.fr

Abstract

GIS Web applications have touched all areas. These applications are a useful tool for people directly or indirectly involved in spatial analysis. They also acquire economic relevance. Using these applications by various users, and even managers, can be a simple, fast, web-based, and inexpensive solution. However, access to information in these GIS web applications depends on the interaction capabilities activated by their user interfaces.

"Green" tourism or ecotourism presents a new aspect of tourism in Tunisia. Several improvements have been made to accommodate thousands of visitors and to present the richness of the Ichkeul as a human area of great importance. Introducing and visiting the Ichkeul National Park virtually to a wider community, raising awareness among visitors to protect the ecosystem is the aim of the "Géoweb Ichkeul" web mapping.

The purpose of this article is to illustrate the concept and techniques of use in the context of web GIS application interfaces. Next, we present an overview on the uses of Web Map by the various Tunisian state organizations and the rendering of their efficiencies. And finally, through a case study on promoting ecotourism services, we show the process of building a web map of Ichkeul National Park (INP).

Keywords: web-mapping, servers, ArcGis online, ecotourism development, Ichkeul National Park

Introduction

Since the development of information technologies and programs focused on the context of GIS, web mapping has experienced a great revolution. The spread of the Internet in everyday life has made it possible for users to interact with geographic data via internet browsers.

Géoweb, web-mapping, Sig-web, Carto-web, interactive cartography, computer graphics, Web design, datvisualization, etc., the names are numerous but the concept is the same. Web-mapping therefore brings together all of the technologies enabling a map to be displayed online. Thanks to the development of open source solutions, geographic information can be manipulated and viewed by different user profiles on the Internet. This increases the complexity of implementing GIS applications, both in terms of functional aspects, user interface and human-machine interaction (Schimiguel and *al*., 2005).

GIS-Web applications have touched all areas, particularly in the urban context, transport, risk management, regional development, environment, society, marketing, politics, etc. These applications represent a useful tool for people directly or indirectly involved in spatial analysis. They also acquire economic relevance. Using these applications by various users, and even managers, can be a simple, fast, web-based, and inexpensive solution. However, access to information in these GIS-Web applications depends on the interaction capabilities activated by their user interfaces. The rapid development of Géoweb tends to deeply modify the ways of visualizing and representing the world through digital data and maps (Mericskay, 2016).

The purpose of this article is to illustrate the concept and techniques of use in the context of GIS-Web application interfaces. Then, we present an overview on the uses of this technology by the various Tunisian state organizations and the rendering of their efficiencies. And finally, through a case study on promoting ecotourism services, we show the process of building a web map of Ichkeul National Park (INP).

1. The process of creating web maps

1.1. At an international level

Since the creation of Google Maps in 2005, web-mapping has grown a lot with the explosion of mobility and geolocation. With the development of smartphones, mobile interfaces and geolocation, it is becoming possible to have large volumes of data concerning tourist mobility (Genevois, 2018).

Basic applications provide interfaces that allow dynamic maps to be produced and published quickly and easily. Google Mymap (program developed by Google) and U-Map (developed by the OpenStreetMap community) are the most famous.

The powerful online GIS, often paid, offer multi-user operations allowing several users to intervene and collaborate on the same project. Among these online GIS is Carto.com, which offers free but limited use, particularly in terms of speed of display and the number of data that can be displayed. ArcGis Online offers simplified but powerful GIS functionality online. The free QGIS server application, an open source solution which has the principle of transposing the free GIS QuantumGIS desktop on the web.

The services offered by the above web applications make it possible to establish relations between the server which loads and stores the geographic data and the client who can configure and display the data. The geographic information stored in the server is organized in the form of attribute tables with geographic coordinates, which makes it possible to make attribute or location queries on the data. A GIS-Web application can provide visualizations of geographic information and can allow certain types of interaction with maps, such as zooming, panning, various queries and images as raster files and using commands languages such as HTML. The uploading of geographic data is done through two standard data exchange protocols. The first, WFS, is vector data. The second, WMS, corresponds to raster data. Among the open source and free computer servers we cite GeoServer (fig. 1) which allows users to share, modify geographic data and preview data layers. It publishes data from all major sources of spatial data using open standards: PostGIS, Oracle Spatial, MySQL, Shapefiles, GeoTIFF, JPEG 2000, etc. It also produces KML, GML, Shapefile, GeoRSS, PDF, GeoJSON, JPEG, GIF, SVG, PNG, etc.

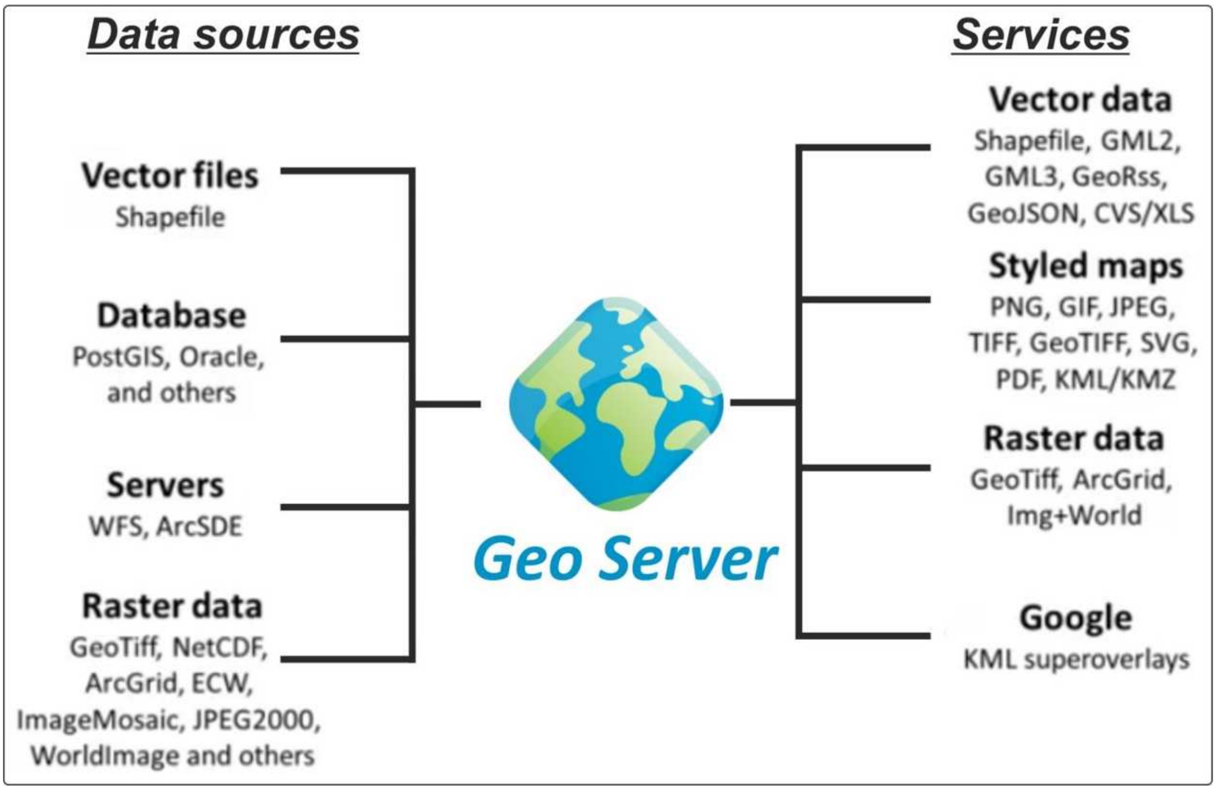

Fig. 1 : The inputs and outputs of the open source server "GeoServer"

Geoweb cartography takes shape in an environment where the traditional cartographic expression rules are no longer. The graphical representation of data has largely taken the step of computer graphics and web design (Mericskay, 2016). The user "cartographer" ignores the basic principles of graphics and does not know the functioning of cartographic communication, or even the foundations of graphic semiology (Griffin, Fabrikant, 2012)

1.2. The Tunisian experience

So many organizations which, to accomplish their private or public mission, have constituted for twenty years geo-spatial databases at variable scales in order to meet the most varied objectives (Joliveau and *a.l*, 2013). It is not a question here of attempting an inventory of them on the various attempts by the various Tunisian organizations to build a geoweb but rather of exposing, briefly, the treated topics and the organization of their databases.

Here we are looking at three departments that have invested in web mapping. The creation of Tunisian digital maps is an official commitment towards transparency and good governance. As part of the development of its tools and the quality of administration services in terms of urban management, decision-making and access to information, the Town Planning Department at the Ministry of Equipment, Housing and Spatial Planninghas set up a geographic information system for urban management and monitoring of urbanization called "SIG PAU". This GIS provides in practice an interface for consulting urbanization instruments, but above all a set of tools for easier management of an urban development plan (PAU) and multiple optimizations (fig. 2). This project makes available to the public 140 PAU in scanned version and 86 in digital vector version[1].

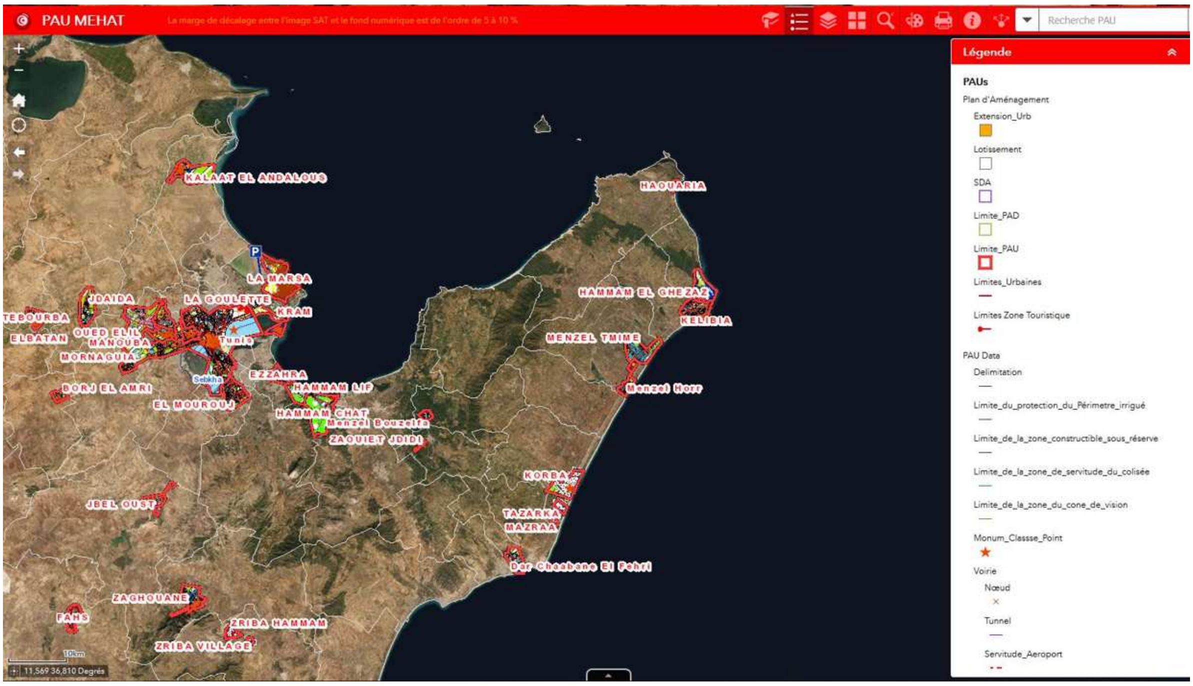

Fig.2 : The graphical interface that provides management and visualization of urban development plans in Tunisia (http://mehat.gov.tn)

The digital map of the Tunisian land domain is the work of the Ministry of State Domains and Land Affairs. It entered service since 2018 through the ministry's electronic site. This card is part of the program to strengthen the provision of public data to citizens, the consecration of good governance and transparency. The digital map of the land domain makes it possible to delimit the state land domain, to protect it, to control it and to ensure its good governance. The public will be able to consult it and use it in economic transactions. Among the areas to appear on the digital map, the geographical points of the archaeological and religious public domain.

The Ministry of Agriculture, Water Resources and Fisheries through its agridata[2] portal provides open source data on several agricultural activities such as plant activities, agricultural land development, water exploitation, the situation of dams, etc. Graphic and cartographic visualization is possible. The data is updated daily which allows users to follow

[1] http://mehat.gov.tn

[2] http://www.agridata.tn/fr

the evolution of the condition of the dams, water consumption and the storage rate in all Tunisian dams (fig. 3).

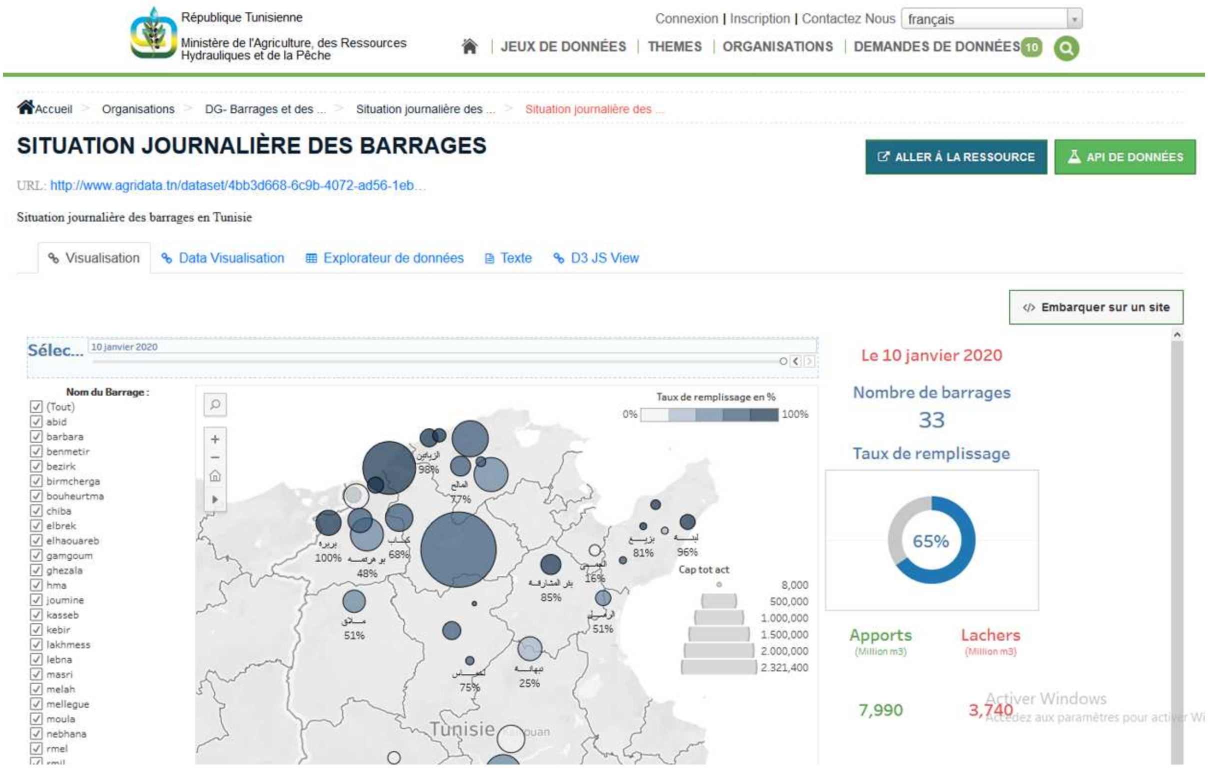

Fig. 3 : The "agridata" portal of the Ministry of Agriculture, Water Resources and Fisheries (http://www.agridata.tn/fr)

2. Development of web-mapping on INP

The aim of carrying out a web mapping on the INP is the promotion of ecological and tourist potential within the park. The study of the location of ecotourism activities at INP involves the use of data available from various official public bodies, NGOs and geolocation work in the field.

Before presenting the characteristics of the site and the stages which led to the implementation of a web-mapping on the INP, it is wise to clarify the concept of ecotourism which presents the generating question in this work.

2.1. The concept of ecotourism

Social conditions and economic crises have prompted communities around the world to seek local solutions and alternatives to achieve sustainable economic growth. This action refers to local "LED" economic development (Rakotozafy, 2005) which brings together cultural, environmental, tourist potential, etc. in order to improve the quality of life of the community. In this section, "ecotourism" is experienced as a form of tourism that focuses on nature (Tardif, 2003). This so-called "ecological" tourism is based on criteria or dimensions relating to the interaction between the social context and nature, the tourism product offered and the management (public or private) of a site.

However, this economic development (formal or informal), which opts for a new local dynamism, must not come at the expense of ecosystems (Boiral, 2004). In this perspective, ecotourism activities must be framed by efforts that combine both conservation and the protection of protected areas and the socio-economic development of communities. We can then say that ecotourism is a multidisciplinary and complex phenomenon, to make it successful, many aspects must be addressed (Rakotozafy, 2005) and diagnose, a participative governance that involves the various actors concerned must be established.

Developing a tourist-ecological activity, without disfiguring and compromising the ecosystem requires, among other things, awareness-raising efforts. These can be widely disseminated through web-mapping. Indeed, the conceptualization and structuring of a database with spatial reference encompassing the assets of the site (Ichkeul national park) and disseminated via the internet tool can constitute a point of influence to promote tourist activity and preserve the ecosystem.

In his encyclopedic dictionary of biological diversity and nature conservation, Triplet P. (2017) considers that in approaches seeking to establish the value of a site, the measurement of tourist attractiveness derives from studies on sites classified for their natural and cultural value which are generally high tourist places. The most common valuation approach consists in evaluating the sums spent by visitors, in particular non-residents of the territory considered. This evaluation must take into account direct and indirect spinoffs.

The direct benefits correspond to the amounts spent by tourists in establishments directly dependent on the site, mainly in the protected area (paid visits and activities, shops, restaurants, parking lots, accommodation).The indirect benefits correspond to the total expenditure made by tourists in shops, services and establishments located near the site or benefiting from its attractiveness.

2.2. Presentation of Ichkeul National Park

2.2.1. The geographic setting

Located at 37 ° 7’ North latitude and 9 ° 40’ East longitude, the Ichkeul National Park occupies the center of the Plain of Mateur. It is part of the relief of the Mediterranean Tell and more precisely of the Mogods (fig. 4). The INP has three components, namely:

- A mountain range.
- A lake.
- A Wetlands.

As for the mountain range, which will be the subject of our study, has an area of 1,363 hectares or 10.8% of the area of the park (Jaziri, 2002). Despite this importance, the INP has not escaped human activities which threaten its fragile natural ecosystem such as mining, overgrazing, salinity of the waters, etc.

Although the altitude is modest (510m), the jbal Ichkeul presents itself as an inselberg which cuts the flatness of the surrounding relief: those of Garaât Ichkeul to the north and those of the

Mateur plain to the south. The crest line has an acute vertex. Some vertices are rounded. They are found at low altitude and at the eastern and western ends of the jbal (fig. 5). The jbal stretches from west to east for 7 km and from north to south for 3 km. On the slopes of the jbal, several rocky outcrops appear especially on the slopes exposed to the South and stripped of dense plant cover (fig. 5). On the south side is a wide plain dating from the quaternary period and dissected by a dense hydrographic network with perennial flow such as the oued Joumine, oued Ghzala, oued el Melah ... (fig. 4). This plain was formerly completely invaded by water (*Lacus Sisara*) giving the island of Ichkeul. It was filled with fine deposits from streams.

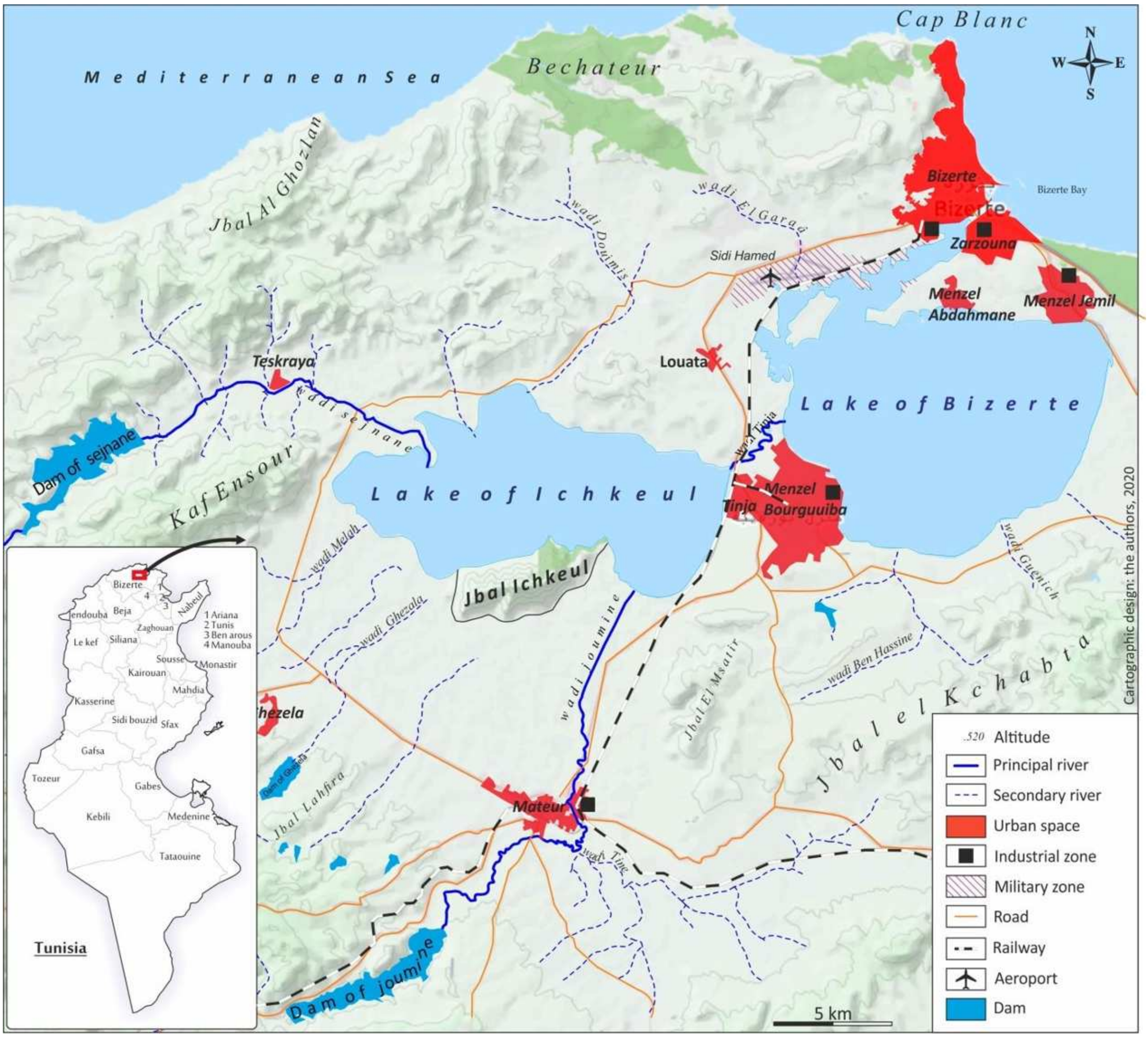

Fig. 4 : Location and delimitation of the Ichkeul national park

The INP constitutes an essential relay for hundreds of thousands of migratory birds. It is home to nearly 600 types of vegetation. The northern slope of the Ichkeul is wetter, more shaded and far from any destructive human activity. It houses the most lush and most advanced formations of the jbal. The luxuriance of the plant cover results in:

- A higher density.

- A complex vertical structure (existence of several strata).
- Greater floristic richness. Most of the rare and endemic species are confined to this slope.

On the southern slope, the plant landscape is different. This slope is located in the upper semi-arid bioclimatic floor. The vegetation is less luxuriant due to the decrease in the amount of rain, the intense sunshine, the presence of skeletal soil, the importance of rock outcrops and the strong anthropic action. The southern slope shelters nearly 9 douars (douar H'ssine, douar Echchardoudi, douar Farch Aniba, douar Drid, douar El-feddane, douar Er-rchada, douar Bel-abed el kader, douar Nachmaïa and douar Es-souima). In addition, the INP is frequented by researchers, naturalists, students and high school students as well as vacationers.

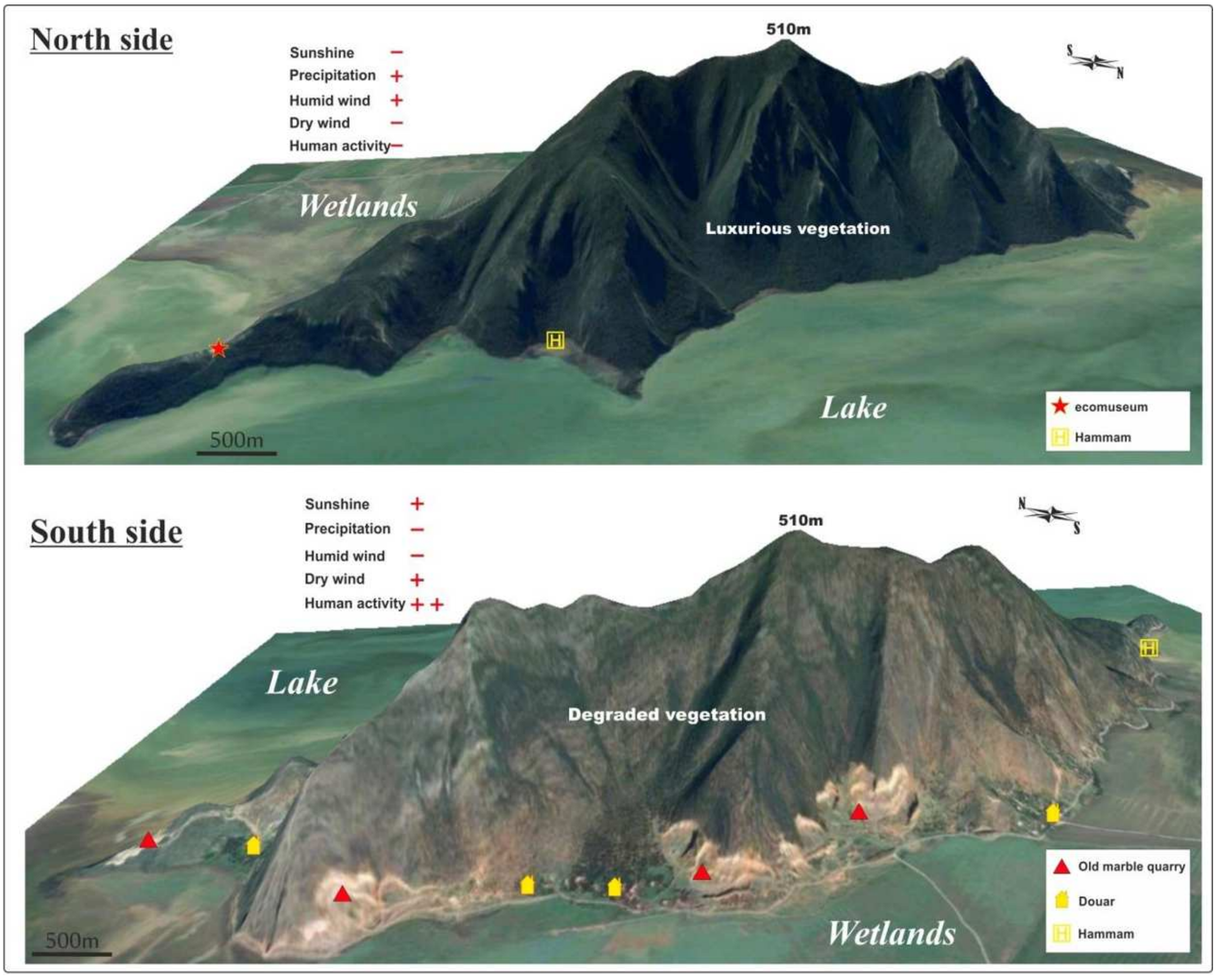

Fig. 5 : Opposition between the two sides of jbal Ichkeul (made with Global Mapper V.19)

2.2.2. Park residents and visitors

Residents of Ichkeul are in a vulnerable position due to lack of employment opportunities, forcing some to move and others to exploit forest resources by cutting and eradicating plant cover to convert land farmland and grazing with herds inside the reserve. All of this has harmful effects on the natural environment. The solution may lie in ecotourism, which would help improve the standard of living of the population by providing services to visitors.

The INP welcomes thousands of Tunisian and foreign visitors annually. However, this number varies depending on the year and the season. For example, in 1996 the number of visitors exceeded 60,000. The lowest number was recorded in 2006 with only 24,000. The period 2011 - 2012 was marked by a significant drop in their numbers, mainly due to the Tunisian revolution and the deterioration of security conditions. Over these two years, they did not exceed 30,000. Since 2014, the rate of visits has been increasing continuously, reaching 42,000 visitors in 2015 (Mosbahi, 2016). In general, the percentage of foreign visitors is much lower than that of domestic visitors. It oscillates between 1000 and 6000 visitors (in 2008).

The greatest number of visitors arriving at the INP occurs during the spring, due to the beauty of the natural landscapes of this period and the weather conditions favorable to hiking. In addition, the coincidence of early spring with the school holidays has an important role in increasing the number of visitors from families, pupils and students. As for the period during which the number of visitors decreases, it begins from June to September and coincides with summer. The decline in the number of visitors during this period explains that most people prefer to go to the coastal areas to swim or not to move to avoid the high temperatures. The fall and winter seasons from October to February see the return of visitors to the park with fewer spring periods. In winter, on rainy days, the number of visitors drops significantly. Then, the arrival of visitors is mainly during school holidays or weekends.

2.2.3. Places frequented by visitors

According to a survey by Mosbahi S. (2016) of 100 visitors, 53.2% of visitors prefer to travel on the ecotourism circuit to the point of panoramic view over a length of 4 km. This circuit is arranged by 26 picnic areas with tables and chairs built in cut stones and which allow to accommodate families. About 26% of visitors go to the baths where thermal springs spring up, such as Hammam Ennagrez, for hospitalization and rest. Among the most visited places is the ecomuseum with 13% of the visits. This eco-museum presents, through boards and display cases, the main plant and animal species in the park. Only 4.3% of visitors go to the cave, because of its fairly large distance from the car parks and the difficulty of accessing it due to the rough terrain. In addition, its visitors must be very careful to avoid accidents such as falls. Sometimes going down into the cave requires the use of expensive special tools such as climbing ropes, shoes and a special helmet that are not accessible to everyone. Visitors to the cave are therefore either members of speleology associations or climbing enthusiasts. The rest of the visitors were lonely and isolated in order to enjoy the scenery and drink alcoholic beverages, especially on the south bank of the mountain near the old quarries.

3. **The implementation of a web-mapping-INP**

At this level, some questions arise. They mainly concern the relevance and reliability of the selected data, the way in which it is possible to integrate the elements of the map into the web and how to ensure the transition from a GIS to a web-mapping?

Several servers are in free access. Some are efficient than others in that they display interactive maps and spatial references. The standard is the Open Geospatial Consortium (OGC), the objective of which is to enhance the assets of the site studied and to make them communicate and visualize geographic information on nested scales, we opted for "ArcGis

Online". The general architecture and the functionalities of our application are represented by the diagram below (fig. 6)

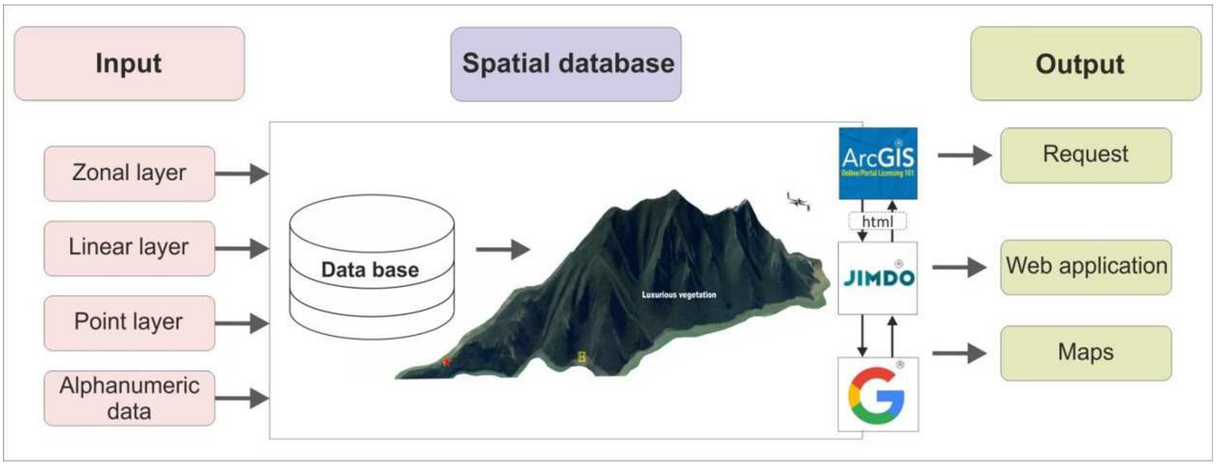

Fig. 6 : General architecture and functionality of web-mapping-INP via the "ArcGis online" application.

The first step is to collect and structure the geographic data (input). Most of the data referenced (Table 1) is collected in the field using the Smartphone application "my GPS coordinates". The latter allowed us to take advantage of direct shooting and a photo-database attached to real Cartesian coordinates. In order to ensure the integration and migration of data on the various GIS software used, the UTM spatial reference system was favored (Universal projection of Transverse Mercator, Zone 32 Nord-Datum WGS 84). Other statistical data was collected from the municipality of Tinja, from organizations involved in the management and governance of the site (Directorate General of Forests (DGF), National Agency for Environmental Protection (ANPE)), NGOs… and served as the basis for completing the attribute tables of the entities.

Table 1: Geographic data used in the INP web-mapping

Geographic entity	Cartographic layout	Source
Rest area	Punctual	Ground
Picnic area	Punctual	Ground
Ecomuseum	Punctual	Ground
Circuit / Track	Linear	Google Earth
Panoramic view area	Punctual	Ground
hammam	Punctual	Ground
Car park	Punctual	Ground
Reception center	Punctual	Ground
Douar	Punctual	Ground
Roman ruin	zonal	Ground
Vegetation	zonal	Phyto-ecological map
Altitude class	zonal	SRTM (www.usgs.gov)

The layers are prepared with classic GIS software such as Q-Gis or Arc Map. The map layers created must be compressed in order to integrate them into the web-mapping server. After importing the data, we are offered several customizable representation modes (size, color, value) but not always necessarily suited to the data to be mapped. From the first access, ArcGis Online offers free mapping space with interactive cartographic support. The work is done with the generator of web applications. The latter offers the possibility of directly creating and drawing the selected entity layers on a ready graphical interface or of associating them from other GIS applications. The environment of ArcGis online also allowed us to configure by scripts (included in html) and to configure the generators of the layers or the generators of the services in order to authorize the users thereafter to explore and manage the windows of displays.

The last step is to save the web project under the name "Géoweb Ichkeul" and authorize sharing. The generated script was incorporated by the free host Jimdo which makes it easier to share and publish for a fairly large audience. The appearance of the layers and the figures used obey roughly the strict rules of graphic semiology. The following figure shows the graphical interface of the web product produced (fig. 7).

Fig. 7 : Graphical interface of the consultation for the web mapping "Géoweb Ichkeul" https://geowebichkeul.jimdofree.com/

Conclusion

Through this work, we realized that platforms and web applications focused on the notion of referenced geographic information have multiplied and developed a lot. The generator of html tags and ArcGis online web applications allowed us to manage and enhance the potential of the environmental and ecological product of Ichkeul National Park. Indeed, within the cartographic environment of the application, certain Open source functionalities are oriented towards geomarketing by integrating the concepts of "competition", "accessibility" and "feasibility".

This is a first attempt in GIS mapping on the web, efforts are still necessary to improve the results obtained, this by more efficient choices of data (data quality) and methods (geometric errors of GPS points) but also through in-depth research on the site's management mode. Indeed, the INP, today shows signs of intolerance. Human pressure increased after the quarries closed. The inhabitants of the park have increased the number of their livestock, thus benefiting from a governance model that shows signs of weakness, and the participatory approach in the management of the site is almost absent. Despite its natural and landscaped potential and the large number of visitors, the production of tourist value for the local population and the park's management stakeholders remains negligible. The governance and promotion of the park must be carried out in a participatory manner where the local population will be considered as an active actor in any decision-making.

Bibliographic references

- Boiral O., 2004. Environnement et Economie : une relation équivoque. In la revue en science de l'environnement, vol.5, n°2. http://journals.openedition.org/vertigo/3386 ; DOI : 10.4000/vertigo.3386

- Genevois S., 2018. «Quels apports du Géoweb et de la géolocalisation pour représenter les mobilités touristiques ? » Mappe-monde, Numéro numéro 124 · Internet · Mise en ligne 05/2018 http://mappemonde.mgm.fr/124int1/

- Griffin A.L., Fabrikant S.I., 2012- « More Maps, More Users, More Devices Means More Cartographic Challenges », Cartographic Journal, (49) n°4, p. 298-301

- Jaziri B., (2002). Le parc national Ichkeul : l'homme et la végétation. Master's thesis, Faculty of Human and Social Sciences of Tunis, 74 p.

- Joliveau Th., Noucher M., Roche S., 2013. «La cartographie 2.0, vers une approche critique d'un nouveau régime cartographique». L'Information géographique, Armand Colin, n° 77 (4), pp.29-46.

- Mericskay B., 2016. «La cartographie à l'heure du Géoweb. Retour sur les nouveaux modes de représentation spatiale des données numériques», French Cartography Committee (CFC), n ° 229-230 September - December 2016) pp. 37-49.

- Mosbahi S., 2016, Valorisation des ressources naturelles dans le parc national de l'Ichkeul, license memory, Faculty of Human and Social Sciences of Tunis, 73p.

- Rakotozafy R., 2005. Perspective de développement de l'écotourisme : cas appliqué à Madagascar. Master of Business Administration, Université de Laval-Québec, 140 p.

- Schimiguel J., Meincke Melo A., Baranauskas C. et Bauzer Medeiros C., 2005. «Accessibility as a quality requirement : geographic information systems on the web. » CLIHC'05, publication of Association for Computing Machinery, pp. 8-19. https://doi.org/10.1145/1111360.1111362

- Tardif J., 2003 « Écotourisme et développement durable », VertigO - la revue électronique en sciences de l'environnement [En ligne], Volume 4 Numéro 1 | mai 2003, mis en ligne le 01 mai 2003. URL : http://journals.openedition.org/vertigo/4575 ; DOI : 10.4000/vertigo.4575

- Triplet P., 2017, Dictionnaire encyclopédique de la diversité biologique et de la conservation de la nature ; 1055p.

Websites

- www.mehat.gov.tn
- www.agridata.tn/fr
- www.usgs.gov
- https://www.ArcGis.com/home/index.html

Titre : Optimisation du drainage routier en relation avec la sécurité routière.

Candidate : Amal Saadi

Directeurs de thèse: Jamel Neji (ENIT)

Résumé

Notre approche, au cours de cette étude, s'articule autour de la relation étroite entre la sécurité routière et l'aménagement adéquat de l'infrastructure tendant à améliorer son assainissement.
Ce travail vise à renforcer la sécurité des conducteurs en améliorant l'adhérence des chaussées, notamment en minimisant la présence d'eau sur celles-ci, et ce en comprenant les phénomènes entrainant une perte d'adhérence néfaste suite à une plus ou moins faible couche d'eau sur la chaussée.
On a commencé par définir les notions physiques liées au phénomène d'adhérence. Puis on a consacré une partie pour l'exploitation et l'analyse de travaux expérimentaux antérieurs autour de la mesure de texture et de frottement d'échantillons de chaussées en présence de films d'eau de différentes épaisseurs.
De même notre travail met en exergue la relation primordiale entre les intempéries, les crues, le drainage et les hauteurs d'eau résiduelle sur la chaussée.
Cette thèse se déroule dans le cadre du projet"Villes prudentes"de l'association tunisienne de la prévention routière.

Mots clés : Drainage, sécurité routière, adhérence, Frottement, Glissement, Hydro-planage

Bearing Fault Diagnosis Method Based on Vibration Image and Convolutional Neural Network

Amarouayache Iskander Imed Eddine
Research Laboratory of Industril Risks, Non-Destructive Control and Operating Safety
University of Badji Mokhtar
Annaba, Algeria
amarouayache23i@gmail.com

Saadi Mohamed Nacer
Research Laboratory of Industril Risks, Non-Destructive Control and Operating Safety
University of Badji Mokhtar
Annaba, Algeria
Mn_saadi@yahoo.fr

Guersi Nourreddine
Research Laboratory of Industril Risks, Non-Destructive Control and Operating Safety
University of Badji Mokhtar
Annaba, Algeria
guersi54@yahoo.fr

***Abstract*— Building an intelligent monitoring system enable to detect incipient bearing faults is still a major challenge for scientists in fault diagnosis domain. The earlier fault detection leads to a real benefits for the economic state of the industrial companies and avoids time and money losses. In this paper, we propose a strong method based on the conversion process of vibration signals into a 2D gray scale images that are used afterward as an input for a convolutional neural network. The proposed method has shown a big reliability and robustness for fault identification where the performance attains a high classification accuracy under different working conditions.**

***Keywords*— vibration, bearing fault diagnosis, vibration image, convolutional neural network**

I. Introduction

Bearings are a fundamental organ and a critical component in rotary machines that are exploited in the industrial systems for light and heavy manufacturing production. The bearing faults are partitioned into two categories. The first category is known as distributed defects that includes misalignment races, waviness, surface roughness and unequal rolling element diameter. These bearing damages are primarily caused by manufacturing mistakes, unsuitable installation or mounting and abrasive wear. The second category is recognized as localized defects that includes each of pits, cracks and spalls. These bearing faults may mainly arise due to fatigue on rolling surfaces. Monitoring and earlier identification of failures affecting bearings conducts to a many advantages such as management of maintenance intervention. There are a diverse condition monitoring techniques that are utilized in bearing fault diagnosis field such as motor current analysis, wear debris analysis, temperature monitoring, oil analysis, acoustic emission and vibration analysis. Actually, vibration analysis technique is the most popular and powerful tool for solving fault diagnosis problems especially in the case of non-stationary signals generated from faulted bearings. These last years, many researchers have been worked on vibration analysis methods that exploits machine-learning algorithms where the artificial intelligence is integrated in fault prognostic domain [1]. Traditional fault detection approaches requires a signal-processing step accompanied with feature extraction stage that need a proficient knowledge. Then, a classification stage is performed via an ML technique where a developed classifier is applied to predict fault occurrence in terms of class and severity. In order to extract and identify the useful features from vibration signals of operating bearing, researchers have applied various manual and empirical analysis techniques that are divided into three principal categories: time domain analysis [2], frequency domain analysis [3] and time-frequency analysis [9]. Time domains features includes statistical features that can capture changes in amplitude and phase resulted from faulted bearing [4]. The frequency analysis methods extract the features more easily to identify the distributed defects with clear sidebands [5]. Time-frequency techniques are the most used approaches in the case of non-stationary vibration signals generated from defected bearings. Among these algorithms, empirical mode decomposition (EMD) [7], wavelet packet transform (WPT) [6] and short time Fourier transform (STFT) [8]. Traditional ML algorithms for performing classification includes SVM [7], KNN, naïve Bayes and decision tree [10]. Recently, deep learning algorithms based on convolutional neural network (CNN) have become the most popular tool due to their self-synthesized feature learning abilities that do not require any signal-processing and manual features extraction steps [11]. CNN algorithms are widely and successfully used by researchers on varied applications including fault diagnosis field [12] [13] [15]. Through this fact, the present investigation aims to explore the efficiency and the performance of CNN algorithm for fault identification and localization of the most frequently occurring bearing defects in rotating machinery.

II. The Proposed Bearing Fault Diagnosis Method

A. *Vibration signal to vibration image conversion*

The idea of this method is to convert the measured bearing vibration signals that are a 1D data form to a 2D vibration images that are fed later as an input to a CNN model. This data processing technique is based on the normalization of each sample amplitude in the raw signal into the range [-1, 1]. Then, the normalized amplitude of each sample becomes the intensity pixel in the corresponding image. The main advantage of this method is that it provides an approach to explore 2D features of the 1D vibration signal where the conversion operation can be realized without any predefined parameters. The following equation describes the transformation process between the normalized amplitude of sample and the corresponding pixel [14]:

$$P[i, j] = A[(i-1)\times M + j] \tag{1}$$

where $i = 1:N$; $j = 1:M$; $P[i, j]$ is the intensity of the corresponding pixel (i, j) (i, j) in the $M \times N$ vibration image. $A = [.]$ is the normalized amplitude of the sample in the raw signal. The number of pixels in the 2D vibration image equals to number of samples in the 1D vibration signal.

B. Introduction to CNN

Convolutional neural network (CNN) is a deep learning technique (DL) that is a feed forward artificial neural network (ANN) with specifics layers, which are used as feature extractors. The main architecture of CNN contains two basic stages, the feature extraction and feature classification stages. The first stage consists of convolution layers, activation layers and sub-sampling layers that are utilized for extracting the significant features from the input signal. Due to this fact, CNN is characterized by the ability of automatic feature learning that does not require any handcrafted features feeding. The second stage is composed by fully connected layers and Softmax function that are used for classification task of the learned features. Recently, CNNs have a successful performance on challenging ambit of pattern recognition and computer visions tasks. Through this paper, we need to explore the efficiency and the capacity of 2D-CNNs models in bearing faults diagnosis field. The particulars components of CNN structure are defined in the following titles.

C. Convolution layer

The convolution layer includes convolution kernels that are also known as kernels filters. Each filter in CL layer has different weights that are computed automatically by an error back propagation algorithm. The input feature maps is convolved by ensemble of learnable kernels filters in order to generate new feature maps that are used afterward as an input to the next layer. In general, the CL model can be defined by the following mathematical equation:

$$(w*a)_{ij} = \sum_{m=0}^{k_1-1}\sum_{n=0}^{k_2-1} w(i-m, j-n)a(m,n) \tag{2}$$

where $*$ denotes the convolution operation, w represents the convolutional kernel and a is the activation function output at the previous layer.

D. Sub-sampling layer

The subsampling layer is also known as pooling layer that is a nonlinear technique. The SL layer is utilized for reducing sampling in order to eliminate redundant information of the input. Consequently, it decreases the learning parameters of the adopted CNN and ameliorates the learning performance of the network. In this work, max pooling $P_{\max}$ is the selected method for performing subsampling operations and it takes the maximum value of x_i in the feature map as the output.

$$P_{\max} = \max\{x_i\} \tag{3}$$

E. Activation layer

Activation layers (FLs) are used for transforming the output values into a highly nonlinear and classifiable transformation by an activation function after a convolution operation. In this work, the selected activation functions $f(x)$ are ReLU (Rectified Linear Unit) for convolution layers and Sigmoid functions for the fully connected layers in order to reinforce the feature separability after the transformation process. Each of chosen activation function is described mathematically by the following equation:

$$\text{ReLU:}\quad f(x) = \begin{cases} x, x \geq 0 \\ 0, x < 0 \end{cases} \tag{4}$$

$$\text{Sigmoid:}\quad f(x) = \frac{1}{1+e^{-x}} \tag{5}$$

F. Fully-connected layer

After alternating convolution, sub-sampling and activation layers, the objective behind the utilization of fully connected layer (FL) is for mapping the features and high-level reasoning. In FL, each neuron is connected to all nodes in the previous layer. The activation function used by the hidden layer is the sigmoid function.

G. Loss function

CNN method calculates the error by comparing the current predicted value to the actual label value in each training data and updates both weight and bias of each layer via a backpropagation algorithm in order to ameliorate accuracy of the training results. The proposed model uses the cross-entropy $H(p,q)$ $H(p,q)$ as a loss function that is defined in theory by the following equation:

$$H(p,q) = -\sum_x p(x)\log q(x) \tag{6}$$

where $p(x)$ denotes the target class probability distribution and $q(x)$ represents the estimated Softmax output probability distribution.

The purpose of this study is to classify accurately the bearing faults from vibration images. Therefore, we use Softmax classifier for obtaining the highest predicted probability among fault types in the diagnosis results. Fig. 1 shows the flowchart of the proposed bearing fault prognostic method.

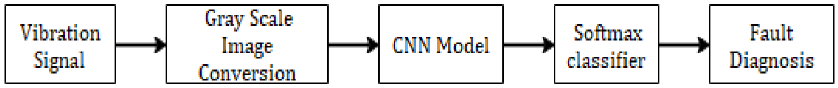

Fig. 1. Flowchart of the proposed diagnosis method.

III. EXPERIMENTS

A. *Dataset source and data preprocessing*

The vibration data are chosen from the open source Bearing Data Center of the Case Western Reserve University (CWRU). Data are collected from accelerometers that are attached to the housing with magnetic bases of the motor driving mechanical system at a sampling frequency of 12 kHz. The operating conditions are considered with bearing 6205-2RS JEM SKM with a single degree of damage diameter that equals to 0.0007 inch. Moreover, the used bearings have three types of defect: inner race fault, outer race fault and ball fault. In this experiment, we prepare four datasets A, B, C and D corresponding to different load conditions 0, 1, 2 and 3 *hp*, respectively. We have a total of 3 different faults and one normal condition (Healthy bearing) therefore, each load condition has 4 classes. Table 1 shows the working bearing states per labels.

In order to have enough samples to train our CNN model, the vibration signals are divided into segments of the same length by an overlapped segmentation. The chosen length of segment must be a square number for easily transforming signal segments into vibration images. We select segment size of 576 data points corresponding to vibration image of size 24 x 24 that contains in total 576 pixels. The conversion process of 1D vibration signal to a 2D gray scale image is explained in the section II.A and fig. 2 shows the obtained vibration images corresponding to load 0 *hp*.

In our experiment, we have 500 vibration images for each fault type. Then, for three fault types including the normal condition, we obtain 2000 vibration images in total for each load condition and Table 2 shows the arrangement of the constructed datasets.

Table1.
The used bearing states per label

Bearing state	**Label**
Normal condition	1
Outer race fault	2
Inner race fault	3
Fault in ball	4

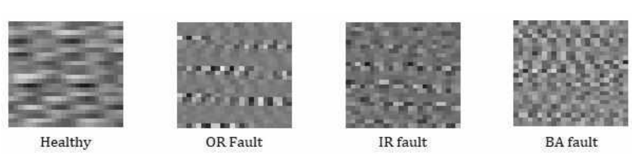

Fig. 2. Vibration images

Table 2.
Dataset arrangement of vibration images.

Dataset Name	**Number of images**	**Load condition**
A	2000	0 *hp*
B	2000	1 *hp*
C	2000	2 *hp*
D	2000	*3 hp*

B. *Structure of the adopted CNN*

The input layer of CNN model must have the same size as the transformed vibration images 24x24 and because of the small size of the gray images, we construct a basic type of CNN structure that contains only two successive convolutional layers of kernel size 5x5 for the first CL and 3x3 for the second CL. Each CL layer is connected to a max-pooling layer (SL) of size 2x2. The number of kernel for each layer is defined experimentally and after several tests, the final selected hyper-parameters of the adopted CNN model are described in table 3.

C. *Results and discussions*

We train the CNN model by 60% of vibration images (1200 training images) from data set A while the rest is left as testing data (800 testing images). The performance of the proposed CNN model reaches 100% of classification accuracy and the detailed classification results are clarified in the confusion matrix presented in Fig. 3.

From the confusion matrix, we can see that the proposed method identifies successfully all fault types under the same load condition (dataset A Load 0) where the diagnosis rate attains a highest accuracy. In the real industrial systems, Bearings as a fundamental component of rotating machinery have to keep operating under diverse conditions. For this fact, we need to examine our bearing diagnosis approach under variable working conditions including both load and noise conditions.
In order to evaluate our diagnosis method under different load conditions and without retraining our diagnosis system, we perform 4 experiments where the selected CNN is trained by 1200 vibration images from one data set as mentioned in table 1 and is tested afterward by 2400 images from three other data sets. The attained performances are shown in table 4.
In the first experiment, we train our CNN model by 1200 vibration images from data set A whilst, 800 vibration images from each dataset B, C and D (total of 2400 images) are utilized for testing the trained CNN model. Each of experiments 2, 3 and 4 is performed by the same way as the

Table 3.
The Structure of our CNN model.

Layer type	Kernel size	Kernel number	Output size
CL1	5x5	30	20x20
SL1	2x2	30	10x10
CL2	3x3	60	8x8
SL2	2x2	60	4x4

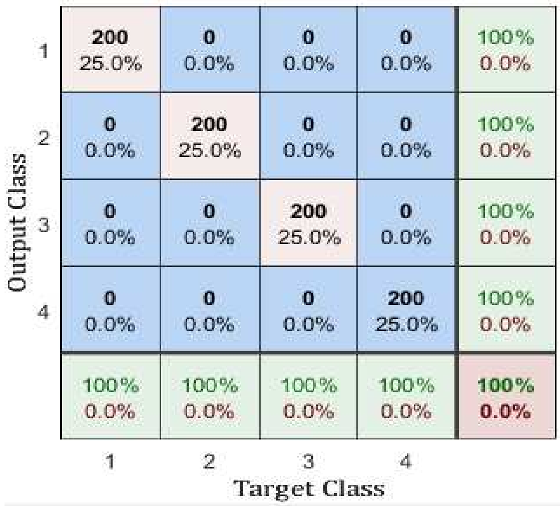

Fig. 3. Confusion matrix of the obtained results under the same load condition

first experiment except that the training-testing datasets are alternated.

As shown in table 3, the lowest performance is noted in the experiment four where the fault identification efficiency attains a high classification accuracy that equals to 99.92%. On the other hand and in each experiment 1, 2 and 3, the diagnosis performances achieve 100% of prognostic precision. As a result, these experiments prove the high efficiency of the proposed method for bearing fault diagnosis where it is clarified that without retraining the CNN model, our approach stills reaching a high performance under different load conditions.

In order to evaluate the proposed diagnosis system under different noise conditions, we add variable standard variances of additive Gaussian white noise (AGWN) to the original vibration signals to form noisy signals as defined by the following mathematical expression of signal-to-noise ratio (SNR):

$$SNR = 10\log_{10}\left(\frac{P_{signal}}{P_{noise}}\right) \tag{7}$$

where P_{signal} and P_{noise} denote the power of signal and noise in that signal respectively. The examination is under low and high SNR values that are varying from -4 dB to 10 dB (decibel).

Table 4.
The Classification accuracy under variable load conditions.

Experiment	Trained dataset	Tested datasets	Accuracy
1	A	B, C and D	100%
2	B	A, C and D	100%
3	C	A, B and D	100%
4	D	A, B and C	99.92%

The same precedents processes are realized on the noisy signals including splitting into segments that are converted afterward into a gray scale images.

Then, the noisy vibration images are considered as an input to the adopted CNN model and the fault diagnosis accuracies of the proposed method under variable values of SNR are shown in fig. 4.

From fig. 4, we can obviously see that the proposed CNN model keeps achieving 100% of classification accuracy under high values of SNR that are varied from 0 dB to 10 Db. However under low values of SNR, the performance degrades and the classification accuracy attains 99% and 95.75% depending to SNR=-2 dB and SNR=-4 dB respectively. The obtained satisfactory results demonstrate the high robustness and effectiveness of the proposed fault diagnosis approach that stills working well under randomly added noise conditions.

IV. CONCLUSION

In this paper, we proposed a robust approach based on CNN algorithm for bearing faults diagnosis. The proposed method exploits the efficiency of CNN to extract automatically the significant features from the transformed vibration images without requiring any signal processing. The adopted diagnosis system has a good performance that reaches 100% of classification accuracy. In addition, when the working load condition is changed and without retraining our CNN model, the proposed diagnosis system still works well by maintaining a high fault identification performance. Furthermore, the proposed method has the reliability, robustness and ability to work under noisy environments without any denoising process.

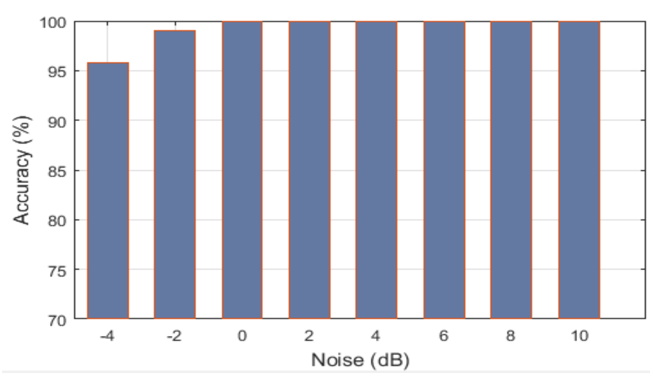

Fig. 4. The performance histogram of the proposed scheme under different noise conditions

References

[2] J. Chang, T. Li, & P. Li, “The selection of time domain characteristic parameters of rotating machinery fault diagnosis”. 2010 International Conference on Logistics Systems and Intelligent Management (ICLSIM), 2010.

[3] C. Bianchini, F. Immovilli, M. Cocconcelli, R. Rubini, and A. Bellini, “Fault detection of linear bearings in brushless ac linear motors by vibration analysis,” IEEE Transactions on Industrial Electronics, vol. 58, no. 5, pp. 1684–1694, December 2011.

[4] B. R. Nayana, P. GEETHANJALI, “Effective Time Domain Features for Identification of Bearing Fault using LDA and NB Classifiers”. International Journal of Mechanical and Production Engineering Research and Development, Vol. 8, pp. 1135-1150, January 2018.

[5] J. ZHOU, Y. QIN, L. KOU, M. YUWONO, & S. SU, “Fault detection of rolling bearing based on FFT and classification”. Journal of Advanced Mechanical Design, Systems, and Manufacturing, 9(5), October 2015.

[6] Sheng-wei Fei, “Fault Diagnosis of Bearing Based on Wavelet Packet Transform-Phase Space Reconstruction-Singular Value Decomposition and SVM Classifier”. Arabian Journal for Science and Engineering, vol. 42(5), pp. 1967–1975, January 2017.

[7] M. Beibei, S. Yanxia, W. Dinghui, & Z. Zhipu, “Three level inverter fault diagnosis using EMD and support vector machine approach”. 2017 12th IEEE Conference on Industrial Electronics and Applications (ICIEA), 2017.

[8] H. Liu., L. Li, & J. Ma, “Rolling Bearing Fault Diagnosis Based on STFT-Deep Learning and Sound Signals”. Shock and Vibration, 1–12, September 2016.

[1] R. Liu, B. Yang, E. Zio, & X. Chen,“Artificial intelligence for fault diagnosis of rotating machinery: A review”. Mechanical Systems and Signal Processing, Vol. 108, pp. 33-47, August 2018.

[9] Z. H. Luo, & Q. J. Xiao, “Time-Frequency Features of Signal Analysis and its Application in Mechanical Fault Diagnosis”. Advanced Materials Research, 834-836, October 2013.

[10] M. Jung, O. Niculita, & Z. Skaf, “Comparison of Different Classification Algorithms for Fault Detection and Fault Isolation in Complex Systems”. Procedia Manufacturing, vol. 19, pp. 111–118, January 2018.

[11] D. Weimer, B. Scholz-Reiter, and M. Shpitalni, “Design of deep convolutional neural network architectures for automated feature extraction in Industrial inspection”.CIRP Ann.-Manuf. Technol., vol. 65, no. 1,pp. 417-420, May 2016.

[12] O. Abdeljaber, O. Avci, S. Kiranyaz, M. Gabbouj, and D. J. Inman, “Realtime vibration-based structural damage detection using one-dimensional convolutional neural networks” J. Sound Vib., vol. 388, pp. 154-170, February 2017.

[13] P. Cao, S. Zhang, & J. Tang, “Preprocessing-Free Gear Fault Diagnosis Using Small Datasets With Deep Convolutional Neural Network-Based Transfer Learning”. IEEE Access, vol. 6, pp. 26241–26253, May 2018.

[14] D. Nguyen, M. Kang, C. Kim, & J. Kim, “Highly reliable state monitoring system for induction motors using dominant features in a two-dimension vibration signal”. New Review of Hypermedia and Multimedia, vol 19(3-4), pp. 248–258, October 2013.

[15] M. Xia, T. Li, L. Xu, L. Liu and C. de Silva, “Fault Diagnosis for Rotating Machinery Using Multiple Sensors and Convolutional Neural Networks”, IEEE/ASME Transactions on Mechatronics, vol. 23, no. 1, pp. 101-110, February 2018.

Bearing Fault Diagnosis Method Based on Vibration Image and Convolutional Neural Network

Amarouayache Iskander Imed Eddine
Research Laboratory of Industril Risks, Non-Destructive Control and Operating Safety
University of Badji Mokhtar
Annaba, Algeria
amarouayache23i@gmail.com

Saadi Mohamed Nacer
Research Laboratory of Industril Risks, Non-Destructive Control and Operating Safety
University of Badji Mokhtar
Annaba, Algeria
Mn_saadi@yahoo.fr

Guersi Nourreddine
Research Laboratory of Industril Risks, Non-Destructive Control and Operating Safety
University of Badji Mokhtar
Annaba, Algeria
guersi54@yahoo.fr

***Abstract*— Building an intelligent monitoring system enable to detect incipient bearing faults is still a major challenge for scientists in fault diagnosis domain. The earlier fault detection leads to a real benefits for the economic state of the industrial companies and avoids time and money losses. In this paper, we propose a strong method based on the conversion process of vibration signals into a 2D gray scale images that are used afterward as an input for a convolutional neural network. The proposed method has shown a big reliability and robustness for fault identification where the performance attains a high classification accuracy under different working conditions.**

***Keywords*— vibration, bearing fault diagnosis, vibration image, convolutional neural network**

I. INTRODUCTION

Bearings are a fundamental organ and a critical component in rotary machines that are exploited in the industrial systems for light and heavy manufacturing production. The operation accuracy and safety reliability of bearings directly influence the overall performance of rotating machinery [1]. The bearing faults are partitioned into two categories. The first category is known as distributed defects that includes misalignment races, waviness, surface roughness and unequal rolling element diameter. These bearing damages are primarily caused by manufacturing mistakes, unsuitable installation or mounting and abrasive wear. The second category is recognized as localized defects that includes each of pits, cracks and spalls. These bearing faults may mainly arise due to fatigue on rolling surfaces. Monitoring and earlier identification of failures affecting bearings conducts to a many advantages such as management of maintenance intervention. There are a diverse condition monitoring techniques that are utilized in bearing fault diagnosis field such as motor current analysis, wear debris analysis, temperature monitoring, oil analysis, acoustic emission and vibration analysis. Actually, vibration analysis technique is the most popular and powerful tool for solving fault diagnosis problems especially in the case of non-stationary signals generated from faulted bearings. These last years, many researchers have been worked on vibration analysis methods that exploits machine-learning algorithms where the artificial intelligence is integrated in fault prognostic domain [2]. Traditional fault detection approaches requires a signal-processing step accompanied with feature extraction stage that need a proficient knowledge. Then, a classification stage is performed via an ML technique where a developed classifier is applied to predict fault occurrence in terms of class and severity. In order to extract and identify the useful features from vibration signals of operating bearing, researchers have applied various manual and empirical analysis techniques that are divided into three principal categories: time domain analysis [3], frequency domain analysis [4] and time-frequency analysis [10]. Time domains features includes statistical features that can capture changes in amplitude and phase resulted from faulted bearing [5]. The frequency analysis methods extract the features more easily to identify the distributed defects with clear sidebands [6]. Time-frequency techniques are the most used approaches in the case of non-stationary vibration signals generated from defected bearings. Among these algorithms, empirical mode decomposition (EMD) [8], wavelet packet transform (WPT) [7] and short time Fourier transform (STFT) [9]. Traditional ML algorithms for performing classification includes SVM [8], KNN, naïve Bayes and decision tree [11]. Recently, deep learning algorithms based on convolutional neural network (CNN) have become the most popular tool due to their self-synthesized feature learning abilities that do not require any signal-processing and manual features extraction steps [12]. CNN algorithms are widely and successfully used by researchers on varied applications including fault diagnosis field [13] [14] [15] [16]. Through this fact, the present investigation aims to explore the efficiency and the performance of CNN algorithm for fault identification and localization of the most frequently occurring bearing defects in rotating machinery.

II. THE PROPOSED BEARING FAULT DIAGNOSIS METHOD

2.1. Vibration signal to vibration image conversion

The idea of this method is to convert the measured bearing vibration signals that are a 1D data form to a 2D vibration images that are fed later as an input to a CNN model. This data processing technique is based on the normalization of each sample amplitude in the raw signal into the range [-1, 1]. Then, the normalized amplitude of each sample becomes the intensity pixel in the corresponding image. The main advantage of this method is that it provides an approach to explore 2D features of the 1D vibration signal where the conversion operation can be realized without any predefined parameters. The following equation describes the transformation process between the normalized amplitude of sample and the corresponding pixel [14]:

$$P[i, j] = A[(i-1) \times M + j] \quad (1)$$

where $i = 1:N$; $j = 1:M$; $P[i, j]$ is the intensity of the corresponding pixel (i, j) (i, j) in the $M \times N$ vibration image. $A = [.]$ is the normalized amplitude of the sample in the raw signal. The number of pixels in the 2D vibration image equals to number of samples in the 1D vibration signal as shown in Fig. 1.

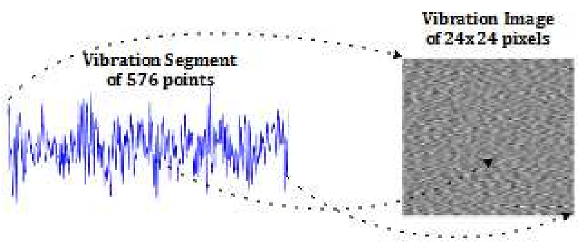

Fig. 1. Conversion process of 1D signal to 2D vibration image

2.2. Introduction to CNN

Convolutional neural network (CNN) is a deep learning technique (DL) that is a feed forward artificial neural network (ANN) with specifics layers, which are used as feature extractors. The main architecture of CNN contains two basic stages, the feature extraction and feature classification stages. The first stage consists of convolution layers, activation layers and sub-sampling layers that are utilized for extracting the significant features from the input signal. Due to this fact, CNN is characterized by the ability of automatic feature learning that does not require any handcrafted features feeding. The second stage is composed by fully connected layers and Softmax function that are used for classification task of the learned features. Recently, CNNs have a successful performance on challenging ambit of pattern recognition and computer visions tasks. Through this paper, we need to explore the efficiency and the capacity of 2D-CNNs models in bearing faults diagnosis field. The particulars components of CNN structure are defined in the following titles.

2.3. Convolution layer

The convolution layer includes convolution kernels that are also known as kernels filters. Each filter in CL layer has different weights that are computed automatically by an error back propagation algorithm. The input feature maps is convolved by ensemble of learnable kernels filters in order to generate new feature maps that are used afterward as an input to the next layer. In general, the CL model can be defined by the following mathematical equation:

$$(w * a)_{ij} = \sum_{m=0}^{k_1-1} \sum_{n=0}^{k_2-1} w(i-m, j-n)a(m,n) \quad (2)$$

where $*$ denotes the convolution operation, w represents the convolutional kernel and a is the activation function output at the previous layer. The schematic diagram presented in Fig. 2 describes the calculation principle of a convolution operation.

2.4. Sub-sampling layer

The subsampling layer is also known as pooling layer that is a nonlinear technique. The SL layer is utilized for reducing sampling in order to eliminate redundant information of the input. Consequently, it decreases the learning parameters of the adopted CNN and ameliorates the learning performance of the network. In this work, max pooling $P_{\max}$ is the selected method for performing subsampling operations and it takes the maximum value of x_i in the feature map as the output. The schematic diagram presented in Fig. 3 explains calculation principle of max-pooling operations.

$$P_{\max} = \max\{x_i\} \quad (3)$$

2.5. Activation layer

Activation layers (FLs) are used for transforming the output values into a highly nonlinear and classifiable transformation by an activation function after a convolution operation. In this work, the selected activation functions $f(x)$ are ReLU (Rectified Linear Unit) for convolution layers and Sigmoid functions for the fully connected layers in order to reinforce the feature separability after the transformation process. Each of chosen activation function is described mathematically by the following equation:

$$\text{ReLU:} \quad f(x) = \begin{cases} x, x \geq 0 \\ 0, x < 0 \end{cases} \quad (4)$$

$$\text{Sigmoid:} \quad f(x) = \frac{1}{1+e^{-x}} \quad (5)$$

2.6. Fully-connected layer

After alternating convolution, sub-sampling and activation layers, the objective behind the utilization of fully connected layer (FL) is for mapping the features and high-level reasoning. In FL, each neuron is connected to all nodes in the previous layer. The activation function used by the hidden layer is the sigmoid function as defined by Eq. 1.

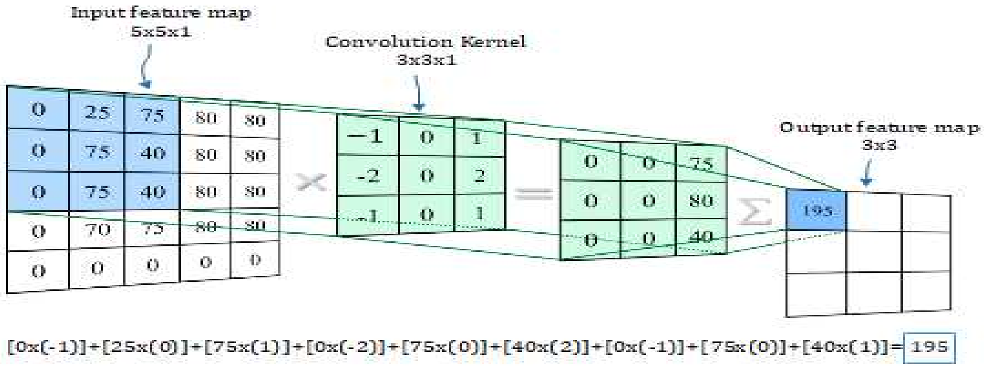

Fig. 2. The schematic diagram of a convolution operation.

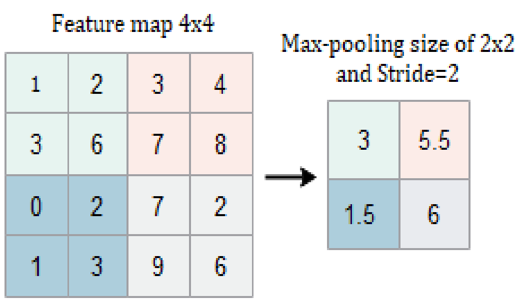

Fig. 3. Schematic diagram of Max-Pooling operation.

2.7. Loss function

CNN method calculates the error by comparing the current predicted value to the actual label value in each training data and updates both weight and bias of each layer via a backpropagation algorithm in order to ameliorate accuracy of the training results. The proposed model uses the cross-entropy as a loss function that is defined in theory by the following equation:

$$H(p,q) = -\sum_x p(x)\log q(x) \qquad (6)$$

where $p(x)$ denotes the target class probability distribution and $q(x)$ represents the estimated Softmax output probability distribution.

The purpose of this study is to classify accurately the bearing faults from vibration images. Therefore, we use Softmax classifier for obtaining the highest predicted probability among fault types in the diagnosis results. Fig. 4 shows the flowchart of the proposed bearing fault prognostic method.

3. EXPERIMENTS

3.1. Dataset source and data preprocessing

The vibration data are selected from the open source Bearing Data Center of the Case Western Reserve University (CWRU) [17]. Data are collected from accelerometers that are attached to the housing with magnetic bases of the motor driving mechanical system at a sampling frequency of 12 kHz. The operating conditions are considered with bearing 6205-2RS JEM SKM with a single degree of damage diameter that equals to 0.0007 inch. Moreover, the used bearings have three types of defect: inner race fault, outer race fault and ball fault. In this experiment, we prepare four datasets A, B, C and D corresponding to different load conditions 0, 1, 2 and 3 *hp*, respectively. We have a total of 3 different faults and one normal condition (Healthy bearing) therefore, each load condition has 4 classes. Table 1 illustrates the working states of bearing per labels and the collected vibration signals belonging to load 0 hp are shown in Fig. 5.

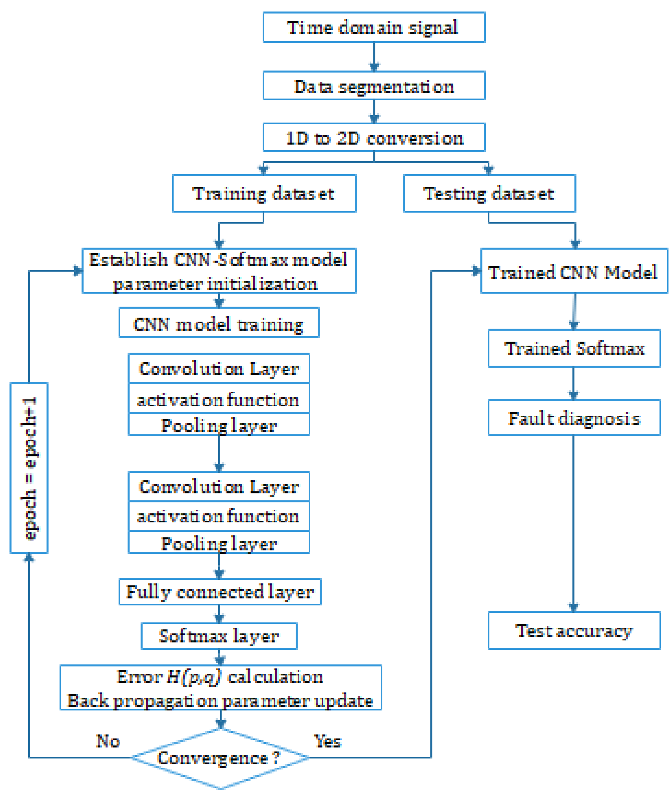

Fig. 4. Flowchart of the proposed fault diagnosis method.

Table1.
The used bearing states per label

Bearing state	Label
Normal condition	1
Outer race fault	2
Inner race fault	3
Fault in ball	4

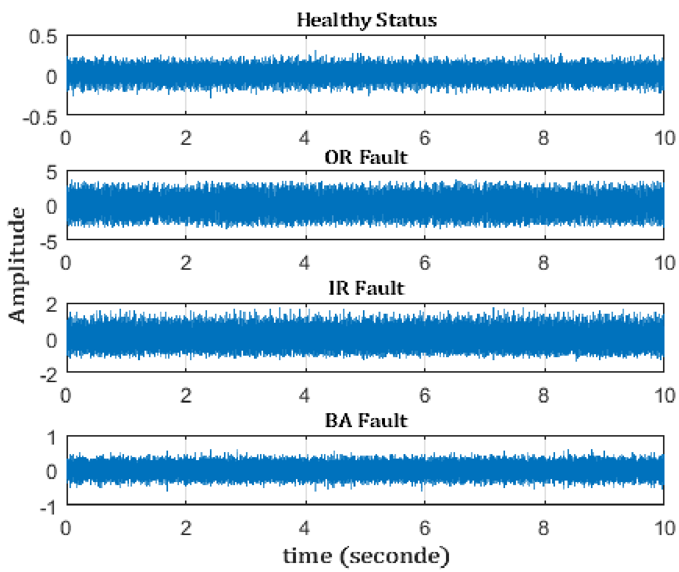

Fig. 5. Vibration signals at load of 0 hp.

In order to have enough samples to train our CNN model, the vibration signals are divided into segments of the same length by an overlapped segmentation. The chosen length of segment must be a square number for easily transforming signal segments into vibration images. We select segment size of 576 data points corresponding to vibration image of size 24 x 24 that contains in total 576 pixels. The conversion process of 1D vibration signal to a 2D gray scale image is explained in the section 2.1 and Fig. 6 shows the obtained vibration images corresponding to load 0 *hp*.

In our study, we have 500 vibration images for each fault type. Then, for three fault types including the normal condition, we obtain 2000 vibration images in total for each load condition and Table 2 shows the arrangement of the constructed datasets.

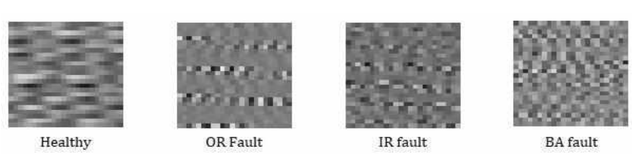

Fig. 6. Vibration images

Table 2.
Dataset arrangement of vibration images.

Dataset Name	Number of images	Load condition
A	2000	0 *hp*
B	2000	1 *hp*
C	2000	2 *hp*
D	2000	*3 hp*

3.2. Structure of the adopted CNN

The input layer of CNN model must have the same size as the transformed vibration images 24x24 and because of the small size of the gray images, we construct a basic type of CNN structure that contains only two successive convolutional layers of kernel size 5x5 for the first CL and 3x3 for the second CL. Each CL layer is connected to a max-pooling layer (SL) of size 2x2. The number of kernel for each layer is defined experimentally and after several tests, the final selected hyper-parameters of the adopted CNN model are described in table 3.

3.3. Results and discussions

3.3.1. Performance evaluation under the same load condition:

In the first experience, we train our CNN model by 60% of vibration images (1200 training images) from data set A while the rest is left as testing data (800 testing images). We are conducted to perform 3 other experiments by the same way as the precedent experiment where the training/Testing vibration images are alternated separately from datasets B, C and D respectively. The classification accuracies of the proposed method are recorded in table 4 and the detailed classification results are clarified in the confusion matrix presented in Fig. 7.

As mentioned in table 4, the proposed fault diagnosis technique reaches a high classification accuracy that equals to 100% in the four performed experiences.
From the confusion matrix, it is distinctly that the proposed method identifies successfully all fault types under the same load condition of operating bearing, where the diagnosis rate attains a highest accuracy.
In the real industrial installations, bearings as a fundamental component of rotating machinery have to keep operating under diverse conditions.

Table 3.
The Structure of our CNN model.

Layer type	Kernel size	Kernel number	Output size
CL1	5x5	30	20x20
SL1	2x2	30	10x10
CL2	3x3	60	8x8
SL2	2x2	60	4x4

Table.4.
Classification accuracy by our fault diagnosis approach.

Experiment	Dataset name Training (60%) / Testing (40%)	Accuracy
1	A	100%
2	B	100%
3	C	100%
4	D	100%

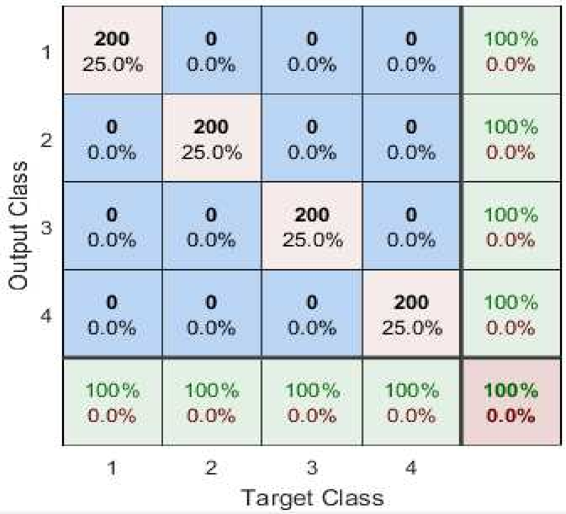

Fig. 7. Confusion matrix of the obtained results under the same load condition

This diversity of working situation comprise either load changes or noise. Load changes are caused by human intervention to accomplish different industrial tasks however, noise is caused by different harmonic interferences in industrial environment. For this fact, we need to examine our bearing diagnosis approach under variable working conditions including both load and noise conditions.

3.3.2. Evaluation the performance under different load conditions:

In order to assess robustness of the considered method under different load conditions, we train our CNN model by 60% of vibration images from each dataset A, B, C and D (4800 training samples) belonging to load 0, 1, 2 and 3 hp, respectively while the rest of the mentioned datasets is taken as testing vibration images (3200 testing samples). The different obtained results are described by the confusion matrix in Fig.8.

It is visibly clear from the summarized results presented in Fig. 8 that the designed fault diagnosis approach attains 100% of classification accuracy. The designed CNN model has successfully predicted the studied bearing status in their correct label with zero misclassification error.

Fig. 8. Confusion matrix of diagnosis results under different load conditions

This proposed test verifies the high reliability of the proposed fault prognostic method to detect the most occurring bearing defects under different load conditions.

3.3.3. Evaluation the performance under variable load conditions:

For the robustness assessment of our diagnosis method under variable load conditions and without retraining our diagnosis system, we perform 4 experiments where the selected CNN is trained by 1200 vibration images from a single set of data from table 2 and is tested afterward by 2400 images from three other datasets. The attained performances are arranged in table 5.

In the first experiment, we train our CNN algorithm by 1200 vibration images from data set A whilst, 800 vibration images from each dataset B, C and D (2400 images in total) are utilized for testing the trained CNN model. Each of experiments 2, 3 and 4 is performed by the same way as the first experiment except that the training-testing datasets are alternated. As shown in table 5, the lowest performance is noted in experiment four where the fault identification efficiency attains a high classification accuracy that equals to 99.92%. On the other hand and in each experiment 1, 2 and 3,

Table 5.
The Classification accuracy under variable load conditions.

Experiment	Trained dataset	Tested datasets	Accuracy
1	A	B, C and D	100%
2	B	A, C and D	100%
3	C	A, B and D	100%
4	D	A, B and C	99.92%

the diagnosis performances achieve 100% of prognostic accuracy. As a result, these experiments prove the high efficiency of the proposed method for bearing fault diagnosis where it is clarified that without retraining the CNN model, our approach stills reaching a high performance under variable load conditions.

3.3.4. Evaluation the performance under different noise conditions:

In order to evaluate the proposed diagnosis system under different noise conditions, we add variable standard variances of additive Gaussian white noise (AGWN) to the original vibration signals to form noisy signals as defined by the following mathematical expression of signal-to-noise ratio (SNR):

$$SNR = 10\log_{10}\left(\frac{P_{signal}}{P_{noise}}\right) \quad (7)$$

where P_{signal} and P_{noise} denote the power of signal and noise in that signal respectively. The examination is under low and high SNR values that are varying from -4 dB to 10 dB (decibel). Fig. 9 shows vibration signals at load 0 hp with added Gaussian white noise with SNR value that equals to -4 decibel.

The same precedents processes are realized on the noisy signals including splitting into segments that are converted afterward into a gray scale images. Then, the noisy vibration images are considered as an input to the adopted CNN model. The fault diagnosis accuracies of the proposed method under variable values of SNR are shown in Fig. 10.

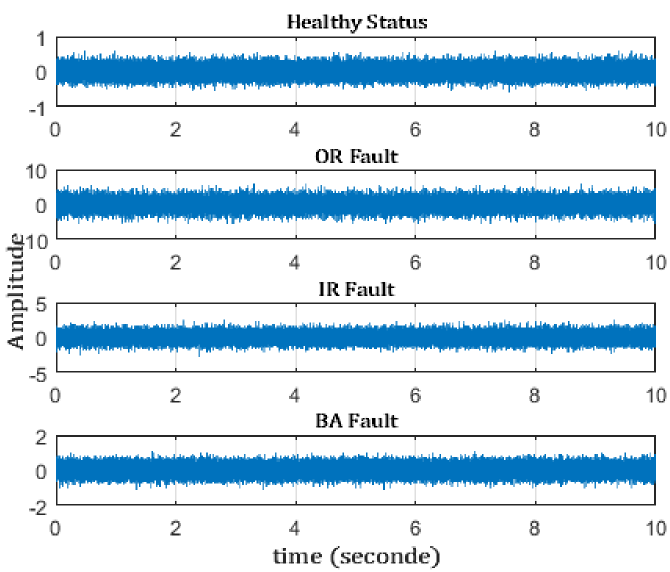

Fig. 9. The noisy vibration signals.

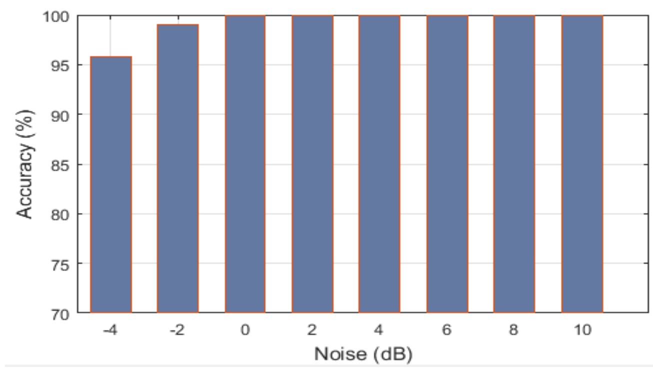

Fig. 10. The performance histogram of the proposed scheme under different noise conditions

From Fig. 10, we can obviously see that the proposed CNN model keeps achieving 100% of classification accuracy under high values of SNR that are varied from 0 dB to 10 Db. However under low values of SNR, the performance degrades and the classification accuracy attains 99% and 95.75% depending to SNR=-2 dB and SNR=-4 dB respectively. For this fact, we tried to improve the performance of our diagnosis system under low SNR values by adding a supplement of hidden layer neuron nodes in both the first and the second convolution layers. Table 6 describes the performed experiences and shows its results.

We can see through this experiment that our CNN model performs better while the number of hidden layer neuron nodes arise in both CL1 and CL2. The classification accuracy reaches 100% for SNR= -2db and attains 98.12% for SNR=-4db. In low SNR Test cases, increasing the number of convolution filters makes our network learns more potential characteristics where the features extraction ability is enhanced. The confusion matrix related to the third experiment with an added SNR value of -4 db, is shown in Fig. 11.

The attained results described by the confusion matrix presented in Fig. 11, shows that our prognostic system misclassifies only 15 samples from 600 faulty vibration images (label 2, 3 and 4) with a misclassification error that equals approximatively to 1.9%. The CNN-Softmax method has successfully detected the Healthy condition (label 1) with 100% of classification accuracy, which proves the strong ability of our method to differentiate Healthy bearing from the faulty ones under noisy working environments.

Table.6.
Classification results per number of convolution filters.

experiment	**Number of neurons**		**Accuracy**	
	CL1	**CL2**	**SNR= -2 db**	**SNR= -4 db**
1	30	60	99 %	95.75 %
2	35	70	100 %	97.6 0%
3	40	80	100 %	98.12 %

Fig. 11. Confusion matrix for added SNR= - 4db.

The obtained satisfactory results demonstrate the high robustness and effectiveness of the proposed fault diagnosis approach that stills working well under randomly added noise conditions.

4. CONCLUSION

In this paper, we proposed a robust approach based on CNN algorithm for bearing faults diagnosis. The proposed method exploits the efficiency of CNN to extract automatically the significant features from the transformed vibration images without requiring any signal processing. The adopted diagnosis system has a good performance that reaches 100% of classification accuracy. In addition, when the working load condition is changed and without retraining our CNN model, the proposed diagnosis system still works well by maintaining a high fault identification performance. Furthermore, the proposed method has the reliability, robustness and ability to work under noisy environments without any denoising process.

References

[1] H. Shao; H. Jiang, L. Ying & X. Li. “A novel method for intelligent fault diagnosis of rolling bearings using ensemble deep auto-encoders”. Mech. Syst. Signal Process, vol. 102, pp. 278–297, 2018.

[2] R. Liu, B. Yang, E. Zio, & X. Chen,“Artificial intelligence for fault diagnosis of rotating machinery: A review”. Mechanical Systems and Signal Processing, Vol. 108, pp. 33-47, August 2018.

[3] J. Chang, T. Li, & P. Li, “The selection of time domain characteristic parameters of rotating machinery fault diagnosis”. 2010 International Conference on Logistics Systems and Intelligent Management (ICLSIM), 2010.

[4] C. Bianchini, F. Immovilli, M. Cocconcelli, R. Rubini, and A. Bellini, “Fault detection of linear bearings in brushless ac linear motors by vibration analysis,” IEEE Transactions on Industrial Electronics, vol. 58, no. 5, pp. 1684–1694, December 2011.

[5] B. R. Nayana, P. GEETHANJALI, “Effective Time Domain Features for Identification of Bearing Fault using LDA and NB Classifiers”. International Journal of Mechanical and Production Engineering Research and Development, Vol. 8, pp. 1135-1150, January 2018.

[6] J. ZHOU, Y. QIN, L. KOU, M. YUWONO, & S. SU, “Fault detection of rolling bearing based on FFT and classification”. Journal of Advanced Mechanical Design, Systems, and Manufacturing, 9(5), October 2015.

[7] Sheng-wei Fei, “Fault Diagnosis of Bearing Based on Wavelet Packet Transform-Phase Space Reconstruction-Singular Value Decomposition and SVM Classifier”. Arabian Journal for Science and Engineering, vol. 42(5), pp. 1967–1975, January 2017.

[8] M. Beibei, S. Yanxia, W. Dinghui, & Z. Zhipu, “Three level inverter fault diagnosis using EMD and support vector machine approach”. 2017 12th IEEE Conference on Industrial Electronics and Applications (ICIEA), 2017.

[9] H. Liu., L. Li, & J. Ma, “Rolling Bearing Fault Diagnosis Based on STFT-Deep Learning and Sound Signals”. Shock and Vibration, 1–12, September 2016.

[10] Z. H. Luo, & Q. J. Xiao, “Time-Frequency Features of Signal Analysis and its Application in Mechanical Fault Diagnosis”. Advanced Materials Research, 834-836, October 2013.

[11] M. Jung, O. Niculita, & Z. Skaf, “Comparison of Different Classification Algorithms for Fault Detection and Fault Isolation in Complex Systems”. Procedia Manufacturing, vol. 19, pp. 111–118, January 2018.

[12] D. Weimer, B. Scholz-Reiter, and M. Shpitalni, “Design of deep convolutional neural network architectures for automated feature extraction in Industrial inspection”.CIRP Ann.-Manuf. Technol., vol. 65, no. 1,pp. 417-420, May 2016.

[13] O. Abdeljaber, O. Avci, S. Kiranyaz, M. Gabbouj, and D. J. Inman, “Realtime vibration-based structural damage detection using one-dimensional convolutional neural networks” J. Sound Vib., vol. 388, pp. 154-170, February 2017.

[14] P. Cao, S. Zhang, & J. Tang, “Preprocessing-Free Gear Fault Diagnosis Using Small Datasets With Deep Convolutional Neural Network-Based Transfer Learning”. IEEE Access, vol. 6, pp. 26241–26253, May 2018.

[15] D. Nguyen, M. Kang, C. Kim, & J. Kim, “Highly reliable state monitoring system for induction motors using dominant features in a two-dimension vibration signal”. New Review of Hypermedia and Multimedia, vol 19(3-4), pp. 248–258, October 2013.

[16] M. Xia, T. Li, L. Xu, L. Liu and C. de Silva, “Fault Diagnosis for Rotating Machinery Using Multiple Sensors and Convolutional Neural Networks”, IEEE/ASME Transactions on Mechatronics, vol. 23, no. 1, pp. 101-110, February 2018.

[17] Bearing Data Center. Available online: https://csegroups.case.edu/bearingdatacenter/pages/12k-drive-end-bearing-fault-data